PL ISSN 0065-1583

POLISH ACADEMY OF SCIENCES
NENCKI INSTITUTE OF EXPERIMENTAL BIOLOGY

# ACTA PROTOZOOLOGICA

VOLUME 25

Number 3

PAŃSTWOWE WYDAWNICTWO NAUKOWE
WARSZAWA 1986

POLISH ACADEMY OF SCIENCES
NENCKI INSTITUTE OF EXPERIMENTAL BIOLOGY

# ACTA PROTOZOOLOGICA

## International Journal of Protozoology



Manuscripts may be submitted to the Editorial Office: Acta Protozoologica, M. Nencki Institute of Experimental Biology, 02-093 Warszawa, 3 Pasteur Street, Poland, or to each member of the Editorial Board.

Subscription orders for all the magazines published in Poland available through the local press distributors or directly through the

Foreign Trade Enterprise
ARS POLONA
00-068 Warszawa, Krakowskie Przedmieście 7, Poland

Our bankers:
BANK HANDLOWY WARSZAWA S.A.

ACTA PROTOZOOLOGICA appears quarterly. The indexes of previous volume will appear in No. 1 of the next volume.

Intexed in Current Contents and in Protozoological Abstracts.

# Relationship Between Cytoskeleton and Motility

Symposium held on 25th June 1985 in Nairobi, Kenya, as a Part of the VII International Congress of Protozoology

It became a tradition of International Congresses of Protozoology to pay special attention to the physiology of movement and behaviour of *Protista*. In that field the protozoologist looking how a unicellular organism behaves and the cell biologist willing to understand how a non-muscle motile cell operates, meet together and work in unison. This tradition was followed by the VII International Congress of Protozoology held in Nairobi on 21 – 29 June 1985. The Symposium "Relationship Between Cytoskeleton and Motility" was one of most successful components of the scientific programme of this Congress. It took 5 hours instead of the 3 originally planned, and was attended by over 100 participants.

The presence of microfilaments and microtubules in the contractile cytoskeletal systems of the unicellular eukaryotes, the differentiations of their fine structure and topography within the cells, as well as the tremendous variety of motile phenomena manifested by *Protista*, made it impossible to review systematically the whole subject during one session. The Symposium concentrated therefore on a few selected topics: (1) organization of the contractile apparatus of giant amoebae and its role in producing the endoplasmic flow and locomotion (W. Stockem, Bonn, FRG), (2) the cytoskeleton and cell-to-substratum adhesion in the small, soil and fresh water amoebae (T. M. Preston, London, U. K.), (3) adhesion-dependent movements of the cytoskeletal cylinder and the traction component of the amoeboid movement (A. Grębecki, Warsaw, Poland), (4) transition from the actin to tubulin motor system during the amoebo-flagellate transformation (C. Fulton, Waltham, USA), (5) assembly and disassembly of the microtubular cytoskeleton in filopodia (M. Hauser, Bochum, FRG), (6) molecular mechanism of operation of the most specialized microtubular system, in the ciliary axoneme (P. Satir, Bronx, USA), (7) calmodulin as a likely universal sensor allowing $Ca^{2+}$ to control the motility of *Protista* (L. Kuźnicki, Warsaw, Poland). A. Grębecki acted as chairman of the Symposium and P. Satir as co-chairman. The chairman's report will appear in the post-congress volume, to be published as a special issue of Insect Science and its Applications (A. Grębecki: Relationship between cytoskeleton and motility. In: Progress in Protozoology, Proc. VII Intern. Congr. Protozool., T. H. Odhiambe ed. in press).

The Editors of Acta Protozoologica decided to invite all the contributors to the Cytoskeleton and Motility Symposium in Nairobi, to publish the integral text of their lectures in our Journal. It is a pleasure to present to the readers (in the pp. 245–304) six papers received in response to this invitation.

ACTA PROTOZOOLOGICA
Vol. 25, No. 3, pp. 245–254 (1986)

# Microfilament Organization and Function in *Amoeba proteus*[1]

W. STOCKEM and H. U. HOFFMANN

Institute of Cytology, University of Bonn, 5300 Bonn 1, FRG

*Received on* 10th September 1985

*Synopsis.* The structural organization and function of the microfilament (MF)-system in *Amoeba proteus* was studied by immunological, fluorescent-analog-cytochemical and electron-microscopical methods. In normal locomoting cells the MF-system is localized beneath the plasma membrane and consists of three different regions: the anterior region of reorganization, the intermediate region of contraction and the posterior region of destruction. Alterations in the polarity and activity of the MF-system as induced by the external application and microinjection of more than 80 different drugs are always combined with characteristic changes in locomotor behavior, plasma membrane dynamics and cytoplasmic organization. Most common phenomena as observed in such experiments are: localized pseudopodium formation and retraction, spherulation and flattening of the amebae, hyalo-granuloplasm separation, cytokinesis and endocytosis. This demonstrates that the microfilament system of *A. proteus* is responsible for a large variety of motile phenomena.

Recent progress in cell motility research has revealed both the stabilizing and dynamical function of a thin layer of microfilaments associated with the internal face of the plasma membrane (Alberts et al. 1983). According to ultrastructural and cell physiological results on non-muscle cells (Weihing 1979, Korn 1982, Weber and Osborn 1982, Jockusch 1983) the cortical filament layer is involved in different movement phenomena, such as (a) generation of motive force for cytoplasmic streaming and cell locomotion, (b) changes in cell form and cell surface morphology, (c) cell body stabilization, (d) movements on and of the cell surface, (e) cell-to-substratum contacts, (f) endo- and exocytosis and membrane turnover, and (g) cytokinetic activities.

In a series of experiments using microinjection, fluorescent analog cytochemistry, immunocytochemistry and electron microscopy we studied the morphology

[1] Lecture presented by W. Stockem on 25th June 1985 at the Symposium "Relationship between Cytoskeleton and Motility", held during the Seventh International Congress of Protozoology in Nairobi, Kenya.

Supported by a grant of the DFG (Sto 126/1–4)

and function of the cortical filament layer in *Amoeba proteus* (Stockem et al. 1978, Wehland et al. 1979, Gawlitta et al. 1980 a, b, Gawlitta et al. 1981, Stockem et al. 1982, Stockem et al. 1983 a, b, Hoffmann et al. 1984). The most important results of these experiments are summarized in this contribution.

## Results and Conclusions

*Amoeba proteus* is a uninuclear organism which exhibits a distinct polarity during normal locomotion. Cytoplasmic streaming originates at the rear end (uroid) and is directed toward the front zone (advancing pseudopodia).

The most striking phenomena of migration are changes in cell shape caused by the continuous formation and retraction of pseudopodia. Detailed studies (Stockem et al. 1969) by cinematographic single-frame analysis (Fig. 1) demonstrate a permanent decrease in contour at the uroid or at retracting pseudopodia (hatch-

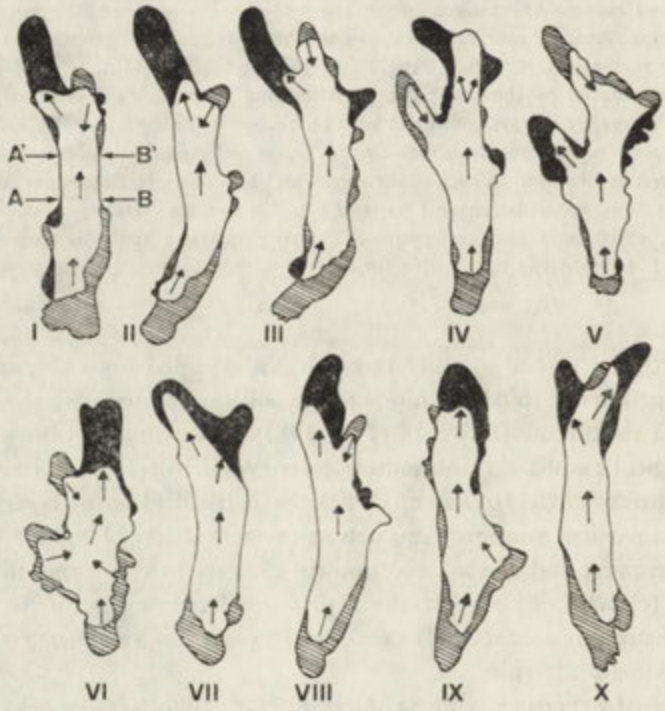


Fig. 1. Drawings obtained from a cinematographic analysis of a movement period over 19 min demonstrating changes in contour and cytoplasm translocation of a polytactic *A. proteus*. The time difference between the 10 consecutive stages (I–X) is 2 min. Each stage is composed of two outlines of the same cell, which differ by 1 min. The first outline, comprised of white and hatched areas, represents the previous time stage, whereas the white and black areas represents the stage the amoeba attained 1 min later. A′, A and B′, B — intermediate region of constant outline, arrows — cytoplasmic streaming direction. Magn. 75× (from Stockem et al. 1969)

ed areas), and a permanent increase in contour at the front or at extending pseudopodia (black areas). The uroid and front region are always separated by an intermediate zone of constant outline (Fig. 1 A A′, B B′).

The streaming endoplasm is transported within a tube, the wall of which consists of stationary ectoplasm (Pl. I EC, EN). Both, endoplasm and ectoplasm exhibit a similar structure and consist of hyaline ground plasm containing the various structured cell components. At the cell periphery ground plasm normally prevails in the ectoplasm and locally forms zones of clear hyaloplasm (Pl. I HP). Different theories localizing contraction either in the posterior or in the anterior pole of amoeba were proposed in the past to explain the phenomenon of amoeboid movement (for recent reviews see Komnick et al. 1973, Allen and Allen 1978, Taylor and Condeelis 1979, Grębecki 1982).

However, these attempts were more or less unsuccessful because morphological and physiological data necessary to understand the mechanism of motive force generation were lacking. In particular, these data include an answer to the question of the (1) nature, (2) spatial arrangement, (3) ultrastructural organization and (4) function of the contractile system in large amoebae.

## Nature of the Contractile System

Direct evidence for the nature of the contractile system was obtained from investigations on glycerinated amoebae (Simard-Duquesne and Couillard 1962, Schäfer-Danneel 1967).

In addition to unspecific spherulation caused by the extraction procedure, the cells specifically react on the addition of ATP and anorganic ions with a distinct volume contraction. The contractile effect of ATP proved to be morphologically manifested in the condensation of a network of microfilaments. In summary, these results indicate that microfilaments provide the structural basis of contractility in *A. proteus* and are equivalent to the actomyosin system of muscle and motile non-muscle cells.

## Spatial Arrangement of the Contractile System

The spatial arrangement of the contractile system in *A. proteus* as a necessary information for understanding the conversion of chemo-mechanical energy transformation on the molecular level into the complicated pattern of amoeboid movement and related phenomena on the microscopical level was recently elucidated by immunocytochemistry (Stockem et al. 1983 b). In normal locomoting specimens fixed for antibody staining in ice-cold methanol actin is mainly located in a cortical layer displayed beneath the plasma membrane or delineating the granuloplasm from the peripheral hyaloplasm. The amount of actin within this layer

increases from the advancing front to the intermediate region of constant outline and decreases again toward the uroid. The distribution of myosin is largely congruent to the display of actin, with the exception that the myosin content of the cortical layer gradually increases from the front to the uroid. It is important to mention that distinct fibrillar-like differentiations in both, the endoplasm and ectoplasm of *A. proteus* are completely lacking.

## Ultrastructural Organization of the Contractile System

The ultrastructural organization of the contractile system in normal locomoting *A. proteus* was investigated using improved fixation and embedding techniques. Best results were obtained after application of PIPES-buffered glutaraldehyde in connection with substances known to prevent depolymerization of microfilaments (PEG, phalloidin), followed by careful dehydration and freeze-substitution (Stockem et al. 1982).

The contractile system is constructed of two components: thin filaments with a diameter of 6 nm (actin) and thick filaments with a diameter of 10–30 nm (myosin). The thin filaments are linked with the plasma membrane by regularly arranged cross bridges of 5–10 nm thickness and 20–30 nm length. The thick filaments are connected to the thin filaments by cross bridges, which measure 60 nm between the two filament types and 30 nm in diameter.

The contractile system is always continuous along the entire cell surface (Fig. 2 A, broken lines) and varies in thickness depending on the cell region. In the front region it is very thin with an average thickness of 0.1 μm (Fig. 2 A, thin broken lines), whereas in the intermediate and posterior region (Fig. 2 A, thick white and black broken lines) it normally increases to 0.5 μm or more. In contrast to thin filaments, which are a general constituent of the contractile system, the display of thick filaments is largely restricted to the uroid region. Both, thin and thick filaments reveal a low degree of order with respect to their spatial orientation. In the front region (Fig. 2 B) the orientation of thin filaments is mostly parallel to the plasma membrane and to the longitudinal axis of the cell. In the intermediate and uroid region (Fig. 2 C), the predominant arrangement of thin and thick filaments is a netlike structure without any visible preferential course of the two filament types.

## Function of the Contractile System

The function of the contractile system in *A. proteus* was investigated by fluorescent-analog-cytochemistry (FAC). This new, high-resolution technique for light-microscopic studies of living cells combines fluorescence microscopy, microinjection, video technology and digital image processing.

Thereby, dynamic processes in the cytoplasm can be observed on the molecular

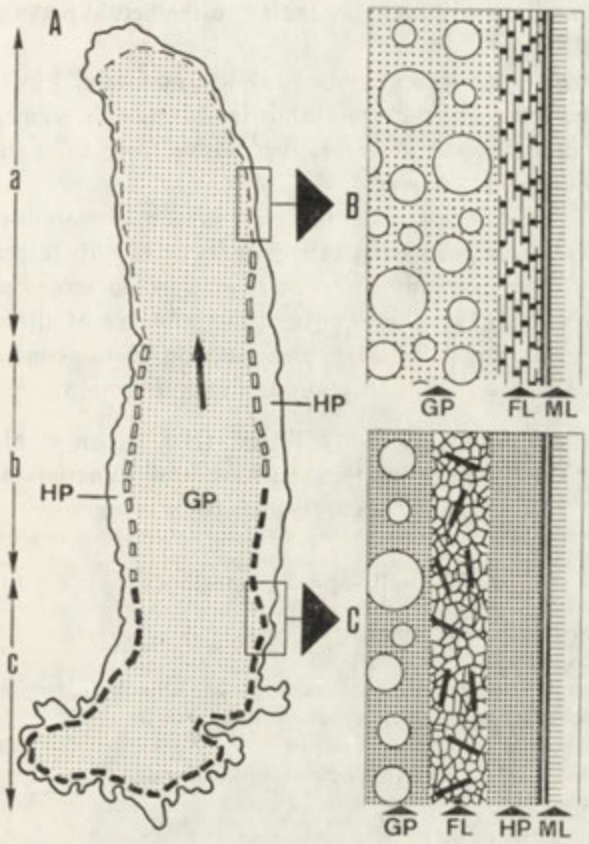


Fig. 2 A — Drawing prepared from an ultrathin section after electron microscopic investigation at high magnification to demonstrate the course of the contractile system in an orthotactic *A. proteus*. The system is divided into three zones: *a* — zone of formation (thin broken lines), *b* — zone of contraction (thick broken white lines), *c* — zone of destruction (thick broken black lines). The length of these zones may actually differ and the transitions between them are fluid. In particular the contraction zone *b* may be much more extended and partly overlap with *a* and *c*, B — Drawing demonstrating the ultrastructure of the cell periphery at the front region. The contractile system (FL) is in close contact with the plasma membrane and contains microfilaments of parallel arrangement which are interconnected by oligomeric myosin cross-bridges, C — Drawing demonstrating the ultrastructure of the cell periphery at the intermediate and uroid region. The contractile system (FL) delineates the peripheral hyaloplasm (HP) from the central granuloplasm (GP), and contains microfilaments and thick (myosin) filaments in a netlike arrangement. The links between the contractile system and the plasma membrane are not shown in the scheme, although they certainly do exist. ML — mucous layer

level, e.g., the intracellular redistribution of fluorescein-labeled muscle G-actin after microinjection into *A. proteus* (Stockem et al. 1983 a). The polymerization-competent protein becomes part of the endogeneous microfilament system undergoing dynamic changes over time periods of several hours. Single-frame analyses of long-term sequences enabled the direct demonstration of both, the contractile activities and morphological transformations of microfilaments in such amoebae. In normally locomoting cells the contractile system undergoes conti-

nuous changes in spatial distribution depending on the actual pattern of cytoplasmic streaming and cell shape.

The highest degree of differentiation is always maintained in the intermediate region between the front and the uroid, thus indicating this segment of the cortex to be the most important site in generating motive force for pseudopodium formation and amoeboid movement.

Individual cellular compartments involved in the excitation-contraction mechanism for motive force generation can be influenced with respect to their functional activity by chemical stimulation or inhibition. In recent series of experiments (Hoffmann et al. 1984) we compared the influence of altogether 88 agents (see the list below) on the morphology and function of the contractile system of *A. proteus* after both, external application and microinjection.

List of Chemical Agents Recently Tested (Hoffman et al. 1984 and Unpublished) for their Action on the Structure and Function of the Contractile Apparatus of *Amoeba proteus*

Externally-applied Substances

Acetylcholine, acridine orange, asparagine, atropine,
benzamide, butyrylcholine,
caffeine, chloral hydrate, chloroform, *p*-chloromercuribenzoic acid, chlorpromazine, cocainhydrochloride, colchicine, collagenase, cysteine, cytochalasin B,
D-600, dibucaine, digitonin, dinitrophenol (DNP)
ether, ethylenediamine, EDTA, EGTA, ephedrine hydrochloride, eserine,
heparin, 8-hydroxyquinoline,
iso-OMPA
lysolecithin
Mono-iodoacetic acid, morphine,
NEM (*n*-ethylmaleimide), noradrenaline,
ouabain,
papain, phalloidin, phloretin, phloridzin, phospholipase, pilocarpine, poly-L-lysine (MG: 500 000, MG: 6 000-9 000), polymyxin-B-sulphate, procaine hydrochloride, prostaglandin $F_{2\alpha}$, puromycin, putrescine,
quinine,
RNase, ruthenium red,
serotonin, spermidine, spermine, sucrose,
theobromine, theophylline, thiourea, trypan red, trypsin,
urea, urethane.

Microinjected Substances

Acetylthiocholine iodide, acridine orange, actin, actinomycin D, ammonium molybdate, ATP, bovine serum albumin,
caffeine, caprylic acid, chlorpromazine, chlortetracycline, cocaine, collagenase, cysteine, cytochalasin B,
D-600, DMSO, DNase I, DNP, $D_2O$,

EDTA, EGTA, eserine, ethanol, ethylenediamine,
ferritin, fluphenazin, fragmin,
heparin, histamine, HMM, $H_2O_2$, hyaluronidase,
iso-OMPA,
lysolecithin,
morphine, NEM,
ouabain,
papain, PCMB, pepsin, phalloidin, phloretin, phloridzin, phospholipase, pH-graded from 3–11, poly-L-glutamic acid, poly-L-lysine, polymyxin B, procaine hydrochloride, putrescine,

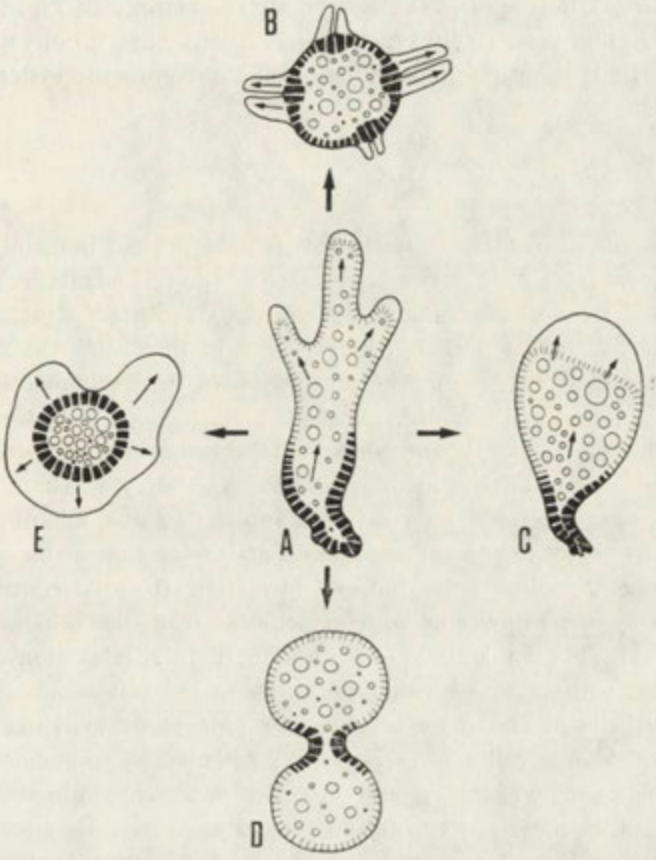


Fig. 3. Schematic drawing to demonstrate some alterations in the polarity and cytoplasmic organization as induced by the external application (B) or microinjection (C–E) of different substances (A→ B — polycations, A→ C — DNAase I, A→ D — spermine, A→ E — phalloidin). A — normal locomoting cell with controlled isotonic contraction of the microfilament system at the intermediate and uroid region (black) and isometric contraction and controlled relaxation at advancing pseudopodia (white), B — pinocytoting cell with total contraction (black) and local detachment of the microfilament system from the cell membrane. Extending pseudopodia containing pinocytosis channels (white), C — monotactic cell with total contraction at the uroid (black) and total relaxation at the front (white), D — dividing cell with local, ring-like contraction in the intermediate region (black), E — total contraction of the microfilament system with detachment from the cell membrane resulting in distinct separation of hyaloplasm (white) from granuloplasm (open circles), arrows inside the cells — cytoplasmic streaming direction (from Stockem et al. 1981)

quinine,
RNase, Ro 20-1724, ruthenium red,
sodium-monovanadate, spermidine, spermine, sucrose,
theophylline, thiourea, trypsin,
vitamin $K_1$.

The different reaction patterns, which were induced by the tested agents mainly depend on two phenomena, i.e., on the localized or general contraction or relaxation of the actomyosin system. Some of the most interesting reactions observed in *A. proteus* after chemical stimulation are summarized in Fig. 3. It is important to mention that these results exactly coincide with observations made by Grębecki (1980, 1981) using photic stimulation of the contractile system in different body regions.

## Final Remarks

The contractile microfilament system of *Amoeba proteus* is mainly represented by a thin cortical layer at the cytoplasmic face of the cell membrane. During normal locomotion the cortical filament layer exhibits a distinct structural and physiological polarity characterized by the existence of three different zones: a zone of formation at the front, a zone of contraction in the medium cell region, and a zone of destruction at the uroid. Experimentally induced alterations in the polarity of the microfilament system cause immobilization in conjunction with characteristic changes in cell shape, membrane dynamics and cytoplasmic organization.

The phenomena observed after external application and microinjection of 88 different substances are: (a) local contraction and relaxation of the microfilament system, i.e., pseudopodium retraction and formation, (b) total contraction of the microfilament system without or with detachment from the cell membrane, i.e., sperulation and hyalo-granuloplasm — separation, (c) total relaxation of the microfilament system without or with destabilization of the cell membrane, i.e., flattening and cell death, and (d) cytokenetic or pinocytotic activities by modified contractions in definite cell areas. The results gathered by immunocytochemistry, fluorescent analog cytochemistry and electron microscopy allow an improved interpretation of ameboid movement and related processes. They seem to favour, among the present broad concepts, the generalized cortical contraction theory (Grębecki 1982) and the solation-contraction coupling hypothesis (Taylor and Condeelis 1979).

## REFERENCES

Alberts B., Bray D., Lewis J., Raff M., Roberts K. and Watson J. D. 1983: Molecular Biology of the Cell. Garland Publishing, Inc. New York and London.
Allen R. D. and Allen N. S. 1978: Cytoplasmic streaming in ameboid movement. Annu. Rev. Biophys. Bioeng., 7, 469–495.
Gawlitta W., Stockem W., Wehland J. and Weber K. 1980 a: Organization and spatial

arrangement of fluorescein-labelled native actin microinjected into normal locomoting and experimentally influenced *Amoeba proteus*. Cell Tissue Res., 206, 181–191.
Gawlitta W., Hinssen H. and Stockem W. 1980 b: The influence of an actin-modulating protein (AM-protein) from *Physarum polycephalum* on the cell motility of *Amoeba proteus*. Eur. J. Cell Biol., 23, 43–52.
Gawlitta W., Stockem W. and Weber K. 1981: Visualization of actin polymerization and depolymerization cycles during polyamine-induced cytokinesis in living *Amoeba proteus*. Cell Tissue Res., 215, 249–261.
Grębecki A. 1980: Behaviour of *Amoeba proteus* exposed to light-shade difference. Protistologica, 16, 103–113.
Grębecki A. 1981: Effects of localized photic stimulation on amoeboid movement and their theoretical implications. Eur. J. Cell Biol., 24, 163–175.
Grębecki A. 1982: Supramolecular aspects of amoeboid movement. Progress in Protozoology, Proc. Sixth Int. Congr. Protozool., 1, 117–130.
Hoffmann H. U., Stockem W. and Gruber B. 1984: Dynamics of the cytoskeleton in *Amoeba proteus*. II. Influence of different agents on the spatial organization of microinjected fluorescein-labeled actin. Protoplasma, 119, 79–92.
Jockusch M. 1983: Patterns of microfilament organization in animal cells. In: Molecular and Cellular Endocrinology, 29, 1–19. Elsevier Sci. Publ. Ireland, Ltd.
Komnick H., Stockem W. and Wohlfarth-Bottermann K. E. 1973: Cell motility: Mechanism in protoplasmic streaming and amoeboid movement. Int Rev. Cytol., 34, 169–249.
Korn E. D. 1982: Actin polymerization and its regulation by proteins from nonmuscle cells. Physiol. Rev., 62/2, 672–737.
Schäfer-Danneel S. 1967: Strukturelle und funktionelle Voraussetzungen für die Bewegung von *Amoeba proteus*. Z. Zellforsch. microsc. Anat., 78, 441–462.
Simard-Duquesne N. and Couillard P. 1962: Amoeboid movement. I. Reactivation of glycerinated models of *Amoeba proteus* with adenosinetriphosphate. Exp. Cell Res., 28, 85–91.
Stockem W. 1970: Untersuchungen mit dem Differential-Interferenz-Kontrast über Morphologie und Cytosen von *Amoeba proteus*. Mikroskopie, 24, 332–344.
Stockem W., Hoffmann H. U. and Gawlitta W. 1981: Funktionell-morphologische Grundlagen der amoeboiden Bewegung. Verh. Dtsch. Zool. Ges., 71–84.
Stockem W., Hoffmann H. U. and Gawlitta W. 1982: Spatial organization and fine structure of the cortical filament layer in normal locomoting *Amoeba proteus*. Cell Tissue Res., 221, 505–519.
Stockem W., Wohlfarth-Bottermann K. E. and Haberey M. 1969: Pinocytose und Bewegung von Amoeben. V. Mitteilung: Konturveränderungen und Faltungsgrad der Zelloberfläche von *A. proteus*. Cytobiologie, 1, 37–57.
Stockem W., Weber K. and Wehland J. 1978: The influence of microinjected phalloidin on locomotion, protoplasmic streaming and cytoplasmic organization in *Amoeba proteus* and *Physarum polycephalum*. Cytobiologie, 18, 114–131.
Stockem W., Hoffmann H. U. and Gruber B. 1983 a: Dynamics of the cytoskeleton in *Amoeba proteus*. I. Redistribution of micro-injected fluorescein-labeled actin during locomotion, immobilization and phagocytosis. Cell Tissue Res., 232, 79–96.
Stockem W., Naib-Majani W., Wohlfarth-Bottermann K. E., Osborn M. and Weber K. 1983 b: Pinocytosis and locomotion of amoebae. XIX. Immunocytochemical demonstration of actin and myosin in *Amoeba proteus*. Eur. J. Cell Biol., 29, 171–178.
Taylor D. L. and Condeelis J. S. 1979: Cytoplasmic structure and contractility in amoeboid cells. Int. Rev. Cytol., 56, 57–144.
Weber K. and Osborn M. 1982: The cytoskeleton. Natl. Cancer Inst. Monogr., 60, 31–46.
Wehland J., Weber K., Gawlitta W. and Stockem W. 1979: Effects of the actin-binding protein DNAase I on cytoplasmic streaming and ultrastructure of *Amoeba proteus*. Cell Tissue Res., 199, 353–372.
Weihing R. R. 1979: The cytoskeleton and plasma membrane. Methods Achiev. Exp. Pathol., 8, 42–109, Karger, Basel.

## EXPLANATION OF PLATE I

Differential-interference-contrast light micrograph of an extending pseudopodium of *A. proteus* EC – ectoplasm, EN – endoplasm, GP – granuloplasm, HP – hyaloplasm, N – nucleus, V – contractile vacuole, arrow – cytoplasmic streaming direction. Bar – 50 μm (from Stockem 1970)

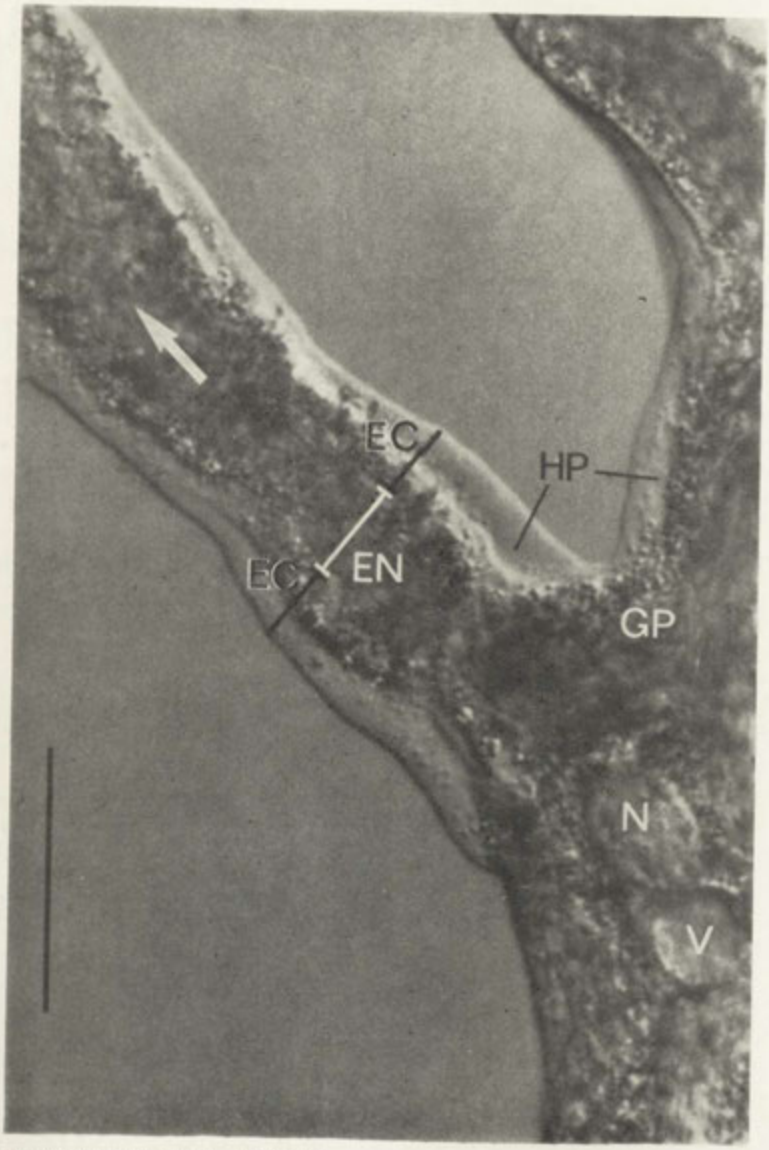


W. Stockem et H. U. Hoffmann auctores phot.

ACTA PROTOZOOLOGICA
Vol. 25, No. 3, pp. 255–268 (1986)

# Adhesion-dependent Movements of the Cytoskeletal Cylinder of Amoebae[1]

Andrzej GRĘBECKI

Department of Cell Biology, Nencki Institute of Experimental Biology, Polish Academy of Science, 3 Pasteur str., 02-093 Warszawa, Poland

*Received on* 4th September 1985

*Synopsis.* The whole peripheral cylinder of amoeba plays as well the contractile as cytoskeletal functions, because the myosin and the actin-binding proteins are both interwoven in the F-actin cortical network. It is therefore a self-contracting and self-retracting structure. In the unattached cells the whole cylinder uniformly withdraws toward its closer rear end, i.e., retracts toward its geometrical centre. That produces a full fountain movement in the cell interior. In amoebae attached to the substrate the peripheral gel layer retracts centripetally from each free body end to the adhesion zone. That results in the tail withdrawal behind the attachement sites as well as in the ectoplasm retreat (= fountain movement) in front of them. Therefore, the fountain phenomenon is not produced by frontal pulling of axial endoplasm, but by self-retraction of the peripheral contractile layer. The velocity of ectoplasm movements always increases linearly from the retraction centre to the distal zones. That confirms the uniform distribution of the contractile and cytoskeletal properties along the cell periphery.

## Pressure Flow and Traction Aspects of Amoeboid Movement

It is well established at least from 15 years that the active component of the ectoplasmic layer of amoebae, responsible for cell locomotion and other motor responses, is built of a three-dimensional network of F-actin microfilaments which can interact either with myosin or with actin-binding proteins. First type of interactions results in filaments sliding which may lead as well to a longitudinal shortening as to the three-dimensional reduction of volume of the whole cortical meshwork, i.e., to its contraction. Interactions of the second type, in which some actin-binding proteins are involved, stiffen the ectoplasmic gel by cross-linking the filaments, i.e., they assign to the ectoplasmic layer its cytoskeletal role (cf. Taylor

[1] Lecture presented by A. Grębecki on 25th June 1985 at the Symposium "Relationship between Cytoskeleton and Motility", held during the Seventh International Congress of Protozoology in Nairobi, Kenya.

and Condeelis 1979, Pollard 1984). Therefore the ectoplasmic cylinder may keep its relatively constant shape and is capable to transmit mechanical tension. We may state in general that it performs simultaneously as well the contractile as the cytoskeletal functions.

Coexistence of these two functions in the ectoplasmic cylinder creates some problems, because on one hand they are complementary and are both needed to produce movements, but on the other hand they are in large extent opposed one to another. Some rigid structure is necessary to transmit the force developed by filaments sliding and to perform work, but too much stiffness would make the contraction impossible or at least constrain it under the isometric régime.

A solution of this contradiction might be proposed on the basis of classical tail contraction theory of amoeboid movement, by assuming that the actin-myosin interactions are restricted to the posterior segment of the ectoplasmic cylinder, which would thus function as the only contractile cell region. The cross-linking of filaments by the actin-binding proteins would prevail in the middle and anterior zones, creating there a system of more stiff tubes built of the stabilized but non-contractile gel (Wehland et al. 1979). In that way the contractile and cytoskeletal functions of the ectoplasmic cortical layer would be spatially separated on the macro-scale of cell organization.

However, it was recently established that the contractility of the cell cortex in amoeba is not limited to the tail but well expressed along the whole cell. The ultrastructural studies of the fixed material and application of the modern fluorescence techniques to living cells lead to the conclusion that the contractile capacities are not restricted to any body pole, but probably are evenly distributed along the cell periphery (Stockem et al. 1982, 1983 a, b). The contractile activity of the whole cortical cylinder of amoeba was directly demonstrated by local application of contracting or relaxing photic stimuli to its different segments (Grębecki 1981). Such structural and functional evidence support the generalized cortical contraction theory of amoeboid movement (Grębecki 1982 a, b).

So, the contractile and cytoskeletal functions seem not to be separated in the ectoplasmic cylinder on the cellular macro-level. They are probably separated on the ultrastructural level, as recently proposed by the solation-contraction coupling hypothesis (Taylor et al. 1979, 1982). It postulates that the whole ectoplasmic gel of amoeba is a mosaic of microdomains in which either the mobilizing effects of myosin or stabilizing effects of actin-binding proteins are respectively prevailing. It means that, at the cellular level, the contractile and cytoskeletal properties of the cortical layer are interwoven along the whole length of amoeba. Thus, the ectoplasm may not only contract in any place, but also transmit mechanical tension to the neighbouring areas. Each contraction spot must interfere with other parts of the peripheral layer by pulling them. As a whole, the ectoplasmic cylinder should behave in an integrated manner as a self-contracting and self-retracting body.

First of all, being a hollow gelated bag built of an unordered meshwork of fila-

ments, it should contract three-dimensionally, in volume, squeezing the endoplasmic sol in its interior. It raises the hydrostatic pressure in the endoplasm, which may be transformed in the movement if a pressure gradient is established. The gradient arises when any place along the contracting cell periphery is being relaxed. Then the endoplasm starts flowing toward the relaxed spot, which becomes the front of locomotion. The contraction-relaxation events in the fronts are under the control of external stimuli. In that way the generalized cortical contraction theory explains the pressure driven and streaming dependent mechanism of locomotion in amoeba (Grębecki 1982 a, b).

That is certainly the most important aspect of movement of the giant amoebae, but not the only one to determine their motor behaviour. As it was stressed before, the contraction force developed by the ectoplasmic cylinder is not only transmitted to its interior in the form of pressure, but also along its own walls in the form of tension. If so, the ectoplasmic material should be also pulled mechanically along and linearly retracted in the plane of the walls of the cylinder. It means that the movements of amoebae are probably in some extent depending on the traction phenomena, besides the pressure mechanism.

The traction mechanism is recognized as locomotion factor in some other *Sarcodina* (e.g., in *Difflugia* — Bovee 1964, Allen 1968), in many crawling tissue cells (e.g., in fibroblasts — Abercrombie 1980) and in *A. proteus* as a factor in pinocytosis (Klein and Stockem 1979). But its general role in the motor behaviour of giant amoebae is little known, based on controversial observations and probably underestimated.

The forward movement of the posterior ectoplasm during locomotion is notorious and was never denied. As far as the ectoplasmic movements in the anterior cell part are concerned, even the account of facts is confusing. Most frequently is reported the massive bulk withdrawal of the whole ectoplasmic tube from the front backwards. The phenomenon is commonly called the fountain movement (Mast 1926, Allen 1961 a, Käppner 1961, Jahn 1964, Seravin 1966 a, b, Stockem et al. 1969, Grębecki 1976). The fountain is formed by the axial arm in which the endoplasmic sol is flowing forward, and the peripheral arm in which the new ectoplasmic gel is transported backwards (cf. Fig. 5).

The origin of the frontal fountain has never been explained in a satisfactory way by any version of the tail contraction theory (Rinaldi and Jahn 1963). But this phenomenon laid at the basis of the frontal contraction theory (Allen 1961 a, b), according to which the motive power is generated during the endoplasm–ectoplasm conversion inside the fountain zone, and the tension transmitted along the viscoelastic endoplasm results in pulling it in the direction of locomotion. It means that, according to this concept, the axial arm of the fountain which moves forward is the active one. Therefore, the explanation of the fountain phenomenon became theoretically important in further testing the validity of the present concepts of amoeboid movement.

## Retraction of the Ectoplasm in Unattached Amoebae

Our recent experimental attempt to reveal some general patterns of the traction dependent movements in the peripheral cell layers of *Amoeba proteus* was undertaken with different morphodynamic types of this species (monotactic, polytactic and heterotactic ones — see Pl. I 1), because the ectoplasmic movements were expected to be strongly dependent on the geometry of amoeba and on the topography of cell-to-substrate adhesion.

The monotactic forms were chosen to start experiments (Grębecki 1984), because of their always single unbranched ectoplasmic cylinder and easy manifestation of the fountain phenomenon. They were suspended either on the surface of fluorinert liquid or on a saturated methylcellulose layer, to prevent them to attach. Such cells are unable to change their position, the endoplasm is, however, streaming in their interior as usually forwards. Under these conditions the ectoplasm moves backwards not only in the frontal zone but along the whole cell length (Fig. 1 A). It means that the unattached monotactic amoebae, in contrast to the attached ones, are characterized by a full fountain movement.

Longitudinal velocity profiles of the backward movement of the ectoplasmic granules were obtained from the cinematographic records of such experiments (Fig. 2 A). Velocity of the ectoplasm withdrawal increases from the tail region up to the frontal cap, always in linear way. The linear slopes of the longitudinal velocity profiles strongly support the view that the contractile and cytoskeletal functions are rather uniformly distributed along the ectoplasm. Any non-contractile, just cytoskeletal, segment of the cylinder would forcibly produce a flat horizontal profile. Such profiles were never obtained. Their linear character indicates that the ectoplasmic cylinder shortens uniformly along its whole length, and

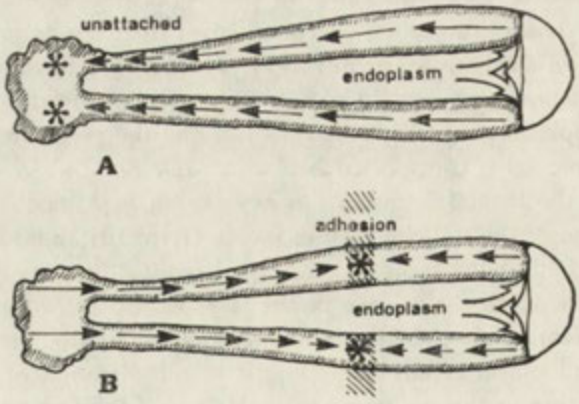


Fig. 1. A scheme explaining the principle of movements of the ectoplasmic cylinder of monotactic amoeba without attachment to the substrate (A) and attached in a narrow centrally located zone (B); the direction and length of arrows represent the character of movements and the asterisks the stationary condition of the ectoplasm

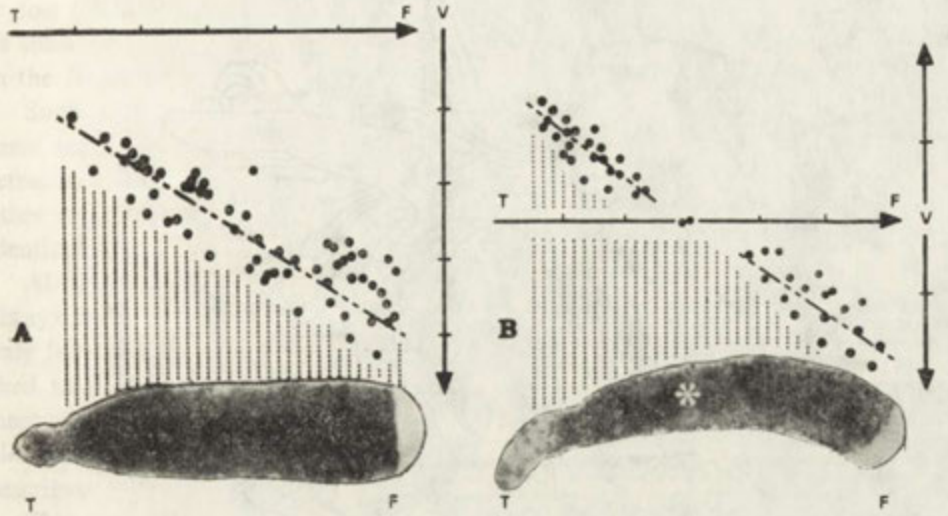


Fig. 2. The longitudinal velocity profiles of ectoplasmic inclusions in an unattached monotactic amoeba (A) and in an attached one (B); the asterisk in B shows the location of the attachment site; the tail-front axis of the body (T–F) is calibrated every 100 μm and the velocity axis (V) at the intervals of 2.5 μm/s each; the negative or positive V values correspond respectively to the backward or forward retraction of the ectoplasmic cylinder; after Grębecki (1984)

the shifting effects are summarized with the growing distance. In the amoeba ectoplasm just the closed posterior end of the cylinder is situated at the maximal distance from any open border of the ectoplasmic layer. Therefore, such velocity profiles prove that in an unattached amoeba displaying a full fountain phenomenon, the ectoplasm is evenly retracted toward its geometrical centre. That is exactly how should behave any self-contracting and self-retracting body freely suspended in the medium.

Monotactic amoebae are the simplest but sporadically occurring forms of *A. proteus*. Therefore, we had to verify each conclusion drawn from the study of this model by confronting it with the behaviour of polytactic forms (Pl. I 1a), which are the most typical for this species. The polytactic amoebae, when the fluorinert fluid or methyl-cellulose layer prevent them to attach, display also a kind of a full fountain along their whole length, but different in form. Together with the principal ectoplasmic cylinder, the lateral pseudopodia and all other elements of the cell outline are also retracted toward the posterior body end, i.e., the whole cell periphery is "flowing" backwards. The velocity changes along the longitudinal body axis are again proportional to the distance from the closed rear end of the ectoplasmic cylinder (Fig. 3 A). It may be concluded that also in the normal polytactic amoebae the contractile cytoskeletal layer retracts as a whole toward its geometrical centre, when the cell is lacking any contact with the ground (Grębecki 1985).

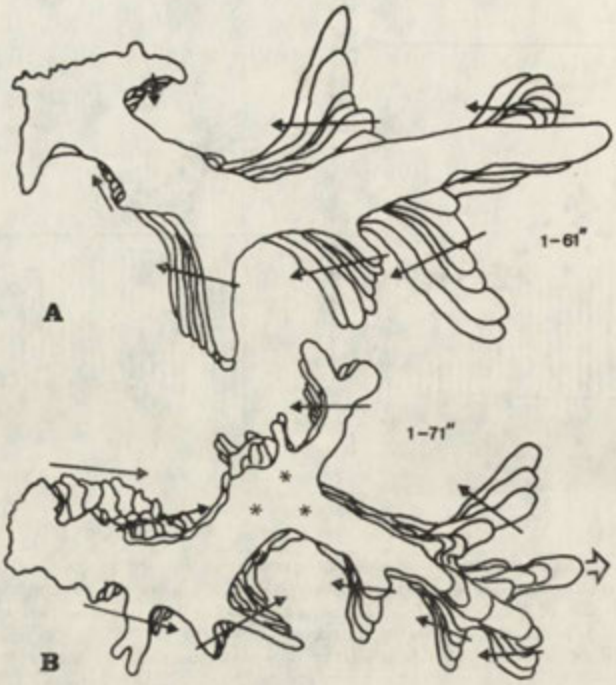


Fig. 3. Superposed cell contours of polytactic amoebae, without attachment to the substrate (A) and attached only by the middle body zone (B, attachment indicated by asterisks); as indicated by arrows, the whole periphery of the unattached cell is retracted backwards, whereas the attached individual retracts its periphery from both free body poles toward the adhesion zone; from Grębecki (1985)

## Ectoplasm Retraction in Amoebae Attached to the Glass

Any uniformly shortening body retracts toward its geometrical centre only when freely suspended in the medium. When in some place attached to the solid substrate, it will retract toward the attachment point. This second situation is that of amoeba locomoting on the surface of glass.

As a matter of fact, the ectoplasmic cylinder of monotactic amoeba migrating on the surface of glass is not retracted toward its geometrical centre, but is withdrawn from both sides toward the cell-to-substrate attachment zone (Grębecki 1984). The adhesion of monotactic individuals is rather weak and vary in time. When locomoting with a moderate speed, they usually adhere to the glass only by the body middle. Then, the stationary ectoplasm is seen just in this narrow attachment zone, whereas the other parts of the peripheral cylinder are longitudinally retracted from both free body poles toward the centre (Fig. 1 B and Pl. I 2a).

When a monotactic individual establishes much more attachment sites scattered over a large part of its lower surface, including the frontal area, almost all ectoplasmic inclusions become stationary and the retraction is restricted to the tail

region (Pl. I 2 b). But the backward motion of the anterior ectoplasm reappears as soon as a new segment of the peripheral cylinder is added without attachment in the front (Pl. I 2 c).

Such a course of events periodically leads the monotactic amoebae to attachment restricted to the rear cell part. In that stage there is no locomotion, no tail retraction, the ectoplasm in the posterior body end remains stationary, but in all other regions is pulled backwards and forms the full fountain pattern (Pl. I 2 d), identical to that manifested by an unattached cell.

All the situations shown in Pl. I 2 coherently prove that the ectoplasmic cylinder always retracts toward the actual adhesion sites. The ectoplasm is either pulled only forwards toward the frontal attachment, or only backwards toward the attached tail, or simultaneously forwards and backwards toward the middle attachment zone. There is no difference in the pattern of ectoplasm retraction in either direction, although traditionally they were considered as separate phenomena and described respectively as tail retraction and fountain movement.

This last statement is further supported by the longitudinal velocity profiles of ectoplasmic granules in monotactic amoebae migrating on the surface of glass (Fig. 2 B). The velocity of ectoplasmic retraction, independently of its direction, is always increasing from the attachment zone up to the free distal ends, in a linear way. It indicates that the ectoplasm uniformly shortens along the cylinder as well in the tail region as in the so-called fountain zone. The shifting effects are therefore summarized with the growing distance from the attachment sites. Consistently with that observation, the maximal velocity of ectoplasm retraction which may be reached at any free body end depends on the length of the unattached segment of cylinder, being slow when it is short, intermediate when about a half of the ectoplasmic tube is free, and the highest when the whole tube is unattached except its opposite end. There is no significant difference, neither in the maximal velocity values nor in the profile slopes, when the forward movement of the posterior ectoplasm is compared to the backward movement of the ectoplasmic walls in the frontal fountain zone.

In polytactic individuals (Grębecki 1985), which adhere very strongly to the glass surface, the major part of the ectoplasm is stationary and the retraction appears only in the tail. There are no conditions for the backward retraction of frontal ectoplasm, and therefore the fountain phenomenon is absent. But in the majority of individuals the young advancing pseudopodia are not attached to the substrate from the very beginning, and at the first phase of their development are free. Their ectoplasmic tubes are then retracted toward the attached body regions and small fountains are recorded. The backward movement of ectoplasmic inclusions is then also revealed by the frame-by-frame film analysis (Pl. II 3). As in the monotactic amoebae, those ectoplasmic markers, which occupy more distal positions, move faster back. The retraction is steady and does not change its character, when the formerly extending pseudopodium begins to retreat. It confirms that the

retraction of the ectoplasmic cytoskeleton from the withdrawing cell regions and from the advancing ones, are not two separate phenomena, but just one integrated continuous process.

## Ectoplasm Retraction Under Deficient Attachment Conditions

The massive bulk withdrawal of the whole anterior part of the ectoplasmic tube system, together with the corresponding elements of the outer cell contour, are easily observed in polytactic amoebae after putting them in experimental situations making a prompt attachment of their fronts impossible (Grębecki 1985).

When the contact with glass surface is restricted, but not completely eliminated, by a thin and partly diluted methylcellulose layer, the polytactic amoebae usually develop the adhesion sites only at their middle body zones. The frame-by-frame contour analysis (Fig. 3 B) demonstrates that in such circumstances the whole anterior cell part (except the endoplasm which as usually flows forward) is withdrawn, like the tail region, toward the stationary central zone. The ectoplasmic cylinders of lateral pseudopodia are not simply retracting along their own axes, but they are simultaneously drawn centripetally from both body poles along the principal motor axis of the whole cell.

The backward movement of the retracting ectoplasmic gel layer, which arises in this experiment in the frontal region, may be further reinforced by activating the anterior cell part by the shade (Pl. II 4). The locomotion becomes then completely inefficient, because the intense inflow of the endoplasmic material into the shaded zone is fully counterbalanced by massive retraction of the whole ectoplasmic structure out of it.

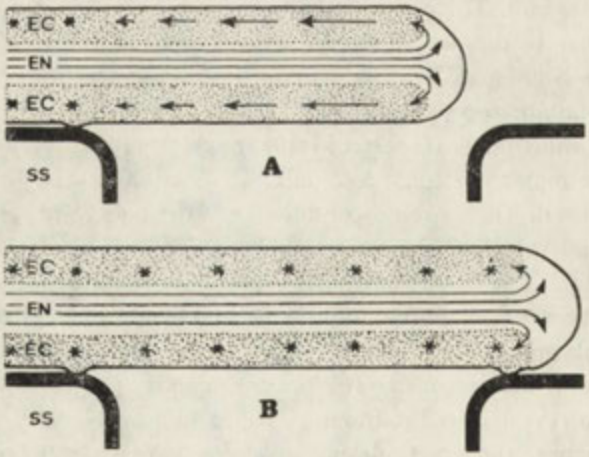


Fig. 4. Scheme of a pseudopodium extending through a ditch in the substrate (A) and reaching its opposite side (B); EC — ectoplasm, EN — endoplasm, SS — solid substratum, arrows and asterisks — as in Fig. 1; after Grębecki (1985)

Polytactic amoebae were also made to migrate on a hanging nylon tissue network, or guided by a strip of shade across a ditch in the bottom of the test chamber. As schematically shown in Fig. 4, in both situations the peripheral cylinders of pseudopodia behave differently, when they are crossing the break between the two solid substrates, and immediately after reaching the opposite border. When the advancing front remains still unattached, the ectoplasm moves backwards and the fountain is manifested. It disappears as soon as the front can re-establish an attachment point on the other side of the gap.

The unattached pseudopodia were also induced on the upper sides of polytactic individuals and guided straight upward by local application of shade (Pl. II 5). When they grew long enough, the bulk backward movement of ectoplasmic inclusions and withdrawal of characteristic elements of the cell contour could be easily observed in them, though the axial endoplasm was still flowing forwards into the shaded distal ends. The experiment clearly demonstrated that: (1) the ectoplasmic layer and the pseudopodium outer contour move strictly together, (2) the speed of retraction gets higher in more distal segments, and (3) the distance between the retracted markers decreases with time. It suggests again that the whole peripheral layer of an unattached pseudopodium is contracting, and the retraction effects are summarized from its basis up to its tip.

When the polytactic amoebae are suddenly exposed to some strong non-directional stimuli (e.g., mechanical shocks), they temporarily assume the heterotactic form (Pl. I 1 b). They lose any motor polarity. From the irregularly rounded main cell body many extremely long pseudopodia protrude radially and are alternately extended and withdrawn. If they grow without adhering to the substrate, or are prevented from doing that, they display prominent fountain movement. Their whole ectoplasmic cylinders regularly and quickly retract from the pseudopodial tips toward their basal regions, that is toward the main cell body, where certainly the centre of mass is located. One should stress the lack of a significant difference in the pattern of ectoplasm retraction between the advancing and retreating heterotactic pseudopodia.

This last observation is further confirmed by the control of vigorous fountains at the tips of heterotactic pseudopodia at their maximal extension stage (Fig. 5). Such a pseudopodium is unable to progress any more, not as result of cessation of the intracellular streaming, but because the cytoplasm input and output are nearly balanced in the fountain zone. Sometimes the balance becomes even negative, i.e., more material is retracted back in the ectoplasmic form than flowing in with the endoplasmic stream. As a result the tip retrogrades, and such pseudopodium is withdrawing in respect to the outer reference points, though it should be qualified as advancing in regard to the intracellular motor mechanism.

The huge heterotactic pseudopodia extended without attachment provide an excellent subject to study the longitudinal velocity profiles of retraction of the ectoplasmic tube (Fig. 6). The profiles were plotted in the same way as before for the

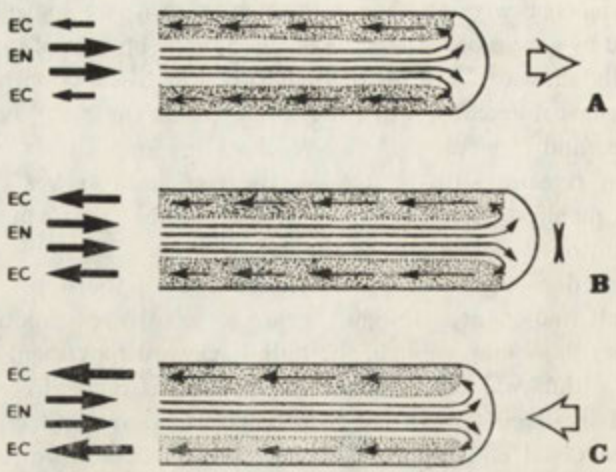


Fig. 5. Scheme of the fountain movement in the tip of a maximally extended pseudopodium of heterotactic type; the black arrows on the left indicate the balance of the inflow of endoplasm and the retraction of ectoplasm, which may be positive (A), null (B) or negative (C); all other symbols as in Fig. 4; after Grębecki (1985)

monotactic amoebae (cf. Fig. 2). They clearly demonstrate that the velocity of backward movement in the ectoplasmic arm of the fountain increases linearly from the basal part of the pseudopodium up to its frontal tip. The slope of the profile does not change when the pseudopodium is growing longer, but the absolute velocity values spectacularly increase. It corroborates well the view that the peripheral ectoplasmic arm of the fountain contracts along its whole length, and the retraction effects are summarized from the pseudopodial basis up to its free distal end.

## Movements of and on the Cell Surface

Many observations prove that the ectoplasmic cylinders of lateral pseudopodia do not only retract along their own axes, but may be simultaneously transported backwards or forwards according to the movements of the ectoplasm along the principal motor axis of the whole cell. Other elements complicating the cell profile behave in the same manner. It was found that their position relative to the neighbour internal markers inside the ectoplasm does not change, what demonstrates that the ectoplasmic cylinder and the outer cell contour move strictly together (Grębecki 1984, 1985).

It opens the question how the cell surface itself and the extracellular particles adjoining it, behave in respect to the intracellular ectoplasmic movements. It was recently demonstrated (Grębecki 1986) that the movement on the surface of amoeba is bidirectional, and has the anterograde and retrograde component. The

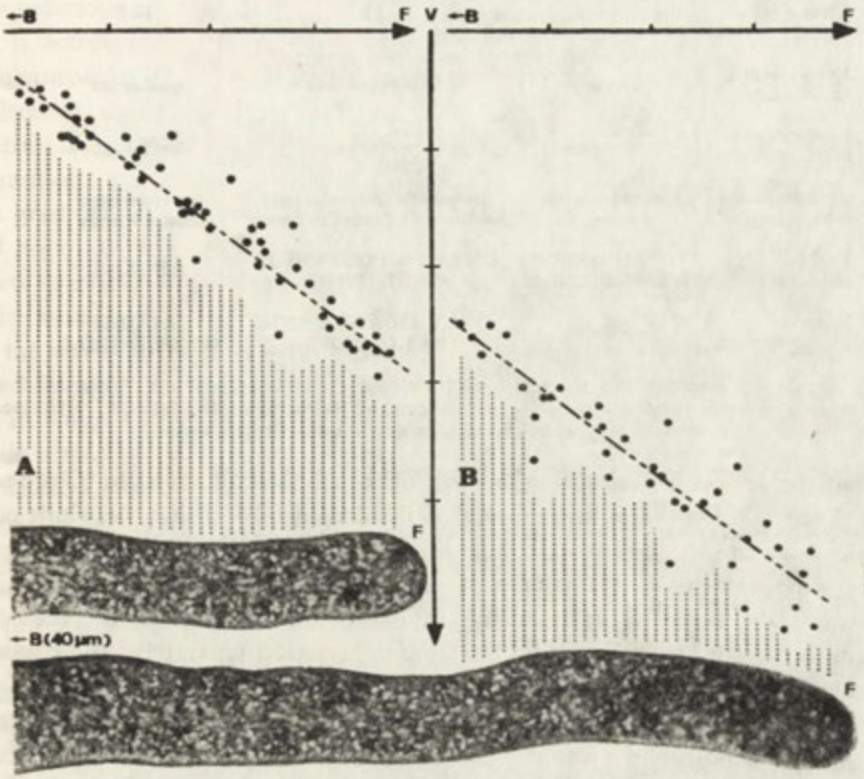


Fig. 6. Two successive velocity profiles in the same heterotactic pseudopodium, recorded at the interval of 30 s (between A and B); the calibration of basis-front (B–F) axis is spaced at 50 μm and the velocity (V) axis at 2 μm/s; after Grębecki (1985)

particles which are not firmly attached to the membrane move forwards, which reflects the general forward flow of the fluid fraction of the surface material, completely independent of the ectoplasmic movements. Simultaneously, however, those particles which are kept on the cell surface by adhesion, precisely follow all the centripetal ectoplasmic movements, as described in this article: forward with the withdrawing tail but backward in the fountain zone. The externally adhering particles and the internal ectoplasmic inclusions, on the both opposite sides of the membrane, move strictly together. This indicates that their adhesion sites are anchored to the cortical layer of microfilaments and hauled by them, exactly as the ligand-receptor complexes during the process of capping in many tissue cells.

## Some General Conclusions

The diagram (Fig. 7) summarizes the data on the direction and extent of ectoplasmic movements, and consequently about the different expression of the tail retraction and fountain phenomena, as depending on the cyclic changes of po-

| Phase | I | II | III |
|---|---|---|---|
| Position of attachment | anterior | intermediate | posterior |
| Locomotion efficiency | maximal | moderate | inefficient |
| Ectoplasmic movement | everywhere forwards | forwards from the tail backwards from the front | everywhere backwards |
| Tail retraction | ALONG WHOLE CELL | ONLY IN POSTERIOR CELL PART | ABSENT |
| Fountain phenomenon | ABSENT | ONLY IN ANTERIOR CELL PART | ALONG WHOLE CELL |

Fig. 7. A diagram summarizing the relations between the changing position of the cell-to-substrate attachment zone and the resulting movements of the ectoplasmic cylinder, with special emphasis on the tail retraction and fountain phenomena

sition of the adhesion sites during locomotion of monotactic amoebae (Grębecki 1984). Theoretically, the most important is the demonstration that the whole ectoplasmic tube may be pulled in either direction, as well forwards as backwards, in the same amoeba in the course of uninterrupted unidirectional locomotion. That cannot be logically explained by any one of the two theories of polar contraction, neither by the tail nor by the front contraction separately. The common feature of these two extreme situations is the movement from a free body pole to the temporarily attached one. If so, during the whole intermediate period of attachment by the middle body regions, the simultaneous forward movement of ectoplasm from behind (tail retraction) and its backward movement from the front (fountain phenomenon), appear as an obvious necessity. The only common denominator is found in the principle that the whole ectoplasmic layer is centripetally retracting toward the actual adhesion sites.

The retraction of ectoplasmic cylinder toward the adhesion sites offers a plausible explanation of mechanism of the fountain phenomenon and a coherent definition of conditions of its manifestation. Our results prove that Allen (1961 a) was perfectly right, when so strongly emphasized that the lack of attachment in the whole cell or in an enough important cell part is the real necessary condition of manifestation of a complete or incomplete fountain. His thesis may be now more specifically formulated: the fountain always arises between the unattached front and the nearest attachment point behind its manifestation zone. Therefore the fountain is spread over the whole cell length when amoeba is attached by the posterior body end or not attached at all, confined to the anterior cell part when the position of the attachment zone is intermediate, and totally absent when the attachment is localized at the front.

But we cannot agree with Allen (1961 a, b) that the axial endoplasmic arm of the fountain is active, being a part of the frontal contraction-pulling mechanism. The centripetal retraction of the whole cytoskeletal layer toward the adhesion

zone indicates, on the contrary, that the peripheral ectoplasmic arm of the fountain is active and moves by self-retraction toward the nearest attachment point. Simultaneously, the endoplasm flows axially forwards, according to the pressure mechanism described before. Both movements together compose the fountain pattern. It appears therefore that in fact the fountain is a hybrid phenomenon, because one of its arms is driven by the traction forces and the other by the pressure gradient.

I hope that the generalized cortical contraction theory, though originally conceived to resolve contradictions in interpretation of the endoplasmic flow aspect of the amoeboid movement, proved to offer also a good starting point to approach the ectoplasmic traction aspects of it. This second aspect is largely underestimated in giant amoebae, though recognized as essential in many other *Sarcodina* and in some tissue cells. The necessity to transport decomposed elements of the motile apparatus forwards by the endoplasmic stream is, on the contrary, underestimated by the students of other forms of amoeboid movement. An artificial hiatus has been created, which led to some reticence in recognizing the basic common features in the motor behaviour of free living amoebae and other crawling cells. It is my feeling that both aspects, as well the pressure as the traction mechanisms, are primarily involved in the basic principles of amoeboid movement. Their respective share may be different in various cells because of a variety of the secondary restricting factors. Among such factors I would pay special attention to the topography and dynamics of cell attachment to the substrate.

## REFERENCES

Abercrombie M. 1980: The crawling movement of metazoan cells. Proc. Roy. Soc. London B, 207, 129–147.

Allen R. D. 1961 a: A new theory of ameboid movement and endoplasmic streaming. Exp. Cell Res. (Suppl.), 8, 17–31.

Allen R. D. 1961 b: Ameboid movement. In: The Cell (J. Brachet and A. E. Mirsky eds.) Academic Press, New York and London, Vol. II, p. 135–216.

Allen R. D. 1968: Differences of a fundamental nature among several types of amoeboid movement. Symp. Soc. Exp. Biol., 22, 151–168.

Bovee E. C. 1964: Morphological differences among pseudopodia of various small amoebae and their functional significance. In: Primitive Motile Systems in Cell Biology (R. D. Allen and Kamiya N. eds.) Academic Press, New York and London, 189–219.

Grębecki A. 1976: Co-axial motion of the semi-rigid cell frame in *Amoeba proteus*. Acta Protozool., 15, 221–248.

Grębecki A. 1981: Effects of localized photic stimulation on amoeboid movement and their theoretical implications. Eur. J. Cell Biol., 24, 163–175.

Grębecki A. 1982 a: Études expérimentales sur la localisation des fonctions motrices chez les amibes. Année Biol., 21, 275–306.

Grębecki A. 1982 b: Supramolecular aspects of amoeboid movement. In: Progress in Protozoology. Proc. VI Int. Congr. Protozool., Part I, 117–130.

Grębecki A. 1984: Relative motion in *Amoeba proteus* in respect to the adhesion sites. I. Behaviour of the monotactic forms and the mechanism of fountain phenomenon. Protoplasma, 123, 116–134.

Grębecki A. 1985: Relative motion in *Amoeba proteus* in respect to the adhesion sites. II. Ectoplasmic and surface movements in polytactic and heterotactic amoebae. Protoplasma, 127, 31–45.

Grębecki A. 1986: Two-directional pattern of movements on the cell surface of *Amoeba proteus*. J. Cell Sci., 83, 23–35.
Jahn T. L. 1964: Relative motion in *Amoeba proteus*. In: Primitive Motile Systems in Cell Biology (R. D. Allen and N. Kamiya eds.) Academic Press, New York and London, p. 279–302.
Käppner W. 1961: Bewegungsphysiologische Untersuchungen and der Amöbe *Chaos chaos* L. I. Der Einfluss des pH des Mediums auf das Bewegungsphysiologische Verhalten von *Chaos chaos* L. Protoplasma, 53, 81–105.
Klein H. P. and Stockem W. 1979: Pinocytosis and locomotion of amoebae. XII. Dynamics and motive force generation during induced pinocytosis in *Amoeba proteus*. Cell Tissue Res., 197, 263–279.
Mast S. O. 1926: Structure, movement, locomotion and stimulation in *Amoeba*. J. Morphol., 41, 347–425.
Pollard T. D. 1984: Actin-binding protein evolution. Nature, 312, 404.
Rinaldi R. A. and Jahn T. L. 1963: On the mechanism of ameboid movement. J. Protozool., 10, 344–357.
Seravin L. N. 1966 a: Monopodial forms of *Amoeba proteus*. (in Russian). Dokl. Akad. Nauk SSSR, 166, 1472–1475.
Seravin L. N. 1966 b: Ameboid locomotion. I. Arrest and resumption of the ameboid locomotion under some experimental conditions (in Russian with English summary). Zool. Zh., 45, 334–341.
Stockem W., Hoffmann H. U. and Gawlitta W. 1982: Spatial organization and fine structure of the cortical filament layer in normal locomoting *Amoeba proteus*. Cell Tissue Res., 221, 505–519.
Stockem W., Hoffmann H. U. and Gruber B. 1983 a: Dynamics of the cytoskeleton in *Amoeba proteus*. I. Redistribution of microinjected fluorescein-labeled actin during locomotion, immobilization and phagocytosis. Cell Tissue Res., 232, 79–96.
Stockem W., Naib-Majani W., Wohlfarth-Bottermann K. E., Osborn M. and Weber K. 1983 b: Pinocytosis and locomotion of amoebae. XIX. Immunocytochemical demonstration of actin and myosin in *Amoeba proteus*. Eur. J. Cell Biol., 29, 171–178.
Stockem W., Wohlfarth-Bottermann K. E. and Haberey M. 1969: Pinocytose und Bewegung von Amöben. V. Konturveränderungen und Faltungsgrad der Zelloberfläche von *Amoeba proteus*. Cytobiologie, 1, 37–57.
Taylor D. L. and Condeelis J. S. 1979: Cytoplasmic structure and contractility in ameboid cells. Int. Rev. Cytol., 56, 57–144.
Taylor D. L., Hellewell S. B., Virgin H. V. and Heiple J. 1979: The solation-contraction coupling hypothesis of cell movement. In: Cell Motility: Molecules and Organization (S. Hatano, H. Ishikawa and H. Sato eds.) University of Tokyo Press, Tokyo, p. 363–367.
Taylor D. L. and Fechheimer M. 1982: Cytoplasmic structure and contractility: the solation-contraction coupling hypothesis. Philos. Trans. R. Soc. Lond., Ser. B, 299, 185–197.
Wehland J., Weber K., Gawlitta W. and Stockem W. 1979: Effects of the actin-binding protein DNAase I on cytoplasmic streaming and ultrastructure of *Amoeba proteus*. An attempt to explain amoeboid movement. Cell Tissue Res., 199, 353–372.

## EXPLANATION OF PLATES I–II

1: Four locomotory types of *Amoeba proteus*: polytactic (a), heterotactic (b), orthotactic (c) and monotactic (d)
2: Pictographic records (10 s exposure time) of the ectoplasmic movements in monotactic amoebae adhering to the substratum in a narrow central zone (a), with a very large attachment zone beginning at the front (b), after rebuilding a new unattached frontal segment (c) and attached only by the tail (d); note the centripetal retraction of ectoplasm (arrows) toward the adhesion sites and its stationary condition (asterisks) in the attachment zones: after Grębecki (1984)
3: Retraction of ectoplasmic granules (shown by markers numbered 1–5) in the unattached tip of a frontal pseudopodium of polytactic type; note the steady character of retraction in the advancing phase (a–b) and during withdrawal of pseudopodium (b–c); after Grębecki (1985)
4: Backward motion of the whole cell contour (note the position of markers numbered 1–3 and the front F) of a very weekly attached polytactic specimen stimulated by a zone of shade; from Grębecki (1985)
5: Pseudopodium stimulated by shade to extend straight upwards (a) and the withdrawal of its ectoplasmic cylinder (shown in b–c by the markers 1–4); after Grębecki (1985)

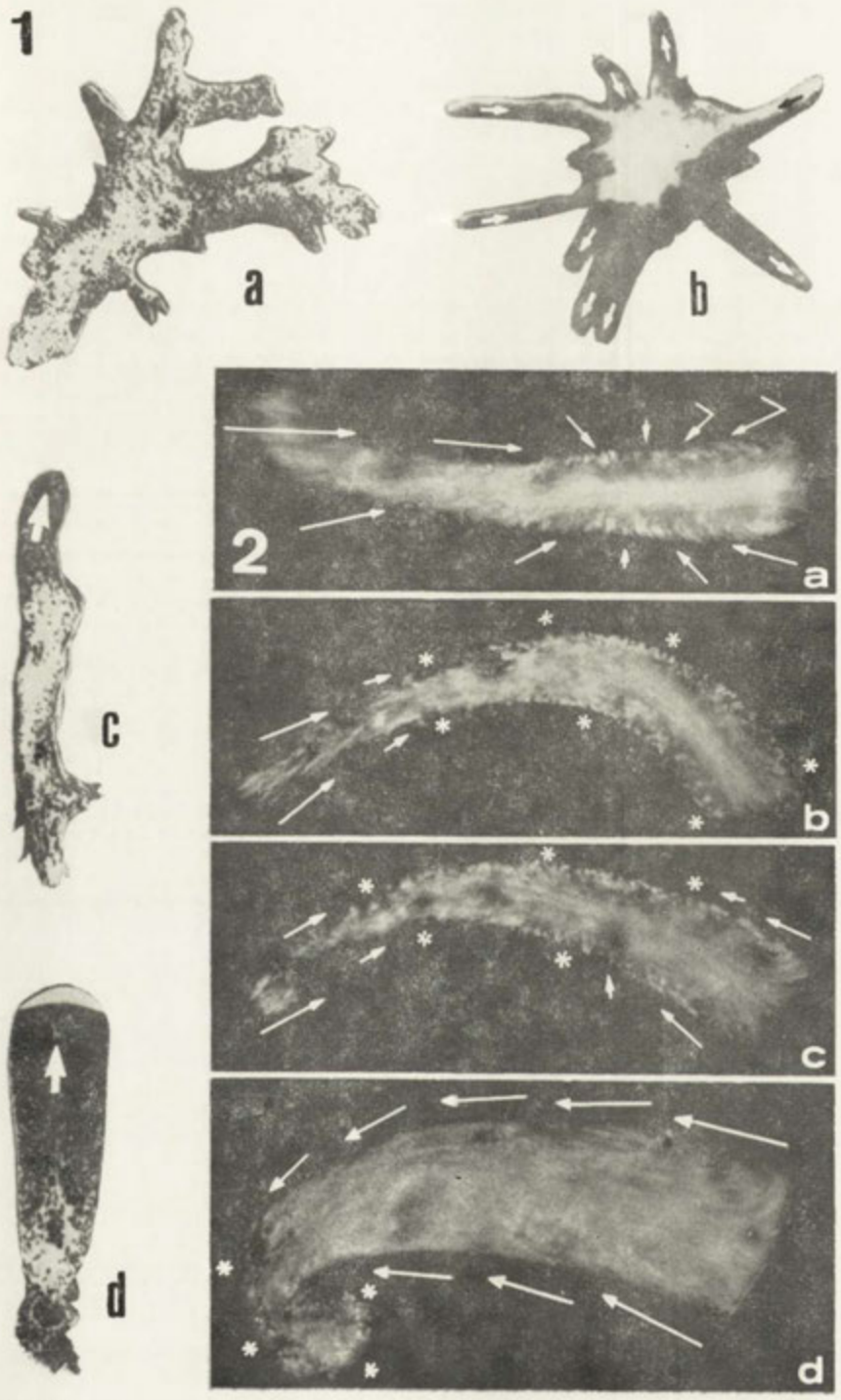


A. Grębecki auctor phot.

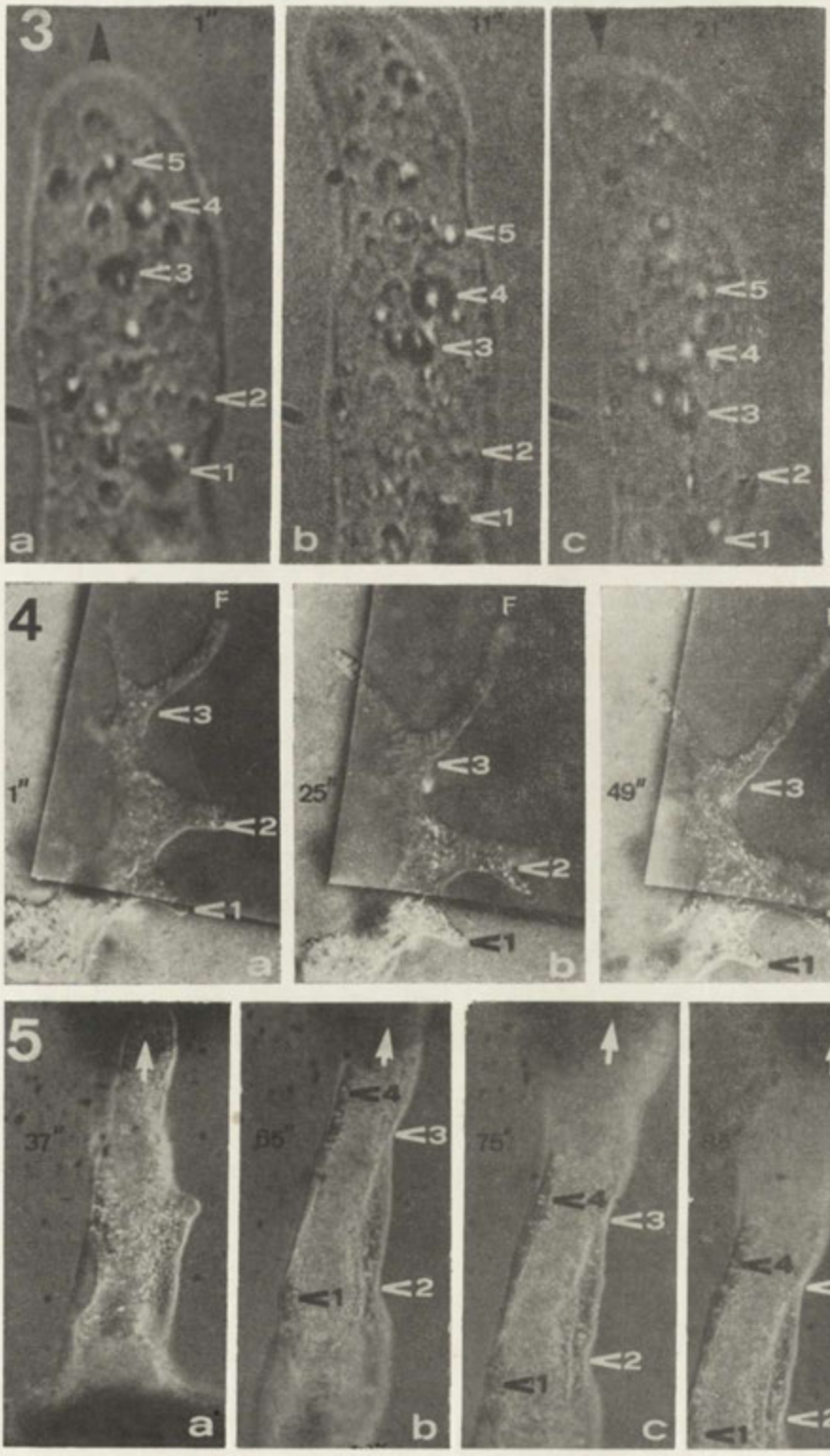


A. Grębecki auctor phot.

ACTA PROTOZOOLOGICA
Vol. 25, No. 3, pp. 269–278 (1986)

# Molecular Biology of Cytoskeletal Proteins in *Naegleria*[1]

Chandler FULTON, Elaine Y. LAI and Stephen P. REMILLARD.

Department of Biology, Brandeis University, Waltham, Massachusetts 02254, U.S.A.

*Received on* 5th October 1985

*Synopsis. Naegleria gruberi*, a common organism of provocative phylogenetic status, undergoes a remarkable differentiation from amoebae with an actin-based motility system to flagellates with a tubulin-based system. The process appears to be regulated, in part, by intracellular free calcium ions, which suggests a possible role for the calcium-modulating protein calmodulin. Actin, the major protein of amoebae, is selectively not synthesized during the hour-long differentiation, and its mRNA rapidly disappears. In contrast, the two subunits of flagellar tubulin and two calmodulins are synthesized *de novo* during differentiation, and the mRNAs for these polypeptides appear, and subsequently disappear, concurrently. We have partially characterized these proteins. Important attributes of the actin, calmodulin, and tubulin have been conserved, but the *Naegleria* proteins show unusual features, especially the absence of 3-methylhistidine from actin and the presence of two differentiation-specific calmodulins in flagellates, one located in flagella and the other in the cell bodies. Our primary interest is the regulation of the synthesis and utilization of these proteins during cell differentiation, and we believe that studying the expression of each gene or gene family in relation to the other selected genes may reveal features that coordinately regulate transcription, mRNA stability, or intracellular localization.

We, and many others, wish to understand the molecular basis of cell differentiation. The choice of a cell differentiation determines which genes and gene products become candidates for study. Our choice of the quick-change act of *Naegleria gruberi* has led us to study three fundamental cytoskeletal proteins — actin, calmodulin, and tubulin — and their genes.

All eukaryotic cells, or at least representatives of all major groups of eukaryotes, share numerous attributes; these shared characteristics indicate a monophyletic origin for eukaryotes at least $1.4 \times 10^9$ years ago. Certain proteins, and their functions, are included in this eukaryotic fingerprint. These proteins include tubulin, a heterodimer of α- and β-tubulin subunits, used for mitosis as well as for the "9+2" axoneme of flagella and cilia and their associated 9-triplet centriole-like basal bodies. They also include actin and other components of the cytoplasmic motility system. Another of these proteins is calmodulin, which allows calcium

[1] Lecture presented by C. Fulton on 25th June 1985 at the Symposium "Relationship between Cytoskeleton and Motility", held during the Seventh International Congress of Protozoology in Nairobi, Kenya.

to regulate many cellular functions. The functions of actin, calmodulin, and tubulin, as well as other fundamental proteins, are so crucial, and their interactions so numerous, that they have been conserved from the ancestral eukaryote to the present.

*Naegleria.* We chose *Naegleria gruberi* as our "model system" to study the regulation of events during cell differentiation and morphogenesis (Fulton 1977 a). *Naegleria* can alternate between two forms, amoeba and flagellate. Some biologists have suggested that because *Naegleria* displays the attributes of two classes of protozoa it is a primitive eukaryote. Perhaps, but *Naegleria* is also a highly evolved organism, probably with more experience (in generations) and success (in numbers, if not biomass) than *Homo sapiens*. Like most unicellular eukaryotes, *Naegleria's* phylogenetic position is uncertain and provocative. To be specific, we do not know how *Naegleria* is related to any other organisms, even other amoebae and flagellates, with the exception of some closely related organisms, such as *Tetramitus rostratus* (Fulton 1970). In its properties, *Naegleria* links amoebae and flagellates (two classes) in the jumbled phylum of *Protozoa*, and jumps across a kingdom by sharing properties with the true slime molds (Fulton 1970).

*Naegleria*, like other organisms, is wonderful and unusual. It is one of the most common organisms on Earth, from the South Pole to the North, in soil and freshwater. Some of its close relatives, such as *N. fowleri*, are opportunistic human pathogens (John 1982), but *N. gruberi* appears to be harmless. *Naegleria* reproduces as an amoeba about 15 μm in diameter. It can reproduce very rapidly for a eukaryote, with doubling times as short as 1.7 hours. The amoebae are haploid and have a small genome, features that are very convenient for the study of gene structure and function. The unique feature of these amoebae is their ability, when transferred from a growth environment to a nutrient-free aqueous environment, to undergo a 1:1 conversion to lively, streamlined swimming flagellates. The flagellates are temporary, and after a time that can vary from seconds to days, depending on the environmental conditions, they revert to amoebae again.

The cells change from amoebae with an actin-based motility system to flagellates with a tubulin-based system (Fulton 1977 b). Thus they alternate between two of the major motility forms used by eukaryotic cells. In addition to the microtubules of the two flagella and basal bodies, the flagellates have a cage of microtubules just beneath the cell surface (Fulton 1977 b, Walsh 1984). The tubulin-based system is more impressive than the actin-based system in the sense that flagellates swim about one-hundred times as fast as amoebae walk. The phenotypic conversion appears to be regulated, in part, by intracellular free calcium ions (Fulton 1977 b), which in turn suggests a possible role for calmodulin.

The differentiation of amoebae to flagellates can be made to occur rapidly, synchronously, and temporally reproducibly. We usually induce differentiation by transferring amoebae from their growth environment to nonnutrient buffer at time zero, and incubating the cells in suspension at 25°C, although several other procedures can be used to initiate differentiation (Fulton 1977 a). Various mor-

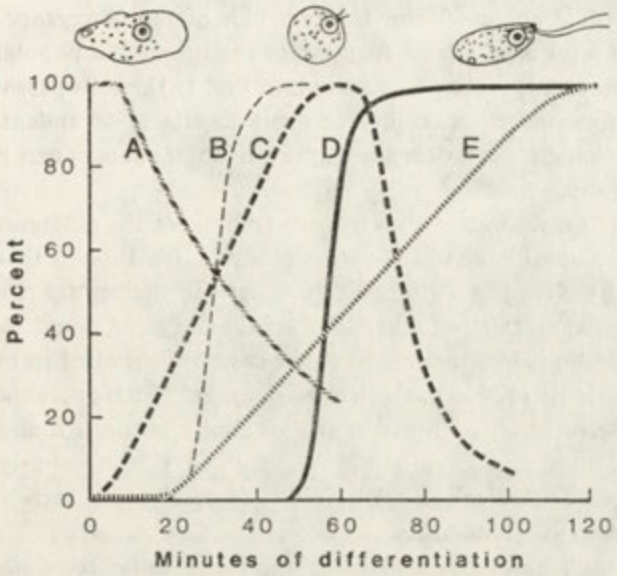


Fig. 1. Temporally programmed events during *Naegleria* differentiation. A — Decrease in abundance of actin mRNA. B — Transition event after which cells have acquired the ability to form flagella without further RNA synthesis. C — Abundance of mRNAs for flagellar α-tubulin, flagellar β-tubulin, and two calmodulins; also the *in vivo* rate of flagellar tubulin synthesis. D — Time course of appearance of cells with flagella. E — Accumulation of flagellar tubulin antigen. Curves B and D represent quantal changes in cell phenotype, whereas the other curves measure quantitative changes in amount or rate. This composite graph is compiled from experiments published elsewhere (Fulton and Walsh 1980, Fulton et al. 1986 a, Kowit and Fulton 1974 b, Lai et al. 1979 a, Sussman et al. 1984 b) as well as work in progress

phological changes of the differentiation can be quantitated by counting the percentage of particular phenotypes among fixed cells. In succession, amoeboid movement becomes latent, the cells round up to spheres, form flagella, and then elongate to the streamlined flagellate shape. Under the conditions of differentiation we use for most of our work, half of the cells form flagella about 60 min after the environmental shift. Figure 1, curve D, shows the time-course of appearance of cells with flagella, one of the many quantal changes in phenotype that can be measured. The reproducible synchronous differentiation allows "time slices" through the process, an important advantage that is difficult with many systems used to study cell differentiation.

Many events during differentiation have been placed on a timetable (Fulton 1977 a, b, Fulton and Walsh 1980, Larson and Dingle 1981, Walsh 1984). As one example, we have used inhibitors of RNA and protein synthesis to map the requirements for RNA and protein synthesis during differentiation (Fulton and Walsh 1980). Actinomycin D, e.g., selectively arrests RNA synthesis if added at any time during differentiation. If added early, such as before 20 min in Fig. 1, the cells remain amoebae and show none of the morphological changes associated with differentiation. If added later, such as at 40 min, the cells proceed to make

flagella on schedule about 20 min later. A plot of the percentage of cells subsequently able to form flagella as a function of the time when populations are transferred to actinomycin D is shown as curve B of Fig. 1. The cells pass through a transition event, before which the ability to form flagella is dependent on RNA synthesis and after which it is independent. Such quantal changes can be mapped with temporal precision.

Tubulin. When we sought to bring our analysis of the differentiation to a molecular level, a natural component to examine was the tubulin that makes up the microtubules of the flagella — the outer doublet and the central pair microtubules. We isolated and characterized outer doublet tubulin, and found that in all tested respects this tubulin is like the tubulins that have been studied in other eukaryotes (Kowit and Fulton 1974 a, P. A. Simpson and C. Fulton, unpublished observations). To our surprise, we found that the tubulin subunits found in the flagella are synthesized during differentiation. We showed this rigorously using isotope dilution experiments (Kowit and Fulton 1974 b, Fulton and Simpson 1976, Simpson et al., in preparation).

Polyclonal rabbit antibodies to outer doublet tubulin recognize the α and β subunits of both outer doublet and central pair tubulin (Kowit and Fulton 1974 a, b, Lai et al. 1979 a, C. Fulton, E. Y. Lai and P. A. Simpson, unpublished observations). These antibodies have not recognized any other tubulin tested, including mitotic tubulin in extracts of *Naegleria* amoebae or purified flagellar tubulins from several other organisms. This unusual specificity allowed us to measure the amount of flagellar tubulin antigen in cells by radioimmunoassay (Fig. 1, curve E). Amoebae have, at most, 3% as much flagellar tubulin antigen as flagellates. The amount of antigen begins to increase beginning at about 20 min of differentiation and reaches a maximum about the time the flagellates have formed full-length flagella (Kowit and Fulton 1974 b).

Amoebae have more than enough tubulin to build flagella; they use this tubulin for mitosis (Kowit and Fulton 1974 b). Yet they make new, antigenically different tubulin for the flagella. These and other observations led us to propose the multitubulin hypothesis, which suggests that cells may use different tubulins, made by different genes, for different functions (Fulton and Simpson 1976). There is now abundant evidence that many organisms, indeed all eukaryotes examined so far except yeast, have and express multiple tubulin genes (reviewed by Cleveland 1983). There still is no definitive evidence whether or not the products of different tubulin genes are used for distinct microtubular organelles; we hope that such evidence will be forthcoming soon.

Our next step was to move backward toward gene expression by asking whether flagellar tubulin mRNA increased in abundance during differentiation. RNA was extracted from cells at successive times during differentiation and translated in the wheat-germ cell-free system. Translation products with the electrophoretic mobility of the α and β subunits of tubulin markedly changed in abundance during

differentiation, at first increasing and then decreasing (Lai et al. 1979 a). We characterized these products, using the translation products of RNA isolated at 60 min of differentiation when these products were most abundant, and showed that these products were indeed flagellar tubulin. In addition, these products were recognized by the antibodies to flagellar tubulin, which permitted us to quantitatively immunoprecipitate flagellar tubulin subunits from translation products. We used cell-free translation followed by immunoprecipitation to quantitate the amount of translatable flagellar tubulin mRNA present at various times during differentiation. Translatable flagellar tubulin mRNA is not detected in amoebae. As is shown in Fig. 1, curve C, it rises to maximum abundance at about 60 min and then declines. The rate of *in vivo* flagellar tubulin synthesis, measured by pulse-chase experiments, follows precisely the same curve (i.e., curve C of Fig. 1). Flagellar tubulin synthesis in these cells clearly is regulated by the abundance of translatable flagellar tubulin mRNA. The simplest interpretation is that flagellar tubulin synthesis during differentiation is regulated by the programmed synthesis, and subsequent degradation, of flagellar tubulin mRNA. This interpretation is supported by experiments using actinomycin D which, added at the beginning of differentiation, prevents both differentiation and the accumulation of flagellar tubulin mRNA (Lai et al. 1979 b). If actinomycin is added during the time when translatable flagellar tubulin mRNA is increasing, such as at 20 min in Fig. 1, further accumulation of this mRNA is arrested.

Calmodulin. If calmodulin plays a role in this differentiation, the synthesis of calmodulin might change during the process. In order to test this possibility, we asked whether we could detect changes in the abundance of translatable mRNA for a calmodulin-like calcium-binding protein during differentiation. We developed a simple assay to quantitate such an mRNA, and obtained a surprising result. Not one but two calmodulin-like calcium-binding proteins are synthesized by RNA from differentiating cells, such as RNA isolated at 60 min (Fulton and Lai 1980, Fulton et al. 1986 a). These polypeptides, synthesized *in vitro*, show the characteristic calcium-dependent mobility shift of the calmodulin family of proteins. The two polypeptides differ in apparent molecular weight. These polypeptides are absent in the translation products of RNA from amebae.

We have characterized the two calcium-binding proteins of flagellates (Fulton et al. 1986 a). Both are typical calmodulins by several criteria. The main polypeptide synthesized is localized in the flagella whereas the minor one is found in the cell bodies. They both are smaller than vertebrate calmodulins, as are the single calmodulins of several other eukaryotic microorganisms, including *Dictyostelium* and *Tetrahymena*. Further evidence that the two *Naegleria* proteins are calmodulins is summarized in Table 1. Both bind to phenyl-Sepharose columns, both give calcium-dependent activation of bovine heart phosphodiesterase, and both react with antibodies to rat testis calmodulin. The finding of two calmodulins is unusual. We have not yet been able to isolate calmodulin from *Naegleria* amoebae,

Table 1

Two Calmodulins of *Naegleria* Flagellates (from Fulton et al. 1986 a)

| | Vertebrate calmodulin | CaM-1 | CaM-2 |
|---|---|---|---|
| Location in flagellates | | flagella | cell body |
| $M_W$apparent | 16,800 | 16,000 | 15,300 |
| $Ca^{2+}$-dependent mobility shift on SDS-polyacrylamide gel electrophoresis | + | + | + |
| Bind to phenyl-Sepharose | + | + | + |
| Activate phosphodiesterase | + | + | + |
| React with antibodies to vertebrate calmodulin | + | + | + |

though radioimmunoassay using the antibodies to vertebrate calmodulin indicates that amoebae contain about 20% as much calmodulin as flagellates. The specific localization of the two calmodulins in different parts of the cells is remarkable, and raises questions about how this localization occurs during differentiation.

We measured the time-course of the appearance of translatable mRNA for these two calcium-binding proteins, and found that translatable mRNA for both polypeptides appear and disappear concurrently with those for flagellar tubulin, i.e., curve C of Fig. 1 (Fulton and Lai 1980, Fulton et al. 1986 a). Many proteins are synthesized during differentiation. We have yet to identify most of these proteins, but pulse-chase experiments indicate that they are not all synthesized on the same timetable. Thus we are excited that mRNAs for two sets of unrelated proteins — the flagellar tubulins and the two calcium-binding proteins — appear and disappear simultaneously. The concurrent rise and fall suggests the possibility that these genes are coordinately regulated, and perhaps we may hope even to find common signals for the synthesis and/or decay of their mRNAs.

Actin. Flagellar tubulin and calmodulin are synthesized as programmed events of differentiation. In contrast, synthesis of actin, the major protein of both amoebae and flagellates, is selectively restricted during this process. Isotope dilution experiments indicate that only about 1% of the actin is synthesized *de novo* during differentiation (Simpson et al., in preparation). Examination of translation products of RNA isolated at successive times during differentiation revealed a major translation product directed by RNA from amoebae that disappears selectively as differentiation progresses (Lai et al. 1979 a). This translation product has the electrophoretic mobility of actin. In order to study this product, we purified and characterized *Naegleria* actin (Sussman et al. 1984 a). In important attributes, *Naegleria* actin is like other actins. For example, *Naegleria* actin forms F-actin filaments which decorate with subfragment-1 of rabbit myosin. *Naegleria* actin also activates heterologous myosin $Mg^{2+}$ — ATPase, has an amino acid composition that is very similar to other actins, and in many respects shares the conser-

Table 2

Unusual Features of *Naegleria* Actin (from Sussman et al. 1984 a and Fulton et al. 1986 b)

(1) Three isoforms
(2) Binds DNase I at low affinity
(3) Absence of 3-methylhistidine
(4) Antibodies specific to actin of *Naegleria*

ved features of actins. This actin is, however, unusual in several respects (Table 2). The actins of vertebrates, *Drosophila*, and several other metazoa have several forms that differ in isoelectric point; in vertebrates and *Drosophila* these isoforms are the products of multiple distinct actin genes (reviewed in Firtel 1981). In contrast, in all lower eukaryotes examined to date a single species of actin accounts for at least 95% of the actin. Yet *Naegleria* actin shows three isoforms. Most actins bind to deoxyribonuclease I with high affinity, and elute only with strong denaturants such as 3 M guanidine. *Naegleria* actin binds to DNase I, but elutes at 0.75 M guanidine. At an extreme, actin of *Entamoeba* does not bind to DNase I at all (Gadasi 1982, Meza et al. 1983). All actins characterized previously have a single residue of 3-methylhistidine as residue 73 of the protein. Although the amino acid composition of *Naegleria* actin is very similar to those of other characterized actins, under conditions where we could detect one 3-methylhistidine per 40 histidine residues, we found no 3-methylhistidine. *Naegleria* actin lacks this posttranslationally added residue, or at least has less than one residue per five actin molecules. Reconstruction experiments indicate that 3-methylhistidine is not lost during the purification of *Naegleria* actin; we conclude it is not present in the actin at the time that amoebae are lysed. Finally antibodies to *Naegleria* actin are specific to *Naegleria* actin; they do not recognize even the actins of other amoeboid organisms such as *Acanthamoeba*, *Dictyostelium*, and *Physarum* (Fulton et al. 1986 b). Of these properties, perhaps the most interesting is the absence of 3-methylhistidine, which indicates that at least some of the measured properties of actin, such as polymerization to microfilaments or interaction with myosin, do not reguire the presence of this post-translationally modified residue.

We used the antibodies to *Naegleria* actin to measure the abundance of translatable actin mRNA at successive times during differentiation (Sussman et al. 1984 b). Figure 1, curve A, shows the rapid decrease in abundance of translatable actin mRNA during differentiation. After a lag of about seven minutes, translatable actin mRNA disappeared exponentially with a half-life of about 25 min. The simplest interpretation is that actin gene expression is turned off, and actin mRNA is selectively destroyed, as early events of differentiation. However, these experiments do not indicate whether the actin mRNA is degraded or somehow rendered untranslatable.

From translatable mRNA to gene expression. DNA clones provide the means to continue our dissection of the structure and expression of these gene families in relation to differentiation. Since we are primarily interested in expressed genes, we prepared complementary DNA (cDNA) clones in the vector system developed by Okayama and Berg (1982). We made libraries of cDNA clones prepared both to 0 min RNA, when translatable actin mRNA is most abundant, and to 60 min RNA, when the flagellar tubulin and calmodulin mRNAs are most abundant. From these libraries we have isolated full-length clones to expressed α- and β-tubulin, calmodulin, and actin genes, and using these clones we have isolated comparable clones from a library of genomic *Naegleria* DNA in a bacteriophage lambda vector. We have sequenced the DNA inserts of several of these clones, including representatives of actin, calmodulin, and α-tubulin genes.

It proved easy to select actin cDNA clones from the 0 min library by screening with a chick β-actin cDNA clone prepared by Cleveland et al. (1980). In general the homology of actin DNAs appears to be well preserved over more than $10^9$ years of evolution; we know of no exceptions to this generalization. Our full-length actin cDNA clones have inserts of about 1.4 kb, which is the size of *Naegleria* actin mRNA. The sequences of two actin cDNA clones show some silent nucleotide substitutions but encode the same actin. Since the actin sequence deduced from the DNA sequence was the most substituted actin described to date, in collaboration with J. Vandekerckhove we obtained the sequence of the major actin protein from *Naegleria*. This protein sequence corresponds perfectly to that deduced from DNA sequencing (Remillard, Vandekerckhove, Lai and Fulton, in preparation). One finding of interest is that *Naegleria* actin contains a histidine at residue 73, which indicates that the absence of 3-methyl histidine in *Naegleria* actin is due to some factor other than the absence of a histidine residue at this position.

All these genes are encoded by multigene families. In other organisms, the actin gene family has as few as one member, as in yeast, or as many as 17 or more, as in *Dictyostelium* and humans (reviewed by Firtel 1981). By the same criteria, *Naegleria* has about a dozen actin genes. Both the heterologous chicken β-actin cDNA clone and homologous *Naegleria* cDNA clones recognize the same set of genomic fragments. The situation for tubulin genes is quite different. Heterologous tubulin DNA probes, from organisms ranging from yeast to chicken, show only limited homology to *Naegleria* α- and β-tubulin genes. There are about seven similar but not identical α-tubulin genes in *Naegleria*. At least several of these are expressed. Two of these expressed α-tubulin genes show differences in their restriction maps which are caused by silent nucleotide substitutions, but encode the same protein. The actin genes we have sequenced are more conserved at the DNA level than the α-tubulin genes, but the actin and α-tubulin proteins are comparably conserved. We are still enumerating the β-tubulin and calmodulin genes.

We are excited about the possibility of using the sequences of these conserved eukaryotic genes and of the polypeptides they encode to deduce the phylogenetic

position of *Naegleria* in relation to other eukaryotic microorganisms, as well as to enhance the overall understanding of the structure, function, and evolution of these genes. Our characterization of actin, calmodulin, and α-tubulin, and the sequencing of their genes, indicate that they share many features with those from other eukaryotic cells, but also suggest that they may be among the most different that have been isolated. The divergence suggests, superficially, that *Naegleria* is rather far from the other organisms for which sequences are available. Unlike ciliates, *Naegleria* uses the universal code. Although the sequences of these conserved proteins have diverged, the characteristics of the proteins indicate that important functional properties have been conserved.

Our main interest remains the regulation of the expression of these genes. With the cDNA clones it became possible to directly measure RNA sequence abundance during differentiation. The results of quantitative RNA dot hybridization are shown in Fig. 1. Curve A shows the superimposible results for both translatable and physical actin mRNA. Curve C shows the results for both translatable and physical mRNA for α-tubulin, β-tubulin, and calmodulin. It is evident that the changes in abundance of translatable mRNAs for these polypeptides is directly proportional to the amount of transcripts in the cell. The rapid increases and decreases in abundance of each mRNA is controlled by the relative rates of transcription and decay, parameters still to be measured. The changes in abundance are remarkable. For example, α-tubulin mRNA increases at least 80-fold in 50 min, and then decays with a half-life of less than 10 min — faster even than actin mRNA.

In conclusion, synthesis of a major cell protein, actin, ceases during differentiation, and mRNA encoding this protein disappears rapidly, beginning as one of the earliest known events in the differentiation. Three other gene families, those that encode the two flagellar tubulin subunits and the family that encodes the calmodulins, are expressed concurrently during differentiation. This coexpression raises question about what turns the genes on and off, and about what targets or controls the rapid destruction of the mRNAs. In the case of the flagellar proteins tubulin and calmodulin-1, we are also intrigued about what signals cause their localization in flagella. If Nature and *Naegleria* are willing, we hope to dissect these questions.

## ACKNOWLEDGMENT

This research was supported by grants from NSF and NIH.

## REFERENCES

Cleveland D. W. 1983: The tubulins: from DNA to RNA to protein and back again. Cell, 34, 330–332.

Cleveland D. W., Lopata M. A., MacDonald R. J., Cowan N. J., Rutter W. J. and Kir-

schner M. W. 1980: Number and evolutionary conservation of α- and β-tubulin and cytoplasmic β- and γ-actin genes using specific cloned cDNA probes. Cell, 20, 95–105.
Firtel R. A. 1981: Multigene families encoding actin and tubulin. Cell, 24, 6–7.
Fulton C. 1970: Amebo-flagellates as research partners: The laboratory biology of *Naegleria* and *Tetramitus*. In: Methods in Cell Physiology (D. M. Prescott, ed.), vol. 4, pp. 341–476. Academic Press, New York.
Fulton C. 1977 a: Cell differentiation in *Naegleria gruberi*. Annu. Rev. Microbiol., 31, 597–629.
Fulton C. 1977 b: Intracellular regulation of cell shape and motility in *Naegleria*. First insights and a working hypothesis. J. Supramol. Struct., 6, 13–43.
Fulton C. and Lai E. Y. 1980: Programmed appearance of translatable mRNAs for two calmodulin-like proteins during cell differentiation in *Naegleria*. J. Cell Biol., 87, 282 a.
Fulton C. and Simpson P. A. 1976: Selective synthesis and utilization of flagellar tubulin. The multi-tubulin hypothesis. In: Cell Motility (R. Goldman, T. Pollard and J. Rosenbaum, eds.), pp. 987–1005. Cold Spring Harbor Laboratory, New York.
Fulton C. and Walsh C. 1980: Cell differentiation and flagellar elongation in *Naegleria gruberi*: Dependence on transcription and translation. J. Cell Biol., 85, 346–360.
Fulton C., Cheng K.-L. and Lai E. Y. 1986 a: Two calmodulins in *Naegleria* flagellates: Characterization, intracellular segregation, and programmed regulation of mRNA abundance during differentiation. J. Cell Biol., 102, 1671–1678.
Fulton C., Lai E. Y., Lamoyi E. and Sussman D. J. 1986 b: Antibodies specific to actin. of *Naegleria*. J. Protozool., 33, (in press).
Gadasi H. 1982: Isolated *Entamoeba histolytica* actin does not inhibit DNAse- I activity. Biochem. Biophys. Res. Commun., 104, 158–164.
John D. T. 1982: Primary amebic meningoencephalitis and the biology of *Naegleria fowleri*. Annu. Rev. Microbiol., 36, 101–123.
Kowit J. D. and Fulton C. 1974 a: Purification and properties of flagellar outer doublet tubulin from *Naegleria gruberi* and a radioimmune assay for tubulin. J. Biol. Chem., 249, 3638–3646.
Kowit J. D. and Fulton C. 1974 b: Programmed synthesis of tubulin for the flagella that develop during cell differentiation in *Naegleria gruberi*. Proc. Natl. Acad. Sci. U.S.A., 71, 2877–2881.
Lai E. Y., Walsh C., Wardell D., and Fulton C. 1979 a: Programmed appearance of translatable flagellar tubulin mRNA during cell differentiation in *Naegleria*. Cell, 17, 867–878.
Lai E. Y., Sussman D. J. and Fulton C. 1979 b: The rise and fall of translatable mRNAs for tubulin and actin during cell differentiation in *Naegleria*: Dependence on transcription. J. Cell Biol., 83, 416 a.
Larson D. E. and Dingle A. D. 1981: Development of the flagellar rootlet during *Naegleria* flagellate differentiation. Dev. Biol., 86, 227–235.
Meza I., Sabanero M., Cazares F. and Bryan J. 1983: Isolation and characterization of actin from *Entamoeba histolytica*. J. Biol. Chem., 258, 3936–3941.
Okayama H. and Berg P. 1982: High-efficiency cloning of full-length cDNA. Mol. Cell. Biol., 2, 161–170.
Simpson P. A., Larson D. E., Sellers J. R., Remillard S. P., Dingle A. D. and Fulton C. 1986: Parsimonious synthesis of differentiation-specific proteins in *Naegleria gruberi*. Synthesis of flagellar tubulins and rootlet protein, but not of actin. (in preparation).
Sussman D. J., Sellers J. R., Flicker P., Lai E. Y., Cannon L. E., Szent-Gyorgyi A. G. and Fulton C. 1984 a: Actin of *Naegleria gruberi*. Absence of $N^{\pi}$-methylhistidine. J. Biol. Chem., 259, 7349–7354.
Sussman D. J., Lai Y. E. and Fulton C. 1984 b: Rapid disappearance of translatable actin mRNA during cell differentiation in *Naegleria*. J. Biol. Chem., 259, 7355–7360.
Walsh C. 1984: Synthesis and assembly of the cytoskeleton of *Naegleria gruberi* flagellates. J. Cell Biol., 98, 449–456.

ACTA PROTOZOOLOGICA
Vol. 25, No. 3, pp. 279–284 (1986)

# Polymorphic Assembly States of *Allogromia* Tubulin[1]

Rainer GOLZ and Manfred HAUSER

Lehrstuhl für Zellmorphologie, Ruhr-Universität Bochum, Postfach 102148, D-4630 Bochum 1, Federal Republic of Germany

*Received on* 15 September 1985

*Synopsis.* Indications for the existence of filopodial tubulin in several polymorphic assemblies (microtubules, helically twisted filaments, paracrystals) under natural conditions were obtained by EM-analysis of the reticulopodial network. By means of IIF with monoclonal anti α-tubulin and after transformation experiments with purified ruthenium red, the tubulin nature of helical filaments and paracrystals was confirmed.

The cytoskeleton of the monothalamous foraminifer *Allogromia laticollaris* provides evidence for the co-existence of several assembly forms of the tubulin dimer under regular physiological conditions. *Allogromia* extends slender, rigid filopodia, repeatedly branching and anastomosing with one another, giving finally rise to a continuous reticulopodial network (RPN) showing bidirectionally saltatory particle transport at velocities often more than 10 μm/s. In response to various external stimuli (e.g., exchange of culture medium, temperature shift etc.) a remarkably rapid outgrowth of filopodia leads within short time to a complex RPN measuring often several millimeters in diameter.

Apart from their different spatial organization forms, both types, flat veil-like lamellipodia or rope-like filopodia, reveal the same extraordinary cytoskeleton, composed mainly of microtubules (MTs) and helically twisted filaments (hFs). Less frequently, paracrystals (PCs) and 5 nm filaments are also detectable.

In the following, we confirm by means of IIF-studies with a monoclonal antibody against α-tubulin, that MTs, hFs and PCs represent only different assembly states of the *Allogromia* tubulin.

---

[1] Lecture presented by M. Hauser on 25th June 1985 at the Symposium "Relationship between Cytoskeleton and Motility", held during the Seventh International Congress of Protozoology in Nairobi, Kenya.

## Filopodial Microtubules

As shown previously (Hauser and Schwab 1974, Travis and Allen 1981) the most prominent cytoskeletal elements within the RPN are MTs, arranged predominantly in thick bundles or thinner cables. Within larger filopodia, often multiple bundles occur, running parallel over long distances, repeatedly branching, splaying out and also rejoining. Often groups or even individual MTs diverge from a bundle and contact neighbouring strands (Pl. I 1).

Obviously, the parallel arrangement of Mt-bundles is achieved by short and solid lateral projections crossbridging adjacent MTs. These bridge-like decorations are arranged in a quite regular 20 nm periodicity closely resembling the dynein arrangement of cilia and flagella and are preferably demonstrable in lysed, demembranated filopodia (Pl. I 4, 7). However, in contrast to the axonemal dynein arms, they are not arranged along the entire length of filopodial MTs, but occupy only short sections within the total length of a bundle. Actually, we investigate the nature of these projections by means of IIF and by *in vitro* model studies, since it is supposed that they may have ATPase activity like the side projections of the *Saccinobaculus* axostyle, which shows sliding in the presence of ATP and $Mg^{2+}$ (Bloodgood 1975, Mooseker and Tilney 1973). These regularly ordered bridging structures contrast distinctly with thinner, fuzzy lateral projections occurring along MTs, which reveal a somewhat more irregular and loosely packed array. The different decorations may also reflect the association of variable MAPs, as indicated by negatively stained MTs prepared under identical experimental conditions, showing a smooth walled type of MT and another type revealing a helical surface pattern (Pl. I 5, 6).

## Filopodial Helical Filaments and Paracrystals

The other main cytoskeletal components, the helical filaments (hFs) with a diameter of approximately 36 nm, are found either in close association with the peripheral region or in continuity with the MT bundles (Pl. I 2, 3). Remarkably, the quantity of hFs increases considerably in reticulopodial regions irritated by chemical or physical stimuli. The ratio of MTs to hFs depends also significantly upon the functional state of each pseudopodial region within the RPN: retracting filo- or lamellipodia possess predominantly hFs whereas in outgrowing areas mainly far-reaching MT bundles are detectable. In order to exclude any physical or chemical artifacts, we were able by means of cryofixation to demonstrate, that hFs are not induced during the preparation procedure, but represent regular cytoskeletal components even in the thinnest filopodia detectable by the light microscope. With cryosubstitution, the occurrence of paracrystals composed of highly registered and densely packed hFs, was likewise demonstrable. Since in a former study (Hau-

ser and Schwab 1974) it was shown that, after application of $D_2O$, paracrystals and hFs disappear in favour of MTs and reversely after VLB, paracrystals and hFs form, it was concluded, that hFs and PCs should be an intermediate assembly or disassembly state of filopodial MTs. The resemblance of these naturally occurring hFs and PCs to those induced under typical *in vitro* conditions by Vinca alkaloids is indeed amazing (Marantz and Shelanski 1970). In negatively stained preparations of lysed filopodia, the same bifilar spiral structure (arrowheads in Pl. II 12), each unit of which was assumed to be a protofilament, as in VLB induced helices (Fujiwara and Tilney 1975, Warfield and Bouck 1974) is detectable. Although there is evidence from thin sections that under physiological conditions the reticulopodial MTs are directly transformed into hFs or *vice versa* (Pl. I 3), no other indications exist, that the helical elements are tubulin.

### IIF with Controls and Ruthenium Red Treated RPNs

Therefore we used the monoclonal antibody YOL 1/34 directed against denaturated α-tubulin to study the tubulin pattern within controls and chemically irritated RPNs. Fully outgrown RPNs exhibit a predominant linear fluorescence pattern, indicating the presence of far-reaching MT bundles (Pl. I 8). Particularly in the extremely flat lamellipodial regions they appear brillant and may be followed continuously into the finest branches of the RPN. Using YL 1/2, a monoclonal antibody directed against the c-terminus of α-tubulin a slightly different staining appeared. Whereas YOL 1/34 sometimes stains also cytoplasmic inclusions, especially in areas irritated during the fixation procedure, YL 1/2 shows an exclusively linear fluorescence.

Since it proved impossible to induce helices by the usual methods (e.g., application of cold temperatures, VBL etc.) without producing retraction and subsequent detachment of the RPN from the coverslips, we looked for a method, which allows the induction of helices while the RPN remains fully intact and adherent. In several systems, the polycation ruthenium red (RR) has been found to interfere with MTs by aggregating them into crystalline structures (Stebbing and Hunt 1982). In experiments with short time incubated RPNs (0.6 μM), we noticed exclusively helices and found the RPN fully adherent. After prolonged treatment (2 min prior to fixation) or after a concentration of 6 μM RR a total aggregation of hFs into paracrystalline structures was obtained (Pl. II 10). Induction of hFs and PCs was achieved even in filopodia after complete lysis and subsequent RR treatment as seen in negatively stained preparations (Pl. II 11–13). Since we affirmed by means of EM-methods that MTs are only sporadically identifiable, we proved with the monoclonal antibody YOL 1/34 the tubulin nature of hFs and paracrystals. As shown in Pl. II 14–16, the resulting fluorescence pattern differs significantly from that of the controls. In short time treated RPNs the usual linear rigid MT pattern is transformed into a wavy one, indicating the formation of

numerous helical elements, which tend to form sinusoid-shaped aggregates. In some lamellipodia of long-time incubated cells, brightly fluorescing patches indicate the formation of paracrystals along former MT cables (Pl. II 16).

Interestingly, the monoclonal antibody YL 1/2 shows almost no affinity to the tubulin crystals and only a very weak one to the helical assembly state.

Without any doubt these intensely staining inclusions, identified as hFs and PCs by means of EM-methods, themselves clearly reveal as tubulin, although there may be some variation in the α-subunit.

## Filaments

At present, we extend our investigations on a third regular component of the filopodial cytoskeleton, which shares some features with another VLB or VCR inducable element: straight 5 to 6 nm filaments interdigitating with filopodial MTs. In addition to PCs, rings and hFs, VLB may also induce the formation of filaments seen in continuity with PCs or helices (Briggs 1984, Krishan and Hsu 1969).

Since these filaments fail to bind HMM or $S_1$-fragments of myosin the possibility that these filaments are actin appear unlikely. There is suggestive evidence that these filaments may also be tubulin representing an additional assembly state in the *Allogromia* RPN. Whereas they are abundant in all filopodial regions, they have totally disappeared in long time Taxol-treated (48 h) RPNs. In the IIF with anti tubulin, unusual dense linear arrays, indicate additional MT assembly. Ultrastructurally, these RPNs reveal solely unusual dense packing of typically Taxol-induced MTs, showing hooks and/or c-shaped profiles. Since in short time Taxol-treated RPNs microtubules and helical filaments appear likewise multiplied, it is suggested, that the 5 nm filaments represent protofilaments, which first assemble to the bifilar helical state.

It is suggested, that the existence of this unique cytoskeleton represents not only phylogenetic variation, but also a specific adaptation to the highly dynamic nature of the RPN, allowing rapid retraction and re-expansion without far-reaching depolymerization of its cytoskeletal main component.

## ACKNOWLEDGEMENTS

The monoclonal antibodies YOL 1/34 and YL 1/2 were a kind gift of Dr. Kilmartin (Cambridge, UK) to Dr. J. Wehland (Göttingen).

This work was supported by a grant of DFG to Dr. M. Hauser (Ha 821/5-2).

## REFERENCES

Bloodgood R. A. 1975: Biochemical analysis of axostyle motility. Cytobios, 14, 101–120.

Briggs R. T. 1984: Vinblastine-induced filaments and crystals in bullfrog leukocytes and erythrocytes. J. Cell Biol., 47, 25 a.

Fujiwara K. and Tilney L. G. 1975: Substructural analysis of the microtubule and its polymorphic forms. Ann. N.Y. Acad. Sci., 253, 27–50.
Hauser M. and Schwab D. 1974: Mikrotubuli und helikale Mikrofilamente im Cytoplasma der Foraminifere *Allogromia laticollaris* Arnold. Untersuchungen mit Vinblastin und Deuteriumoxid zum Nachweis einer engen Wechselbeziehung. Cytobiologie, 9, 263–279.
Krishan A. and Hsu D. 1969: Observations on the association of helical polyribosomes and filaments with vincristine-induced crystals in Earle's L-cell fibroblasts. J. Cell Biol., 43, 553–559.
Marantz R. and Shelanski M. L. 1970: Structure of microtubular crystals induced by vinblastine *in vitro*. J. Cell Biol., 44, 234–241.
Mooseker M. S. and Tilney L. G. 1973: Isolation and reactivation of the axostyle. J. Cell Biol., 56, 13–26.
Stebbing H. and Hunt C. 1982: The nature of the clear zone around microtubules. Cell Tissue Res., 227, 609–618.
Travis J. L. and Allen R. D. 1981: Studies on the motility of the *Foraminifera*. I. Ultrastructure of the reticulopodial network of *Allogromia laticollaris* (Arnold). J. Cell Biol., 90, 211–221.
Warfield R. K. N. and Bouck G. B. 1974: Microtubule-Macrotubule transitions: Intermediates after exposure to the mitotic inhibitor vinblastine. Science, 186, 1219.

## EXPLANATION OF PLATES I–II

1–8 — Control pseudopodia
1: Longitudinally sectioned filopodium exhibiting MT bundles and hFs (arrows). Each MT may join separate bundles (arrowhead). Bar 1 μm
2, 3: The hFs are closely associated with MTs and appear in some cases to emerge directly from MTs (arrow). Bars 0.2 μm
4: Adjacent MTs are interconnected by globular cross-bridges (arrows) arranged in distinct patches along the entire length of MT bundles. Bar 0.2 μm
5: Another type of MT decoration is demonstrable in negatively stained preparations. MAPs with a longitudinal distance of 36 nm are helically arranged along the MT long axis (arrowheads). Bar 0.1 μm
6: Negatively stained preparations of whole mounted lysed pseudopodia reveal a protofilament arrangement comparable to usual *in vitro* MT preparations. Bar 0.2 μ,m
7: Negatively stained MT bundle with cross-bridges (arrowheads). Bar 0.2 μm
8: Lamellipodium stained with YOL 1/34, a monoclonal antibody against α-tubulin, showing a predominant linear fluorescence pattern of MT bundles. Bar 10 μm

9–16 — Ruthenium red treated pseudopodia

9: Longitudinal section. After application of 0.6 μm RR for 10 s all MTs are converted into paracrystalline aggregates (PC). Bar 0.5 μm
10: Cross-section. Longer incubation times (up to 30 s) cause the formation of large paracrystals, which may fill out thinner filopodia. Bar 0.5 μm
11, 12: Negatively stained hFs (11) after RR treatment (6 μM for 10 s) exhibit the same ultrastructure as hFs in control pseudopodia (12). Arrowheads indicate the double-stranded composition of the helices. Bars 0.1 μm
13: Some hFs may appear more irregularly twisted. Bar 0.1 μm
14, 15: Lamellipodia stained with YOL 1/34 after 0.6 μM RR incubation (10 s). The linear fluorescence pattern of the MT bundles has changed into a wavy one, demonstrating the formation of hFs. Bars 10 μm
16: The aggregation of hFs into paracrystals after incubation in 0.6 μM RR (30 s) is documented by an irregular spotted fluorescence. Bar 10 μm

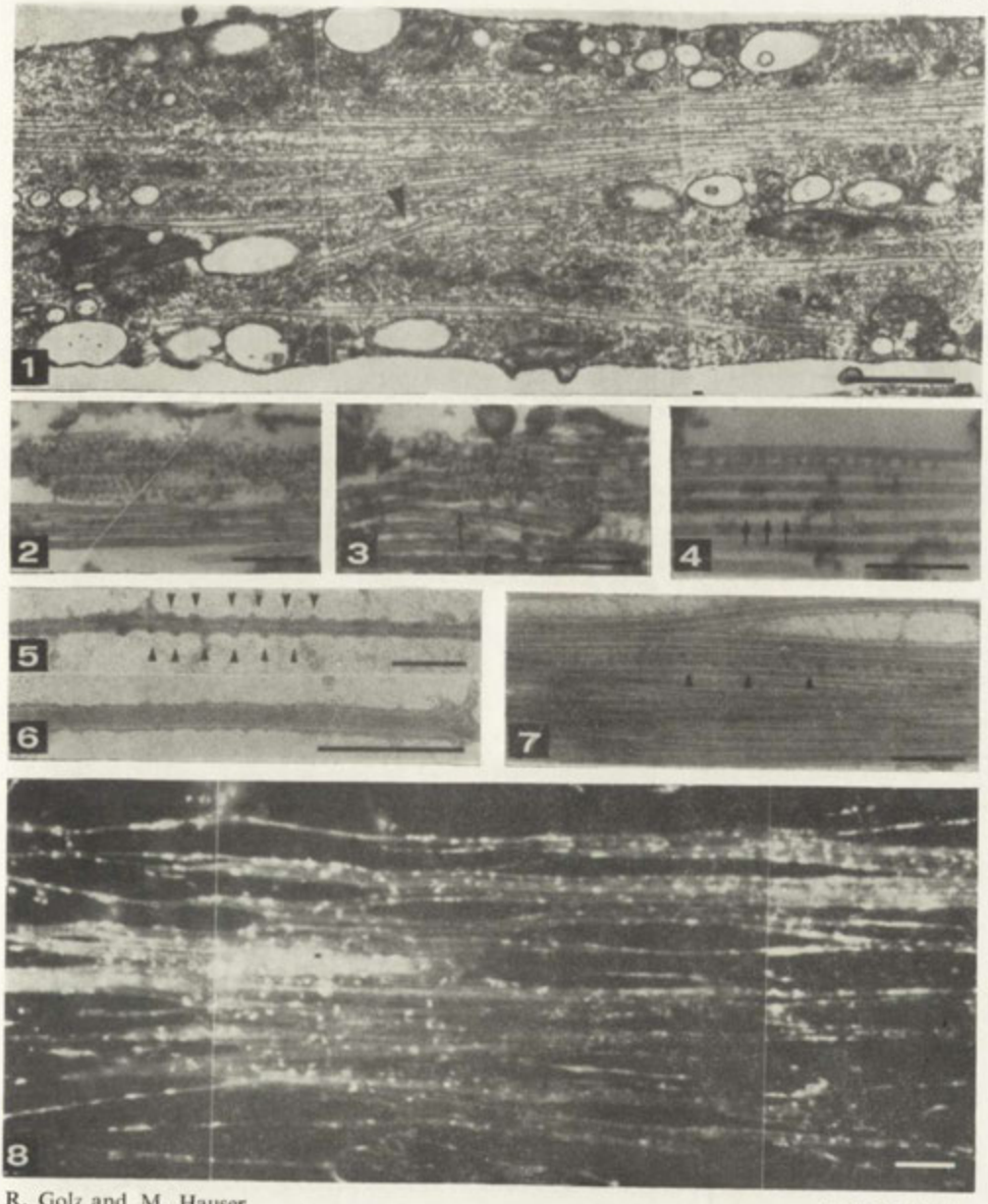


R. Golz and M. Hauser

auctores phot.

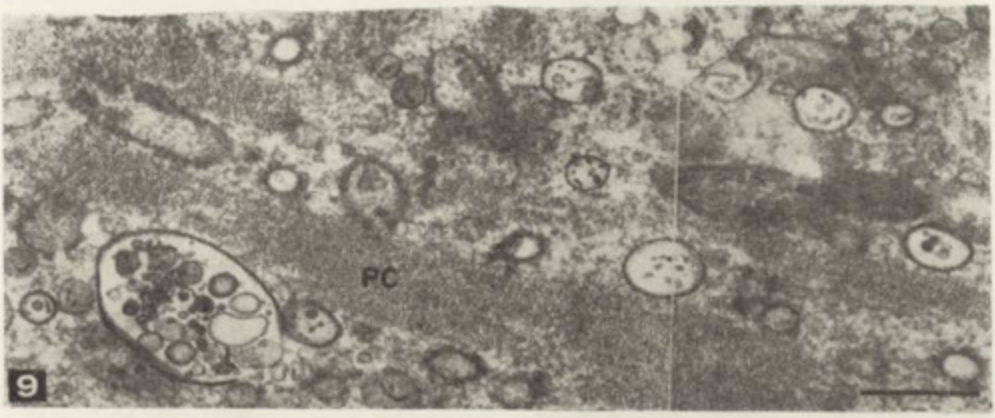


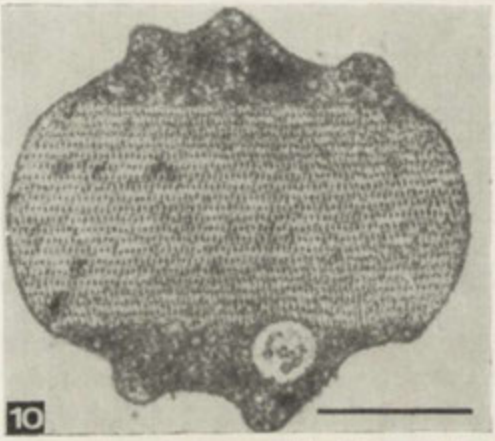


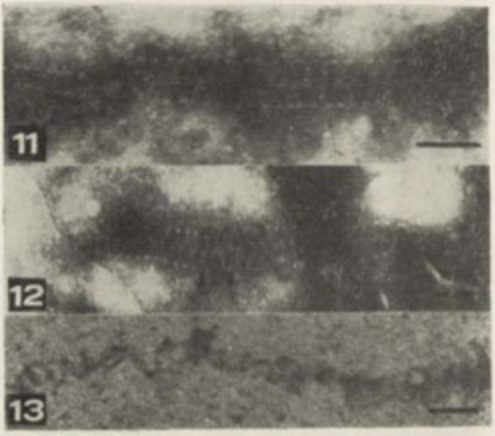




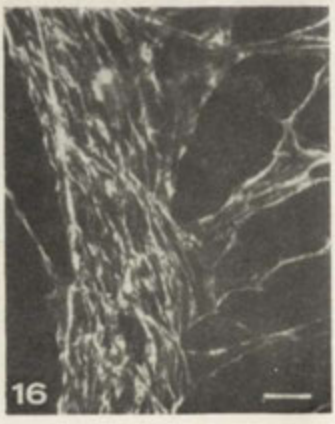


R. Golz and M. Hauser auctores phot.

ACTA PROTOZOOLOGICA
Vol. 25, No. 3, pp. 285–304 (1986)

# Dynein Structure and Function in Protozoan Cilia: Current Status[1]

Peter SATIR

Department of Anatomy and Structural Biology, Albert Einstein College of Medicine, Bronx, New York 10461, USA

*Received on* 26 September 1985

*Synopsis.* Ciliary dynein studied *in situ* and after alloaffinity purification is a complex molecule composed of heavy, intermediate and light chains. The heavy chains are the likely sites of ATPase activity and form the major part of the globular domains of isolated dynein. *In situ* the major domains forming an arm extend transversely across the interdoublet gap. The head of the arm attaches to the doublet N+1. Its barbed end makes two attachments to the doublet N, at least one of them is ATP-insensitive. A computer model of the doublet microtubule has been constructed. It incorporates the positional relationships of the appended structures and the details of fine structure of the dynein arms. To produce ciliary motion, active sliding of the microtubule doublets is switched on and off at various times in the beat cycle. Metabolic regulation of the intrinsic axonemal switches that control dynein arm activity ultimately governs the ciliary behavior. $Ca^{2+}$ and c-AMP are the usual regulators. The $Ca^{2+}$ switch operates *via* calmodulin sensor that is a structural part of the axoneme. It seems that the $Ca^{2+}$ and c-AMP switches operate antagonistically at other parts of the beat cycle, probably by changing the phosphorylation state of axonemal proteins including dynein.

Dynein is the mechanochemical transducer protein responsible for microtubule sliding and consequently motility of protozoan cilia and flagella. In the past four years, since the previous review of tubulin-based cell motility in these pages, considerable attention has been focused on this molecule. There is now significant information and agreement about the structure, biochemistry and function of dynein, or rather of several different dyneins of various organisms, although some specific details remain controversial. The information is briefly reviewed in this article, with particular emphasis on *Tetrahymena* dynein to which my laboratory

[1] Lecture presented by P. Satir on 25th June 1985 at the Symposium "Relationship between Cytoskeleton and Motility", held during the Seventh International Congress of Protozoology in Nairobi, Kenya.

has contributed. Recent reviews of this subject from other perspectives have been published by Warner and Mitchell (1980), Bell et al. (1982) and Johnson (1985).

### Dynein is a hetero-oligomeric ATPase with heavy (H), intermediate (I) and light (L) chains

Dynein has previously been prepared by salt extraction from various axonemes, followed by sucrose density gradient fractionation. In this way, Bell et al. (1979) established that a particular 21S sea urchin sperm flagellar dynein was a complex of H, I and L chains. The two major heavy chains, Aα and Aβ, are present in equimolar amounts, and both chains are associated with ATPase activity. Analysis of the release of these chains by ATP and salt after proteolytic cleavage of intact axonemes suggests that Aα chain is closely associated with the *in situ* dynein binding site on subfiber A of each doublet microtubule, while the Aβ chain is associated with the transient *in situ* attachment site on subfiber B (Bell and Gibbons 1982). I shall refer to the Aβ side as the head end, the Aα side as the barbed end of the arm.

### Both inner and outer arms are composed of dyneins. The polypeptide composition of inner and outer arms may be different. There is more than one ATPase per dynein arm

Piperno and Luck (1982) have analyzed the dynein arms of *Chlamydomonas* comparing the polypeptide components of the isolated dyneins with polypeptides that are deficient in arm defective mutants. Four dyneins were identified by ATPase activity in the extraction experiments. All polypeptides deficient in outer arm mutants are associated with the 12S and 18S species; a 12.5S and 11S species comprise the inner arms. Each individual dynein has 1–3 distinct polypeptide components of high molecular weight and one or more lower molecular weight substituents. Pfister and Witman (1984) have subfractionated the 18S dynein into two unique subunits, each containing an H chain. Both subunits have ATPase activity. Pfister et al. (1984) have shown that the photoaffinity probe 8-azido ATP selectively labels the H chain of *Chlamydomonas* 12S dynein.

### Some dyneins associate with microtubules in an ATP-sensitive manner. This can form the basis of purification of these molecules

Takahashi and Tonomura (1978) have shown that *Tetrahymena* dynein, extracted from axonemes by low ionic strength dialysis, will rebind to isolated axonemal microtubules at multiple loci. Addition of ATP releases the arms, but if sufficient time elapses for hydrolysis of the ATP, the arms will rebind. Release and rebinding are easily monitored by electron microscopy. Satir et al. (1981) have shown that the released arms remain in the supernate when the microtubules are sedimented by centrifugation. Nasr and Satir (1985) have utilized this obser-

vation as a basis for purification. Dynein-decorated microtubules are placed on a filter, washed with buffer to remove impurities and unbound dyneins; subsequently ATP is added and the eluate collected. We refer to this procedure as alloaffinity purification, since it depends on the affinity of dynein to two unrelated ligands, microtubules and ATP. Release also depends on the ionic strength of the buffer used. The ATP eluate contains an alloaffinity purified dynein that corresponds to conventional 30S *Tetrahymena* dynein (Porter and Johnson 1983).

Alloaffinity purified *Tetrahymena* dynein contains H, I and L chains. On gel electrophorograms, the major H peak is at $M_r$ about $3\times10^5$; the I region usually consists of 1–3 bands with $M_r$ $6–9\times10^4$ and the L region consists of 4 bands of $M_r$ between 23 and 14,000. The molecular weight of the H chains cannot be accurately determined from gel electrophoresis and may be underestimated. For every heavy chain in the molecule, there is approximately one light chain; for every two heavy chains approximately one I chain. Alloaffinity purified *Tetrahymena* dynein will rebind to microtubules in the absence of ATP, with a periodicity and length resembling *in situ* arms. Heterologous, as well as homologous dyneins can be prepared by alloaffinity purification. Alloaffinity purified *Chlamydomonas* dynein is a set of polypeptides including the four heavy chains that characterize the outer arm.

In solution, dyneins have a structure containing a major globular domain of about 4–5 nm radius attached to a thin flexible strand. In dynein arms, the strands associate together into bouquets with 2–3 globular domains

Johnson and Wall (1983) have examined isolated 30S *Tetrahymena* dynein using scanning transmission electron microscopy (STEM). These images show the dynein as a bouquet of three globular heads connected by three separate strands to a base (Fig. 1 A). Mass measurement indicates that the structure has a mass of $1.95\pm0.24\times10^6$ daltons and that each head is $420\pm80$ kdaltons. Witman et al. (1983) have found that the *Chlamydomonas* outer dynein arm also has this construction: the 18S particle is two headed and has a net mass of $1.25\times10^6$ daltons, while the 12S particle is a single globular unit with a mass of 470 kdaltons. The 21S sea urchin dynein studied by Gibbons and his colleagues is evidently a two headed molecule.

Each globular domain contains at least 1 H chain with ATPase activity

The STEM determined mass of the molecule divided by the $M_r$ of the H chains suggests that at least 3 and no more than 6 H chains comprise *Tetrahymena* alloaffinity purified dynein or the *Chlamydomonas* outer arm; that is one or two H chains are present in each globular domain. A parsimonious assumption is that the globular domains with a tail are isomorphs that are constructed homologously, say of 2H, 1I and 2L chains. This subunit would have a $M_r$ of ca. $7\times10^5$.

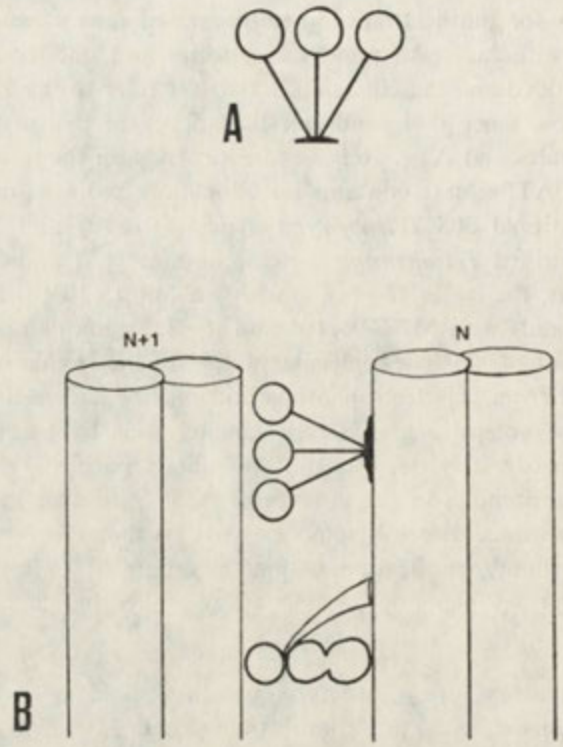


Fig. 1. A — Representation of isolated 30S *Tetrahymena* dynein as seen in STEM (after Johnson and Wall 1983), B — Orientation of the dynein molecule *in situ*, *Above* — Vertical disposition of subunits as proposed by Johnson and Wall (1983), *Below* — Transverse orientation of subunits as proposed by Avolio et al. (1984). (From Satir and Avolio (1986). Courtesy N.Y. Acad. Science)

The *in situ* arm is composed of a cape, body and head. The globular domains are aligned transversely across the interdoublet gap with ATPases at either end of the molecule

The substructure of the *in situ* arm has been re-studied in *Tetrahymena* and *Chlamydomonas* using rapid freeze methods (Goodenough and Heuser 1982, 1985, Tsukita et al. 1983) and improved negative stain and thin section methods (Avolio et al. 1984, Satir and Avolio 1986). In each case, the arm appearances in profile are quite similar. The main portion of the arm is suspended basally from a fiber or cape and it extends across the interdoublet gap from subfiber A of doublet no. N toward subfiber B of doublet N+1, ending in a head, that probably corresponds to one of the globular domains seen in the isolated molecule (Fig. 1 B). The remainder or body of the arm probably corresponds to the other globular domains. At the barbed end of the arm, the cape and body form a two-point attachment to subfiber A; at least one of the barbed end attachments is ATP-insensitive, since *in situ* the arm always is associated with subfiber A. The globular domains

of the *in situ* arm are aligned perpendicular to rather than parallel to the doublets so that the arm can attach by both ends. In cross-section, the arm is triangular in shape with the head at the apex of the triangle (Avolio et al. 1986).

Dynein arm orientation found after decoration of axonemal microtubules is more promiscuous and less stringent in orientation than that seen *in situ*. For the reattached arms, there is no single unique structural orientation, and attachment occurs by either the barbed or the head end. These attached arms release upon addition of ATP regardless of their orientation. Taken together with the results of Bell and Gibbons (1982), this suggests that one or more of the ATPase H chains of the arm is associated with the head end of the molecule; one or more with the barbed end. For the *Chlamydomonas* outer arm, this would be consistent with the 12S portion of the arm forming the head; the 18S portion forming the body.

Despite compositional differences, inner and outer arms are similarly constructed across the interdoublet gap. In *Tetrahymena*, image reconstruction suggests that for every outer arm, there is a corresponding inner arm

The inner arm of *Chlamydomonas* has been studied by Goodenough and Heuser (1985), who conclude that there are differences in construction and placement of these arms in relation to the outer arm. However, Avolio et al. (1986) have examined individual *Tetrahymena* doublet microtubules in en face views. A computer model of the doublet and its appendages has been generated, incorporating the detailed head, body, cape substructure for both inner and outer

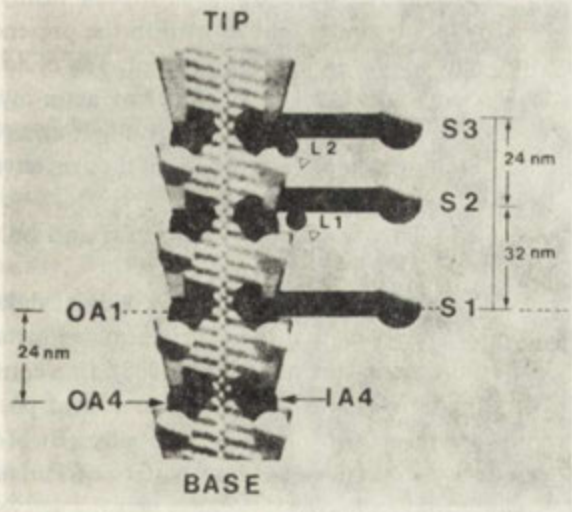


Fig. 2. Computer reconstruction of an axonemal doublet showing alignment of outer (OA) and inner (IA) arms, radial spokes (S1-S3), and interdoublet links (L1, L2). Arms are seen en face. Note subunit arrangements. OA1 and IA1 are aligned with S1. (From Avolio et al. (1986)

arms (Fig. 2). Images of the arms in longitudinal view and cross-section are successfully modelled in this way, suggesting that inner and outer arms are structurally similar. The inner and outer arms occur in register with the same periodicity; inner arm 1 (IA 1) and outer arm 1 (OA 1) are aligned with spoke (S1) of each spoke group. It seems likely that the inner arm is transversely oriented across the interdoublet gap in the same way as the outer arm and that it too has an ATPase containing head at one end and an ATPase containing body at the other.

### The dynein arm has a mechanochemical cycle that produces force in a fixed spatial direction. Morphologically, this cycle is reflected in changes in the relative positions of the subunits comprising the arm

Sale and Satir (1977) showed that doublet microtubule sliding in *Tetrahymena* has a fixed polarity, such that doublet N+1 is always displaced tipwards with respect to doublet N. This has been confirmed in *Paramecium* by Mogami and Takahashi (1983). Using thin-section and negative stain electron microscopy, Satir et al. (1981) described three distinct morphological configurations of the dynein arm including an extended, rigor, and compact form. A scenario for the mechanochemical cycle which couples these configurations to the events of ATP hydrolysis during ciliary microtubule sliding and to the direction of active sliding was proposed. Avolio et al. (1984) have re-interpreted these configurations in terms of subunit movements of the head and body of the arm, which, more recently, can be reconstructed dynamically with the computer (Avolio et al., 1986). Using the non-hydrolyzable ATP analog AMP–PCP, Avolio et al. (1984) have demonstrated that *in situ* the head of the arm can firmly attach to subfiber B of doublet N+1 across the interdoublet gap. In the presence of ATP, head attachment must be transient so that sliding can proceed. The cycle itself is formally analogous to the Lymn and Taylor (1971) model of actin-myosin interaction (Satir et al. 1981, Johnson 1985). Complexities that might arise because of ATP sensitive dynein-microtubule interactions at both ends of the arm have been neglected.

### Dynein arm activity can be switched off and on

A growing body of evidence that suggests that active doublet sliding within a ciliary axoneme is asynchronous, implying that the dynein arms of certain doublets are active at the same time as other arms are not (Satir 1985). In a complete beat cycle, there would be a defined pattern of arm activity for each beat position and differing sets of arms would be turned on or off sequentially. Sugin and Naitoh (1982, 1983) have been able to reproduce the beat pattern of *Paramecium* cilia with considerable precision by a trial and error procedure that fits active sliding patterns to beat form in this manner.

Although the cyclic pattern of arm activity is intrinsic, extrinsic controls can be superimposed to effect the switching on or off of a subset of arms. Inner and outer arms may subserve different behavioral functions

Two main controls -$Ca^{2+}$ and c-AMP-appear to act on the intrinsic axonemal switches. The $Ca^{2+}$ control mechanism probably operates via a calmodulin sensor that is a structural part of the axoneme. At $Ca^{2+}$ of $10^{-7}$M or less, beat is normal; at $10^{-6}$M $Ca^{2+}$ many cilia become quiescent and at higher $Ca^{2+}$ concentrations the pattern of dynein arm activity is changed and may produce ciliary reversal. *Chlamydomonas* mutants with an altered inner arm component and altered phosphoproteins move backwards only with symmetrical beat that characterizes ciliary reversal in this organism (Segal et al. 1984). Axonemes prepared from this mutant beat similarly regardless of the $Ca^{2+}$ concentration of the reactivation medium. Another type of mutant, which lacks outer arms, swims forward with the asymmetric beat that characterizes normal forward swimming (Kamiya and Okamoto 1985, Mitchell and Rosenbaum 1985). These mutant axonemes reactivate normally in media with little $Ca^{2+}$, but become quiescent as $Ca^{2+}$ is raised. They do not show the reversal response when $Ca^{2+}$ is raised above $10^{-6}$M. The presence of one row of normal arms is sufficient for ciliary beat at a reduced frequency, but the form of the beat and the behavioral responses apparently depend on which row is present.

The complexity of dynein polypeptide composition affords opportunity for alteration of arm activity *via* post-translational modifications such as phosphorylation or dephosphorylation

The $Ca^{2+}$ and c-AMP controls, and perhaps the intrinsic arm activity cycle itself, may operate *via* changes in the phosphorylation state of polypeptides, including those comprising the dynein arms. Piperno and Luck (1981) have shown that several components of the *Chlamydomonas* inner arm, including the H chains, are phosphoproteins. One problem with hypotheses dependent on such mechanisms it that the enzymatic machinery necessary for the modification must be part of the axoneme and possibly of the arm itself; a second problem is the time necessary for repeated cycling of activity, which might be less than a few ms for cilia beating at 100 Hz. The possibility that there is an ATPase H chain at either end of the arm suggests a simple structural mechanism for activation of the arm: an active arm is attached by its body to subfiber A of doublet N; an inactive arm has detached. In this way, activation, which would depend on body attachment to subfiber A of doublet N (regulated in some simple way by post-translational modification?), might be separated from mechanochemical cycle producing sliding, which depends on head attachment to subfiber B of doublet N+1.

## ACKNOWLEDGEMENTS

I thank J. Avolio, S. Lebduska and M. E. J. Holwill. The help of C. Hubertus in typing and assembly of this manuscript is greatly appreciated. This work was supported by a grant from the USPHS (HL22560).

## REFERENCES

Avolio J., Glazzard A. N., Holwill M. E. J. and Satir P. 1986: Structures attached to doublet microtubules of cilia: computer modelling of thin section and negative stain stereo, images. Proc. Nat., Acad. Sci. USA, 83, 4804–4808.

Avolio J., Lebduska S. and Satir P. 1984: Dynein arm substructure and the orientation of arm-microtubule attachments. J. Mol. Biol., 173, 389–401.

Bell C. W., Fronk E. and Gibbons I. R. 1979: Polypeptide subunits of dynein 1 from sea urchin sperm flagella. J. Supramol. Struct., 11, 311–317.

Bell C. W. and Gibbons I. R. 1982: Structure of the dynein-1 outer arm in sea urchin sperm flagella. J. Biol. Chem., 257, 516–522.

Bell C. W., Fraser C., Sale W. S., Tang W-J. Y. and Gibbons I. R. 1982: Preparation and purification of dynein. Methods Cell Biol., 24, 373–397.

Goodenough U. W. and Heuser J. E. 1982: Substructure of the outer dynein arm. J. Cell Biol., 95, 798–815.

Goodenough U. W. and Heuser J. E. 1985: Substructure of inner dynein arms, radial spokes and the central pair/projection complex of cilia and flagella. J. Cell Biol., 100, 2008–2018.

Johnson K. A. 1985: Pathway of the microtubule-dynein ATPase and the structure of dynein: a comparison with actomyosin. Annu. Rev. Biophys. Chem., 14, 161–188.

Johnson K. A. and Wall J. S. 1983: Structure and molecular weight of the dynein ATPase. J. Cell Biol., 96, 669–678.

Kamiya R. and Okamoto M. 1985: A mutant of *Chlamydomonas reinhardtii* that lacks the flagellar outer dynein arm but can swim. J. Cell Sci., 74, 181–191.

Lymn R. W. and Taylor E. 1971: Mechanism of adenosine triphosphate hydrolysis by actomyosin. Biochem. J., 10, 4617–4624.

Mitchell D. R. and Rosenbaum J. L. 1985: A motile *Chlamydomonas* flagellar mutant that lacks outer dynein arms. J. Cell Biol., 100, 1228–1234.

Mogami Y. and Takahashi K. 1983: Calcium and microtubule sliding in ciliary axonemes isolated from *Paramecium caudatum*. J. Cell Sci., 61, 107–121.

Nasr A. and Satir P. 1985: Alloaffinity filtration: A general approach to the purification of dynein and dynein-like molecules. Anal. Biochem., 151, 97–108.

Pfister K. K. and Witman G. 1984: Subfractionation of *Chlamydomonas* 18S dynein into two unique subunits containing ATPase activity. J. Biol. Chem., 259, 12072–12080.

Pfister K. K., Haley B. E. and Witman G. 1984: The photoaffinity probe 8-azidoadenosine 5′ triphosphate selectively labels the heavy chain of *Chlamydomonas* 12S dynein. J. Biol. Chem., 259, 8499–8504.

Piperno G. and Luck D. J. L. 1981: Inner arm dyneins from flagella of *Chlamydomonas reinhardtii*. Cell, 27, 33–340.

Piperno G. and Luck D. J. L. 1982: Outer and inner arm dyneins from flagella of *Chlamydomonas reinhardtii*. Cell Motility, (Suppl.) 1, 95–99.

Porter M. E. and Johnson K. A. 1983: Characterization of the ATP sensitive binding of *Tetrahymena* 30S dynein to bovine brain microtubules. J. Biol. Chem., 258, 6575–6581.

Sale W. S. and Satir P. 1977: Direction of active sliding of microtubules in *Tetrahymena* cilia. Proc. Natl. Acad. Sci. U.S.A., 74, 2045–2050.

Satir P. 1985: Switching mechanisms in the control of ciliary motility. Mod. Cell Biol., 4, 1–46.

Satir P. and Avolio J. 1985: Dynein as a microtubule-associated protein. Ann. N.Y. Acad. Sci., 466, 269–274.

Satir P., Wais-Steider J., Lebduska S., Nasr A. and Avolio J. 1981: The mechanochemical cycle of the dynein arm. Cell Motility, 1, 303–327.

Segal R. A., Huang B., Ramanis Z. and Luck D. J. L. 1984: Mutant strains of *Chlamydomonas reinhardtii* that move backwards only. J. Cell Biol., 98, 2026–2034.

Sugino K. and Naitoh Y. 1982: Simulated cross-bridge patterns corresponding to ciliary beating in *Paramecium*. Nature (London), 295, 609–611.

Sugino K. and Naitoh Y. 1983: Computer simulation of ciliary beating in *Paramecium*. J. Submicrosc. Cytol., 15, 37–42.

Takahashi M. and Tonomura Y. 1978: Binding of 30S dynein with the B-tubule of the outerl doublet of axonemes from *Tetrahymena pyriformis* and the adenosine triphosphate-inducedl dissociation of the complex. J. Biochem., (Tokyo), 84, 1339–1355.

Tsukita S., Tsukita S., Ugukura J. and Tshikana H. 1983: ATP-dependent structura changes of the outer dynein arm in *Tetrahymena* cilia: A freeze-etch replica study. J. Cel Biol., 96, 1480–1485.

Warner F. D. and Mitchell D. R. 1980: Dynein: The mechanocl emical coupling adenosine triphosphatase of microtubule-based sliding filament mechanisms. Int. Rev. Cytol., 66 1–43.

Witman G. B., Johnson K. A., Pfister K. K. and Wall J. S. 1983: Fine structure and molecular weight of the outer arms of dyneins of *Chlamydomonas*. J. Submicrosc. Cytol., 15, 193–197.

ACTA PROTOZOOLOGICA
Vol. 25, No. 3, pp. 295–304 (1986)

# Calmodulin Regulated Processes in Protistan Motility[1]

Leszek KUŹNICKI

Department of Cell Biology, Nencki Institute of Experimental Biology, Pasteura 3, 02-093 Warszawa, Poland

*Received on* 10 October 1985

*Synopsis.* Calmodulins (CaM) are probably involved in all motile systems of protists. (1) It is generally believed that calmodulin shares regulatory roles is stimulus-contraction coupling as a plasma membrane component and a messenger (sensory transducer). (2) In some contractile systems CaM regulates actin-myosin interaction. (3) Both CaM · Ca and cAMP are fundamental regulators of cilia and flagella activity. In spite of great deal of research, most details of the mechanism of CaM action are unknown and the role of calmodulin in particular motile systems of protists has not been determined. The best known $Ca^{2+}$-mediated motile event among protists is the ciliary reversal. The binding of mono- and divalent cations to $Ca^{2+}$-binding sites of calmodulin as well as to other $Ca^{2+}$-binding proteins is suggested as the initial molecular mechanism of ciliary reversal.

Over the last few years calmodulin (CaM) has been extensively studied. This topic was comprehensively reviewed by Klee and Vanaman (1982), Means et al. (1982), Burges et al. (1983), Marmé and Dieter (1983), Seamon and Kretsinger (1983), Cox et al. (1984), Manalan and Klee (1984).

Recently it is clear that: (1) CaM is the general name of a class of calcium binding proteins with extremely similar structural and functional properties. (2) CaM is present in all eukaryotes but has not been found in prokaryotes. (3) CaM binds $Ca^{2+}$ in the presence of $Mg^{2+}$ and other physiological ions and modulates calcium transport and concentration inside the cell. (4) CaM · Ca complex in multiple specific interaction with enzymes (E) and other proteins regulates overall activity of each eukaryotic organism.

## General Mechanism of Action

Calmodulin harbors four $Ca^{2+}$-binding sites: in cellular processes only $CaM \cdot Ca_{n \geq 3}$, plays its role. $Ca^{2+}$ and calmodulin alone are not active in the cytoplasm (Cheung 1984, Cox 1984, Dedman 1984).

[1] Lecture presented by L. Kuźnicki on 25th June 1985 at the Symposium "Relationship between Cytoskeleton and Motility", held during the Seventh International Congress of Protozoology in Nairobi, Kenya.

It is generally believed that the mechanism that links excitation with intracellular events involves two sequentional steps. In response to stimulus, $Ca^{2+}$ dissociates from cell membranes or flows from the medium across the plasma membrane into the cell and then binds to the calmodulin (first step). Saturation of calmodulin binding sites causes a conformation change toward a more helical structure. Binding $Ca^{2+}$ ions proceeds sequentially. Saturation of the three or four $Ca^{2+}$-binding domains on calmodulin exposes a hydrophobic site that appears to interact with the receptor enzyme to form activated complex (second step).

Calmodulin has been implicated in many cellular events because in cytoplasm and organelles numerous calmodulin dependent enzymes and proteins operate. *In vitro* these enzymes or CAPs (calmodulin acceptor proteins) are defined as molecules that bind only to calmodulin (nonbinding to the troponin C) in high ionic strength buffer in a $Ca^{2+}$-dependent manner and are inhibitable by trifluoperazine (Dedman 1984).

In living cell the reactions between calcium and calmodulin as well as $CaM \cdot Ca_n$ and CAP are reversible and regulated by the concentration of calcium ions in cytoplasm. A decrease of $Ca^{2+}$ ions favors dissociation of calmodulin-CAP complex, an increase favors its formation. All eukaryotic cells contain calmodulin at exceedingly high levels in comparison with intracellular concentration of $Ca^{2+}$; that is the mechanism of keeping calcium ions on physiological level $\geqslant 10^{-7}$M.

On the molecular level $CaM \cdot Ca$ exerts its effects directly or indirectly. The direct effects were found on plasma membrane ATPase, dynein ATPase, and on cyclic nucleotide metabolizing enzymes. $CaM \cdot Ca$ exerts its effect indirectly by activiting protein kinases or phosphatases.

## The Possible Role of Calmodulin in Protista

The first hint that calmodulin exists in various protists (*Euglena gracilis*, *Amoeba proteus*, *Physarum polycephalum*) and plays a role in modulating the effects of $Ca^{2+}$ on motile systems was obtained by J. Kuźnicki et al. (1977, 1979). Since that time this protein has been isolated from other species of Protista: *Tetrahymena pyriformis*, *T. termophila*, *Paramecium tetraurelia* (Jamieson Jr. et al. 1979, 1980, Jamieson Jr. and Vanaman 1980, Maihle and Satir B. H. 1980), *Dictyostelium discoideum* (Bazari and Clarke 1980, Clarke et al. 1980, Jamieson Jr. and Frazier 1983), *Chlamydomonas reinhardtii* (Gitelman and Witman 1980).

The calmodulin has been localized in the cilia (Maihle et al. 1981, Ohnishi et al. 1982). The study of Blum et al. (1980, 1983). Jamieson Jr. et al. (1980), demonstrated that CaM may play a role in regulation of the ciliary dynein ATPase system in *Tetrahymena pyriformis*. It was showed that bovine brain CaM is effective in the activation of *Tetrahymena* 14S and 30S dynein ATPases, while *Paramecium* CaM activate *in vitro* brain phosphodiesterase.

The CaM · Ca dependent regulation was also found in ameboid locomotion. Maruta et al. (1982, 1983) demonstrated the role of CaM · Ca in the regulation of myosin heavy chain kinases of *Dictyostelium* aggregating cells. CaM · Ca activated myosin heavy chain kinase, while cAMP had opposite effect.

The ciliary and flagellar system is another one in which CaM · Ca and cAMP produce opposite effects. The stimulation of motility by cAMP is contrasted with the inhibition by CaM · Ca (Jamieson et al. 1979, Means et al. 1982). The study of general molecular mechanism of the axonemal motility well progressed *in vitro*. Much less progress, however, has been made in the physiological experiments *in situ*.

Calmodulin antagonists have been applied to intact protists to probe for involvement of calmodulin in $Ca^{2+}$-dependent processes. The chloropromazine affects photophobic response and alters the phototaxis of *Chlamydomonas* (Hirschberg and Hutchinson 1980). According to B. H. Satir et al. (1980), *Paramecium tetraurelia* in the presence of trifluoroperazine in the medium swim slowly, somewhat contracted and deciliated after prolonged exposure. In *Paramecium caudatum*, W-7 inhibits the voltage-dependent calcium current (Hennessey and Kung 1984). The messenger mediating the hyperpolarization of the axoneme has not been identified, although recent studies implicate cAMP (Gustin et al. 1983).

On the basis of these data we can conclude that calmodulin and calcium play central roles in regulating actin-myosin and tubulin-dynein locomotory systems and other phenomena, like mitosis as well as excitation, $Ca^{2+}$ transport and sensory transduction. However, specific involvement in any particular protozoan movement has not been well defined experimentally. The major experimental difficulty is that each motile event is complex and involves intersecting systems like membranes and cytoskeleton elements.

## The Major Experimental and Theoretical Complications

Two steps calcium-calmodulin intracellular second messengers mechanism presents a rather simplified model based on the *in vitro* experiments, than a common process occurring in cell. CaM · $Ca_n$ has a variety of action mechanism, often acting simultaneously. It may act by direct effect on ATPase activity or through kinases or phosphatases.

The molecular basis of motility regulation is not a simple equation consisting $Ca^{2+} + CaM \rightleftharpoons CaM \cdot Ca_{n\geq 3}$ and $CaM \cdot Ca_{n\geq 3} + E \rightleftharpoons E \cdot CaM \cdot Ca_{n\geq 3}$. After excitation, concentrations of both messengers $Ca^{2+}$ and cAMP increase in the cell. Probably all motile systems of protists are regulated by the cAMP to $Ca^{2+}$ ratio. The effects of these two intracellular messengers can be antagonistic, additive or synergistic. The continuing discovery of $Ca^{2+}$-binding proteins different from calmodulins (Van Eldik et al. 1980, Manalan and Klee 1984), much more com-

plicates the postulated mechanisms of CaM action. Each of this new $Ca^{2+}$-birding proteins may have its own role in the regulation of motility.

*In vivo*, this complexity is a major problem in searching for calmodulin-modulated reactions. For instance, the sequestration of $Ca^{2+}$ with EGTA or other calcium chelator in effect alters the reaction rate or completely inhibits a well-characterized enzyme. $Ca^{2+}$ affects, however, so many processes that the same result *in vivo* is incomplete, because it is difficult to distinguish between a direct and indirect effect of EGTA.

A commonly used calmodulin antagonist is trifluoperazine. Calmodulin which binds this compound becomes inactive. All fluoperazines as well as the napthalensulfonamide W-7, W-12 and its chloro-derivative W-13 are hydrophobic. It is necessary to ascertain that the action of used antagonists results from inactivation of calmodulin and not from general hydrophobic effect. This can be done with a purified enzyme, but is very difficult with a living cell under physiological setings. Despite these limitations two strains of *Volvox certari* have been described as possessing phenothiazine-insensitive calmodulin (Kurn and Sela 1981).

This complexity and technical limitations of experimental methods make the evidence for involvement of calmodulin in any particular motile system of protista still fragmentary. Much of the current literature concerning calmoduin is aimed at demonstrating that a known calcium-mediated event, involves CaM as an intermediate. In fact that still is the only disposible way for a combined physiological, biochemical and immunological research on calmodulin.

The study of the existing evidence of the involvement of $Ca^{2+}$ in the motile responses of protists, leads to the conclusion that the ciliary reversal is the only case where the physiological experiments demonstrated calcium translocation as a direct response to external stimuli.

## Calmodulin in Ciliary Reversal

Since the XIX century it is well known, that paramecia placed in KCl solution of concentration ranging from over ten to several tens mM, immediately manifest a ciliary reversal lasting several seconds. It was evident from Kamada (1938, 1940) and Kamada and Kinosita (1940) experiments that $Ca^{2+}$ ions should play a role in this motor responses of *Paramecium caudatum*. The ciliary reversal evoked by $K^{1+}$ ions may be at any moment interrupted by introduction of more calcium ions into the medium. Kamada and Kinosita (1940) also showed that without $Ca^{2+}$ in the medium the ciliary reversal cannot be induced by any concentration of KCl. Injection of KCl into *Paramecium* cytoplasm has no effect on the direction of ciliary beat, but introduction of oxalates into the cell, evoked ciliary reversal. On the basis of this data, Kamada (1940) put forward the hypothesis that in the cytoplasm $Ca^{2+}$ ion is bound with a rather unprecised anion X. The

external action of $K^{1+}$ diffusing into the cell, or internal binding of $Ca^{2+}$ by oxalates, in consequence would liberate anion X, which initiates ciliary reversal.

Jahn (1962) calculated Kamada and Kinosita (1940) data on the duration time of ciliary reversal in *P. caudatum*, in relation to $[K^{1+}]/\sqrt{[Ca^{2+}]}$ in the terms of Gibbs-Donnan ratio. It was clear that the maximum time of ciliary reversal duration is the same independently of the absolute $K^{1+}$ concentration if:

$$\frac{[K^{1+}]}{\sqrt{[Ca^{2+}]}} = \text{const.}$$

On this basis Jahn (1962, 1967) put forward the hypothesis that loss of $Ca^{2+}$ from the outer surface of *Paramecium* membrane evokes ciliary reversal. Grębecki (1965) and Kuźnicki (1966) raised objections against Kamada and Jahn ideas. Grębecki (1965) and Kuźnicki (1966) found that paramecia with decalcified superficial cellular complex become fully insensible to any chemical stimulation except $Ca^{2+}$ ions — a recalcification of their medium evokes ciliary reversal.

The experiments with models of ciliates show that the undulating cilium movement and its reversal are independent phenomena. The cilia on the models of *Paramecium* are reactivated to beat by ATP+$Mg^{2+}$ solutions, while the ciliary reversal occurs when free $Ca^{2+}$ concentration is raised above $10^{-6}$M in presence of ATP (Naitoh and Kaneko 1972). In living ciliates the ciliary reversal is preceded by membrane depolarization. According to Eckert (1972) and Eckert and Naitoh (1972), depolarization causes a transient increase in the $Ca^{2+}$ conductance of the surface membrane of *Paramecium*. Calcium inward current raises the concentration of free $Ca^{2+}$ within cilia which results in changing their beat from the forward to reversed direction. The calcium current hypothesis postulating that ciliary reversal is coupled to membrane potential by a membrane-limited influx of $Ca^{2+}$ from the medium, fails, however, to explain the following facts: (1) The ciliary reversal in *Paramecium* could be evoked by chemical, electrical and mechanical stimuli at $10^{-6}$M $Ca^{2+}$ concentration in the medium. (2) In all membranes $Mn^{2+}$ and $La^{3+}$ ions blockage the calcium permeability, however, both cations induce long-lasting ciliary reversal of *Paramecium* (Kuźnicki 1970, 1973).

In the seventies it became clear that the ciliary reversal is not fully understood. It was then discovered that $Ca^{2+}$ might not act in its free ionic state but requires the presence of a binding protein, especially the calmodulin. Simultaneously with isolation and localization of calmodulin in axoneme of mammalian spermatozoa (Jones et al. 1980) it was established that cAMP is positively correlated with motility in sperm. In contrast, elevation of intracellular $Ca^{2+}$ arrests flagellar motility of sperm (Gibbons 1980). In the majority of experiments the flagellar motility was maintained at low levels of $Ca^{2+}$ ($10^{-7}$M) but inhibited at higher levels of $Ca^{2+}$ ($10^{-6}$M). These results suggest that CaM · Ca may exert an effect on flagellar

movement *via* secondary rather than a primary interaction with ATPase component of the flagellum.

The ciliary system is probably like the flagellar one in that cAMP and CaM · Ca produce opposite effects. Jamieson et al. (1980) suggested that the CaM is required for the initiation and transduction of responses to axoneme. Reed and P. Satir (1980) have shown that the calmodulin may be a part of an axonemal switch that evokes ciliary arrest in ciliated epithelial cells from the gill of freshwater mussels. On the basis of these data the involvement of CaM · Ca in the ciliary reversal has been postulated by B. H. Satir et al. (1980), Kuźnicki (1981), Kuźnicki and Mikołajczyk (1982).

In this regard there are number of specific questions that I would submit to further discussion. Is the calmodulin which participates in the control of the direction of ciliary beat a multifunctional protein, or specialized for the tubulin-dynein system? *Naegleria gruberi* differentiation from amoebae to flagellate forms is associated with synthesis of two calmodulins, one located in flagellum (CaM-1) and the other (CaM-2) in the cell body (Fulton et al. 1986). These data suggest that protists may use different calmodulins for different functions. At second, how calmodulin might be involved in regulating the ciliary reversal? It is generally accepted that all calcium dependent motile systems are regulated by the $Ca^{2+}$ ions bound to calmodulin. An alternative interpretation is offered by the view of Chao et al. (1984) and Cheung (1984) that certain cations ($Mn^{2+}$, $Tb^{3+}$, $Cd^{2+}$, $Sm^{3+}$, $La^{3+}$, $Hg^{2+}$, $Sr^{2+}$, $Pb^{2+}$) are toxic because they effectively activate calmodulin and thus upset its normal regulator by the cellular flux of $Ca^{2+}$. According to the conventional hypothesis the heavy metals like $Hg^{2+}$ and $Pb^{2+}$ cause toxic effects by interacting with essential sulphydryl groups of enzymes, while others like $Cd^{2+}$, have lower affinities and are less toxic. Chao et al. (1984) found that the cations with an ionic radius close to that of $Ca^{2+}$ (0.99 A) effectively substitute for $Ca^{2+}$ ions in calmodulin. In the range 0.74–1.20 A of ionic radii metals activate calmodulin-dependent phosphodiesterase and change the intrinsic fluorescence of calmodulin. It is possible that these cations also support the activity of other calmodulin dependent enzymes. This would create a stimulation in which the activity of calmodulin is no longer regulated by the cellular flux of $Ca^{2+}$ ions.

These findings from Cheung laboratory offer a new interpretation to the unsolved data concerning toxicity and ciliary reversal of *Paramecium* (Table 1). For *Paramecium caudatum* the toxicity series of heavy metal cations was established (Grębecki and Kuźnicki 1956). All these cations in some concentrations induced ciliary reversal and majority effectively activate calmodulin. The lanthanides have higher affinities than $Ca^{2+}$ to calmodulin and also form biologically active complex (Wallace et al. 1982). At the concentrations used for evoking ciliary reversal in *Paramecium* the ability of calmodulin to bind monovalent cations like potassium was also shown (Klee and Vanaman 1982). On the basis

Table 1

Relation between cation toxicity for *P. caudatum*, their ionic radius and the ability of cation induced calmodulin fluorescence and calmodulin dependent phosphodiesterase activity

| Cation* toxicity | | $Ca^{2+} < Sr^{2+} < Ba^{2+} < Mn^{2+} < Zn^{2+} \leq Pb^{2+} \leq Cd^{2+} < Hg^{2+}$ | | | | | | | |
|---|---|---|---|---|---|---|---|---|---|
| Radius A | | 0.99 | 1.13 | 1.34 | 0.80 | 0.74 | 1.20 | 0.97 | 1.10 |
| Phosphodiesterase activity** | % | 100 | 86 | 23 | 70 | 67 | 92 | 90 | 73 |
| | $A_{50}$ μM | 2.8 | 25.0 | — | 4.0 | 5.0 | 2.0 | 3.0 | 3.7 |
| Fluorescence** | Changes % | 100 | 72 | 4 | 54 | 52 | 47 | 81 | 75 |
| | $F_{50}$ cation/CaM | 1.7 | 13.0 | 0 | 2 | 0.9 | 1.2 | 0.8 | 5.0 |

* Modified from Grębecki and Kuźnicki (1956)

** Modified from Chao et al. (1984)

of these data a competition for binding sites on calmodulin between $Ca^{2+}$ and other cations may be suggested as initial molecular mechanism of ciliary reversal. According to it, the ciliary reversal in response to an external stimulation will be initiated by temporary upset of the normal functions of CaM in the membrane and in the axoneme.

In spite of potential artifacts introduced by CaM-antagonists, the voltage-dependent $Ca^{2+}$ current in *Paramecium* is inhibited by W-7 (Hennessey and Kung 1984). This observation is in agreement with the study of the ciliary membrane composition. In the ciliary membrane of *Paramecium tetraurelia*, the presence of calmodulin and guanylate cycles modulated by CaM · Ca has been demonstrated (Klumpp et al. 1983 a, b). The same proteins occur in the ciliary membrane of *Tetrahymena* (Yazawa et al. 1981, Schultz et al. 1983). The discoveries of calmodulin, CaM · Ca-regulated cycles, cGMP and cGMP-dependent kinase in ciliary membrane of *Paramecium* have major contributions to our understanding of the mechanism of $Ca^{2+}$ permeability. The interpretation of these data is in agreement with my assumption that calmodulin in the ciliary membrane, as well as in the axoneme is involved in ciliary reversal This assumption, however, has to be verified, because a soluble protein controlling Ca-channel activity in *Paramecium* does not have the properties of calmodulin (Haga et al. 1984). Actually, the presence of calmodulin in the ciliary membrane is well established, while protein(s) constituting the $Ca^{2+}$ channels in ciliates have not been identified (Kung and Saimi 1985).

The idea that binding of several cations to calmodulin causes ciliary reversal in *Paramecium* needs to be substantiated with new evidence. Further experiments should also confirm that tubulin and dynein are in fact subject to regulation by the ratio of CaM · Ca to cAMP.

## REFERENCES

Bazari W. and Clarke M. 1980: Calmodulin from *Dictyostelium discoideum*. In: Calmodulin and cell function. Ann. N. Y. Acad. Sci., 356, 358–359.

Blum J. J., Hayes A., Jamieson G. A. Jr. and Vanaman T. C. 1980: Calmodulin confers calcium sensitivity of ciliary dynein ATPase. J. Cell. Biol., 87, 386–397.

Blum J. J., Hayes A., McCartney J. E. and Schachat F. H. 1983: Enzymatic and molecular heterogeneity of *Tetrahymena* dynein ATPase: activation of different forms by calmodulin and heat. J. Submicrosc. Cytol., 15, 237–242.

Burgess W. H., Schleicher M., Van Eldik L. I. and Watterson D. M. 1983: Comparative studies of calmodulin. In: Calcium and Cell Function (ed. Cheung W. Y.), Vol. IV, Academic Press, New York, 209–261.

Chao S. H., Suzuki Y., Zysk J. R. and Cheung W. Y. 1984: Activation of calmodulin by various metal ions as a function of ionic radii. Mol. Pharmacol., 26, 75–82.

Cheung W. Y. 1984: Calmodulin; its potential role in cell proliferation and heavy metal toxicity. Fed. Proc., 43, 2995–2999.

Clarke M., Bazari W. L. and Kayman S. C. 1980: Isolation and properties of calmodulin from *Dictyostelium discoideum*. J. Bacteriol., 141, 397–400.

Cox J. A. 1984: Sequential events in calmodulin on binding with calcium and interaction with target enzymes. Fed. Proc., 43, 3000–3004.

Cox J. A., Comte M., Malnoë A., Burger D. and Stein E. A. 1984: Mode of action of the regulatory protein calmodulin (ed. Sigel H.). In: Metal Ions in Biological Systems. New York, Marcel Dekker Inc., 17, 215–273.

Dedman J. R. 1984: The role of calmodulin in the mediation of intracellular calcium. In: Mechanisms of Intestinal Electrolyte Transport and Regulation. Alan R. Liss, New York, 135–146.

Eckert R. 1972: Bioelectric control of ciliary activities. Science, (Wash.), 176, 473–481.

Eckert R. and Naitoh Y. 1972: Bioelectrical control of locomotion in the ciliates. J. Protozool., 19, 237–243.

Fulton Ch., Lai E. Y. and Remillard S. P. 1986: Molecular biology of cytoskeletal proteins in *Negleria*. Acta Protozool., (in press).

Gibbons B. H. 1980: Intermittent swimming in live sea urchin sperm. J. Cell Biol., 84, 1–12.

Gitelman S. E. and Witman G. B. 1980: Purification of calmodulin from *Chlamydomonas*: Calmodulin occurs in cell bodies and flagella. J. Cell Biol., 98, 764–770.

Grębecki A. 1965: Role of $Ca^{2+}$ ions in the excitability of protozoan cell. Decalcification, recalcification, and the ciliary reversal in *Paramecium caudatum*. Acta Protozool., 3, 275–289.

Grębecki A. and Kuźnicki L. 1956: Autoprotection in *Paramecium caudatum* by influencing the chemical properties of its medium. Acta Biol. Exp., 17, 71–107.

Gustin M. C., Bonini N. M. and Nelson D. L. 1983: Membrane potential regulation of cAMP: Control mechanism of swimming behavior in the ciliate *Paramecium*. Neurosci. Abstr., 9, 167.

Haga N., Forte M., Ramanathan R., Hennessey T., Takahashi M. and Kung C. 1984: Characterization and purification of a soluble protein controlling Ca-channel activity in *Paramecium*. Cell, 39, 71–78.

Hennessey T. and Kung C. 1984: An anticalmodulin drug, W-7, inhibits the voltage-dependent calcium current in *Paramecium caudatum*. J. Exp. Biol., 110, 169–181.

Hirschberg R. and Hutchinson W. 1980: Effect of chlorpromazine on phototactic behavior in *Chlamydomonas*. Can. J. Microbiol., 26, 265–267.

Jahn T. L. 1962: The mechanism of ciliary movement. II. Ion antagonism and ciliary reversal. J. Cell. Comp. Physiol., 60, 217–228.

Jahn T. L. 1967: The mechanism of ciliary movement. III. Theory of suppression of reversal by electrical potential of cilia reversed by barium ions. J. Cell. Comp. Physiol., 70, 79–90.

Jamieson G. A. Jr., Bronson D. D., Schachat F. H. and Vanaman T. C. 1980: Structure and function relationship among calmodulins and troponina C-like proteins from divergent eukaryotic organisms. In: Calmodulin and Cell Functions. Ann. N.Y. Acad. Sci., 356, 1–13.

Jamieson G. A. Jr. and Frazier W. A. 1983: *Dictyostelium calmodulin*: affinity isolation and characterization. Arch. Biochem. Biophys., 227, 609–617.

Jamieson G. A. Jr., Vanaman T. C. and Blum J. J. 1979: Presence of calmodulin in *Tetrahymena*. Proc. Natl. Acad. Sci. USA, 76, 6471–6475.

Jamieson G. A. Jr. and Vanaman T. C. 1980: Affinity chromatographic isolation of highly

purified Ca-CaM sensitive dynein ATPases from *Tetrahymena* cilia. In: Calmodulin and Cell Functions. Ann. N. Y. Acad. Sci., 356, 391–392.
Jamieson G. A. Jr., Vanaman T. C., Hayes A. and Blum J. 1980: Affinity chromatographic isolation of highly purified Ca-CaM sensitive dynein ATPase from *Tetrahymena* cilia. In: Calmodulin and cell functions. Ann. N.Y. Acad. Sci., 356, 391–392.
Jones H. P., Lenz R. W., Palevitz B. and Cormier M. 1980: Calmodulin localization in mammalian spermatozoa. Proc. Natl. Acad. Sci., USA 77, 2772–2776.
Kamada T. 1938: Intracellular calcium and ciliary reversal in *Paramecium*. Proc. Imp. Acad. Japan, 14, 260–262.
Kamada T. 1940: Ciliary reversal of *Paramecium*. Proc. Imp. Acad. Japan, 16, 241–247.
Kamada T. and Kinosita H. 1940: Calcium-potassium factor in ciliary reversal of *Paramecium*. Proc. Imp. Acad. Japan, 16, 125–130.
Klee C. B. and Vanaman T. C. 1982: Calmodulin. In: Advances in Protein Chemistry, 35, 213–321.
Klumpp S., Kleefeld G. and Schultz J. E. 1983 a: Calcium/calmodulin-regulated guanylate cyclase of the excitable ciliary membrane from *Paramecium*. J. Biol. Chem., 258, 12455–12459.
Klumpp S., Steiner A. L. and Schultz J. E. 1983 b: Immunocytochemical localization of cyclic GMP, cGMP-dependent protein kinase, calmodulin, and calcineurin in *Paramecium tetraurelia*. Eur. J. Cell Biol., 32, 164–170.
Kung C. and Saimi Y. 1985: $Ca^{2+}$ channels of *Paramecium*: a multidisciplinary study. In: Current Topics in Membranes and Transport. 23, 45–65.
Kuran N. and Sela B. A. 1981: Altered calmodulin activity in fluphenazine-resistant strains: pleiotropic effect on development and cellular organization in *Volvox cartei*. Eur. J. Biochem., 121, 53–57.
Kuźnicki J., Kuźnicki L. and Drabikowski W. 1977: $Ca^{2+}$-regulation of motility and troponin C-like proteins in Protozoa and Myxomycete. Proceedings of the 6th Meeting of the European Muscle Club, Saclay, 29–30 September, Abstr. 67–68.
Kuźnicki J., Kuźnicki L. and Drabikowski W. 1979: $Ca^{2+}$-binding modulator protein in protozoa and myxomycete. Cell Biol. Int. Rep., 3, 17–23.
Kuźnicki L. 1966: Role of $Ca^{2+}$ ions in the excitability of protozoan cell. Calcium factor in the ciliary reversal induced by inorganic cations in *Paramecium caudatum*. Acta Protozool., 4, 241–256.
Kuźnicki L. 1970: Mechanism of the motor responses of *Paramecium*. Acta Protozool., 8, 83–118.
Kuźnicki L. 1973: Excitation-contraction coupling in ciliary reversal. Progress in Protozoology, Fourth Int. Congr. Protozool., U.E.R. Sciences, Clermont-Ferrand, 236.
Kuźnicki L. 1981: Comparison between the ciliary reversal of *Paramecium* and the rapid reorientation in flagellum position of *Euglena*. In: Progress in Protozoology, Abstr., Fourth Int. Congr. Protozool., Warszawa, 208.
Kuźnicki L. and Mikołajczyk E. 1982: Motility and behaviour: Contributed paper session in Memory of Professor Theodore J. Jahn. Progress in Protozoology. Proceeding of VI Inter. Congr. of Protozool., Special Congress Vol. Acta Protozool., Part I, 149–157.
Maihle N. J. and Satir B. H. 1980: Calmodulin in the ciliates *Paramecium tetraurelia* and *Tetrahymena thermophila*. In: Calmodulin and cell functions. Ann. N. Y. Acad. Sci., 356, 408–409.
Maihle N. J., Dedman J. R., Means A. R., Chafouleas J. G. and Satir B. H. 1981: Presence and indirect immunofluorescent localization of calmodulin in *Paramecium tetraurelia*. J. Cell Biol., 89, 695–699.
Manalan A. S. and Klee C. B. 1984: Calmodulin. In: Advances in Cyclic Nucleotide and Protein Phosphorylation Research, 18, 227–278.
Marmé D. and Dieter P. 1983: Role of $Ca^{2+}$ and calmodulin in plants. In: Calcium and Cell Function (ed. Cheung W. Y.), Academic Press, New York, Vol. IV, 263–311.
Maruta H., Baltes W., Gerisch G., Dieter P. and Marmé D. 1982: Signal transduction in chemotaxis of *Dictyostelium discoideum*: role of $Ca^{2+}$ and calmodulin in the regulation of myosin heavy chain kinases and other protein kinases. In: Plasmalemma and Tonoplast: Their Functions in the Plant Cell. (eds. Marmé D., Marre E. and Hertel R.), Elsevier, Amsterdam, 331, 335.
Maruta H., Baltes W., Dieter P., Marmé D. and Gerisch G. 1983: Myosin heavy chain kinase inactivated by $Ca^{2+}$/calmodulin from aggregating cells of *Dictyostelium discoideum*. EMBO, 2, 535–542.
Means A. R., Tash J. S. and Chafouleas J. G. 1982: Physiological implications of the presence, distribution, and regulation of calmodulin in eukaryotic cells. Physiol. Rev., 62, 1–39.

Naitoh Y. and Keneko H. 1972: Reactivated triton-extracted models of *Paramecium*: Modification of ciliary movement by calcium ions. Science, (Wash.), 176, 523–524.
Ohnishi K., Suzuki Y. and Watanabe Y. 1982: Studies on calmodulin isolated from *Tetrahymena* cilia and its localization within the cilium. Exp. Cell Res., 137, 217–227.
Reed W. and Satir P. 1980: Calmodulin in mussel gill epithelial cells: Role in ciliary arrest. In: Calmodulin and cell functions. Ann. N.Y. Acad. Sci., 356, 423–426.
Satir B. H., Garofalo R. S., Gilligan D. M. and Maihle N. J. 1980: Possible functions of calmodulin in Protozoa. In: Calmodulin and cell functions. Ann. N.Y. Acad. Sci., 356, 83–91.
Schultz J. E., Schonefeld U. and Klumpp S. 1983: Calcium/calmodulin-regulated guanylate cyclase and calcium-permeability in the ciliary membrane from *Tetrahymena*. Eur. J. Biochem., 137, 89–94.
Seamon K. B. and Kretsinger R. H. 1983: Calcium modulated proteins. In: Metal Ions in Biology, Vol. 6, Academic Press, New York.
Van Eldik L. J., Piperno G. and Watterson D. M. 1980: Comparative biochemistry of calmodulins and calmodulin-like proteins. In: Calmodulin and cell functions. Ann. N.Y. Acad. Sci., 356, 36–42.
Wallace R. W., Tallant E. A., Docker M. E. and Cheung W. Y. 1982: Calcium binding domains of calmodulin. Sequence of fill as determined with terbium luminescence. J. Biol. Chem., 257, 1845–1854.
Watanable Y. and Nozawa Y. 1982: Possible roles of calmodulin in a ciliated protozoan *Tetrahymena*. In: Calcium and Cell Function. (ed. Cheung W. Y.), Academic Press, New York, Vol. II, 297–323.
Yazawa M., Yagi K., Toda H., Kondo K., Narita K., Yamazaki R., Sobue K., Kakiuchi S., Nagao S. and Nozawa Y. 1981: The amino acid sequence of the *Tetrahymena* calmodulin which specifically interacts with guancylate cyclase. Biochem. Biophys. Res. Commun., 99, 1051–1057.

ACTA PROTOZOOLOGICA
Vol. 25, No. 3, pp. 305–314 (1986)

# Helical Torsion of Cell Cortex Affects Phagotrophy of *sc 6* *Paramecium tetraurelia*

Janina KACZANOWSKA and Teresa GOLC

Institute of Zoology, Warsaw University, Warszawa 00-927/1, Poland

*Received on* 19 December 1985

*Synopsis.* During clonal ageing the *sc 6* mutant of *Paramecium tetraurelia* manifests the morphological heterogeneity of phenotypes (Whittle and Chen-Shan 1972, Kaczanowska 1977). The isolation of *sc 6* twisted dividers from early stationary clones yielded cell-division products of different morphology: the anterior cell represented a normal, straight phenotype, whereas the posterior cell manifested an anticlockwise twist of its cortex along the main body axis. Both daughters are able to twist if introduced to the culture medium promoting expression of *sc 6* trait, but they maintained their different morphologies if supplemented with a portion of fresh bacterized culture medium. *sc 6* cells of different morphologies were used to study their ability to form and to egest the food vacuoles.

It has been ascertained that helical torsion of the cortex and the altered swimming behaviour of *sc 6* twisted *Paramecium tetraurelia* depressed both the uptake and release of food vacuoles with respect to these activities performed by the control wild type and *sc 6* straight cells.

The aim of the present report is to examine the effects of the cortical twist and altered swimming behaviour upon the rate of food vacuoles formation and release.

Phagotrophy in *Paramecium* occurs by a sequent formation of food vacuoles at the bottom of the oral apparatus (Hanson 1962, Allen 1974). During phagotrophy the beating of the oral membranelles within the oral cavity produces a current which facilitates food accumulation, whereby food is swept into the oral pouch. Food vacuoles circulate within the cytoplasm of *Paramecium* (Allen 1974, Berger and Pollock 1981). During this circulation digestion and release of metabolites to the cytoplasm occur. Food vacuoles are eliminated at random through the cellular anus (a cytoproct) (Berger and Pollock 1981). Food vacuoles randomly enter into position at the cytoproct and the actual extrusion of their contents takes a part of a second. The remaining vacuolar membrane is retrieved and recycled for new food vacuole production (Allen and Wolf 1974).

The question arises whether the cortical twist impairing general swimming behaviour and the resulting displacement of the cytoproct in *Paramecium* may affect the rates of ingestion and egestion of food vacuoles. For this purpose, the *sc 6 Paramecium tetraurelia* was used. *sc 6* mutation in homozygozity promotes under some specific external conditions a helical twisting of the cell along its main axis. For instance at the early stationary phase of clones the *sc 6* cells readily begin to twist (Sonneborn 1974). However, the rates of formation and egestion of digestive vacuoles in the wild type and *sc 6* cells decline with clonal ageing (Smith-Sonneborn and Rodermel 1976 and unpublished observation). Therefore in order to obtain *sc 6* cells that would be able to feed but would maintain a different morphology, the twisted dividers were produced and then their daughters were supplemented with a fresh bacterized medium. *sc 6* dividers virtually yielded the anterior straight, morphologically normal and posterior twisted daughters and both these cells were able to feed. *sc 6* cells and wild type controls of the same interfission ages were tested for their ability to form food vacuoles and next to egest them.

It has been ascertained that helical torsion of the cortex of *Paramecium tetraurelia* alters its swimming behaviour. This morphology affects the uptake of food vacuoles and ingested food vacuoles reside longer within the cytoplasm than it occurs in wild type and morphologically normal *sc 6* cells.

The role of mechanical factors upon the rates of the uptake and release of food vacuoles in *Paramecium* is briefly discussed.

## Material and Methods

Two stocks of *Paramecium tetraurelia* were employed. The one used as a control was a wild type wt 51S standard stock (Sonneborn 1970). The experimental stock screwy 6 (*sc 6*) kept as line d4-75 (Sonneborn 1974) was a mutant of stock 51S. This mutant resembles a normal cell twisted about its long axis. Mutants of *sc* group develop heterogeneity of the phenotypes during their clonal ageing as arrays of phenotypes of morphologically normal, moderately and heavily twisted cells (Whittle and Chen-Shan 1972). *wt* and *sc 6* paramecia were cultured in lettuce medium inoculated with *Klebsiella cloacae* (Sonneborn 1970). Lettuce medium inoculated with bacteria for 24–28 h and kept at 27°C will be referred to as "fresh culture medium".

Initial stocks were kept in test tubes at room temperature about 22±2°C and fed only twice a week. Cells diluted 1:9 vol/vol with the fresh culture medium entered after 3 days into a stationary phase. In test tubes containing *sc 6* cells the heterogeneity of phenotypes was checked under dissection microscope. Some cells assigned *in vivo* as straight or twisted were isolated, then fixed and silver stained according to Chatton-Lwoff method (Frankel and Heckmann 1968).

Supernatant from stationary *sc 6* cells that revealed heterogeneity of phenotypes was collected for immediate use as described in section Results. For this purpose test tubes were spun down by centrifugation 500 g×3 min and the supernatant is referred to as "used medium". This supernatant diluted with fresh culture medium, approximately 1:2 vol/vol is referred to as "partially used medium" or P.U.M.

Assay on food vacuole formation: Three groups of cells: wild type, *sc 6* straight and *sc 6* twisted postdividers kept in P.U.M. were supplemented at 0 time with latex beads (PLP Dovex 0.76 μm diam.) at final concentration $10^5$ beads/ml. These groups of cells were periodically assayed for the total number of labelled food vacuoles. Individual cells were picked up, put on the specimen slide and fixed with Peronyi fixative (Preer 1975) and examined under light microscope to score number of individual food vacuoles. Pooled data from four independent replicas of experiment are used to get means and standard deviation for about 30 individual cells for each tested period of feeding for every type of cells.

Assay on kinetics of loss of labelled food vacuoles: Three groups of cells: wild type, *sc 6* straight and *sc 6* twisted postdividers kept in P.U.M. were prelabelled with PLP beads during 5 min. During the next 5 min these labelled cells were individually reisolated into the PLP-deprived P.U.M. The number of labelled food vacuoles was periodically assayed in individual cells. Pooled data of three independent replicas of experiment were used to get particular means and standard deviation exactly as described above.

Estimation of rates of the uptake and egestion in *wt*, *sc 6* straight and *sc 6* twisted cells: Total numbers of food vacuoles taken up during 10 min by every kind of cells and their gradual egestion were calculated as described for *Chilodonella steini* (Sawicka et al. 1983). Statistical calculations followed the methods described by Sokal and Rohlf (1969).

## Results

### Test of Reliability of *in vivo* Specification of *sc 6* Phenotypes

Whittle and Chen-Shan (1972) noted that twisted cells heavily rotate during their forward swimming. To test this notion, three days old mass cultures of *sc 6* were used. Under dissection microscope the cells were *in vivo* classified as "straight" or "twisted", depending on their swimming behaviour, and then isolated, fixed and stained.

Morphometrical and cytogeometrical studies on the cortical pattern of 51S and *sc 6* cells designated *in vivo* as "straight" revealed a virtual stability of cortical parameters of all nondividing cells (to be published elsewhere). This pattern is consistent with the detailed descriptions of Sonneborn (1963) and Kaneda and Hanson (1974). In brief: the oral sector is marked by a complex comprising the preoral suture, the oral apparatus and the postoral suture with a cytoproct. This sector extends along the main body axis from anterior to posterior poles. The postoral suture is flanked to the right by nearly meridional ciliary rows. At the postoral suture there is a long silver-stained line representing the lips of the cytoproct (Allen and Wolf 1974). The cytoproctal slit extends along the main body axis.

In 30 cells asigned *in vivo* as "straight", 28 represented wild type morphological phenotype, and only two manifested a slight helical twist of the postoral suture. This suture was slightly rotated to the left.

Twisted *sc 6* phenotypes that manifested *in vivo* apparent rotation during forward swimming, in stained preparations displayed the helical spiralization of the oral sector. Preoral suture slightly twisted to the left was followed with the obli-

quely positioned oral apparatus. The postoral suture was highly spiralized and the cytoproct was displaced onto the lateral or even dorsal side of the cell.

All the cells designated *in vivo* as "twisted", in fact represented morphologically twisted phenotypes (30 cells tested).

## Preparation of Phagocytic *sc 6* Sister Cells of Different Phenotypes

Although principle in culture medium promoting expression of twisted phenotypes remains unknown (Whittle and Chen-Shan 1972) it was noted that these phenotypes appear readily at early stationary phase and/or in slowly dividing *sc 6* cells. The aim of the present paper was to find out medium that maintains slow fission rate and phagocytotic activity of *sc 6* cells at a time. We made it as follows:

(1) test tubes containing one aliquote of initial *sc 6* stock manifesting heterogeneity of phenotypes were supplemented with 9 aliquotes of fresh culture medium for 72 h at room temperature,

(2) test tubes were examined for heterogeneity of *sc 6* phenotypes. Tubes containing many twisted cells were sampled. Samples were diluted with fresh culture medium roughly 1:1 vol/vol to induce cell divisions. It appeared that both straight and twisted cells were able to divide,

(3) twisted dividers found during 20 min in samples (see point 2) collected either in used medium or in P.U.M. to get postdividers of the same ages,

(4) eighteen straight and 12 apparently twisted postdividers introduced into used culture medium were re-isolated again to used culture medium and examined morphologically the next day. Twenty straight and 18 twisted postdividers from P.U.M. were isolated again to P.U.M. to examine their fission rate during three subsequent days. After three days the derived clones were tested for heterogeneity of phenotypes within the progeny,

(5) most postdividers (point 3) were split into straight and twisted groups of cells for subsequent studies on food vacuole formation and egestion. These cells were introduced into P.U.M. and assayed with PLP after about 3 h,

(6) control wild type postdividers were parallely received (points 2–4) and introduced into P.U.M. They were also tested for their phagocytotic activities 3 h later.

## Study on the Fates of Straight and Twisted Sisters

Straight cells introduced into P.U.M. yielded a nearly straight progeny at first division, but heterogeneity of the phenotypes was resumed during three days. Twisted cells introduced into P.U.M. yielded anterior straight and posterior twi-

sted daughters. This heterogeneity of the phenotypes was maintained during three days. Hence, both straight and twisted isolates during their clonal reproduction yielded the same pattern of intraclonal polymorphism.

All clones, regardless of the morphology of stem isolates introduced into P.U.M., revealed uniform circadian daily fission rate during three days (about 1.0 for straight founder isolates, and 1.1 for twisted founders).

Straight divider yielded two straight daughters. Twisted divider yielded a virtually straight anterior and twisted posterior offspring. Both kinds of daughters, straight and twisted, are able to gain the same twisted phenotype if introduced to the used medium that promotes the appearance of twisted phenotypes. The twist of a straight cell within the used medium may occur without cell division. Thus, under a stimulus of external medium, all cells are able to twist irrespective of their origin as anterior or posterior cell during preceding division.

## Changes of the Total Numbers of Ingested Labelled Food Vacuoles during Constant Feeding in *wt*, *sc 6* Straight and *sc 6* Twisted Cells

Pooled data concerning the three groups of cells are presented in Fig. 1. It appears that all kinds of cells were strongly stimulated to feed with PLP at the start of the experiment and subsequently the total number of ingested labelled food vacuoles residing in the cells gradually declined.

Mean numbers of labelled food vacuoles found at a time in *wt* cells fed during 15 to 50 min and next during 100–120 min are statistically ($p = 0.05$) different from those found in *sc 6* twisted cells. *wt* cells possessed high numbers of labelled food vacuoles during the first 50 min of feeding, followed by an abrupt decline during the second hour of the experiment, whereas *sc 6* twisted cells kept low numbers of food vacuoles during the first hour of feeding and the decrease of these numbers during the second hour of the experiment was slow. Behaviour of *sc 6* straight cells follows the kinetics of changes of *wt* cells.

## Loss of Prelabelled Food Vacuoles in Label-deprived Medium in *wt*, *sc 6* Straight and *sc 6* Twisted Cells

Pooled data on the decline of the total numbers of prelabelled food vacuoles in three kinds of cells as a function of time that elapsed from the removal of label are presented in Fig. 2. *wt* and *sc 6* straight cells manifested a very rapid loss of labelled food vacuoles. Twisted cells revealed significantly different ($p = 0.05$) kinetics of decline. These cells manifested a very slow rate of decrease of the total numbers of labelled food vacuoles.

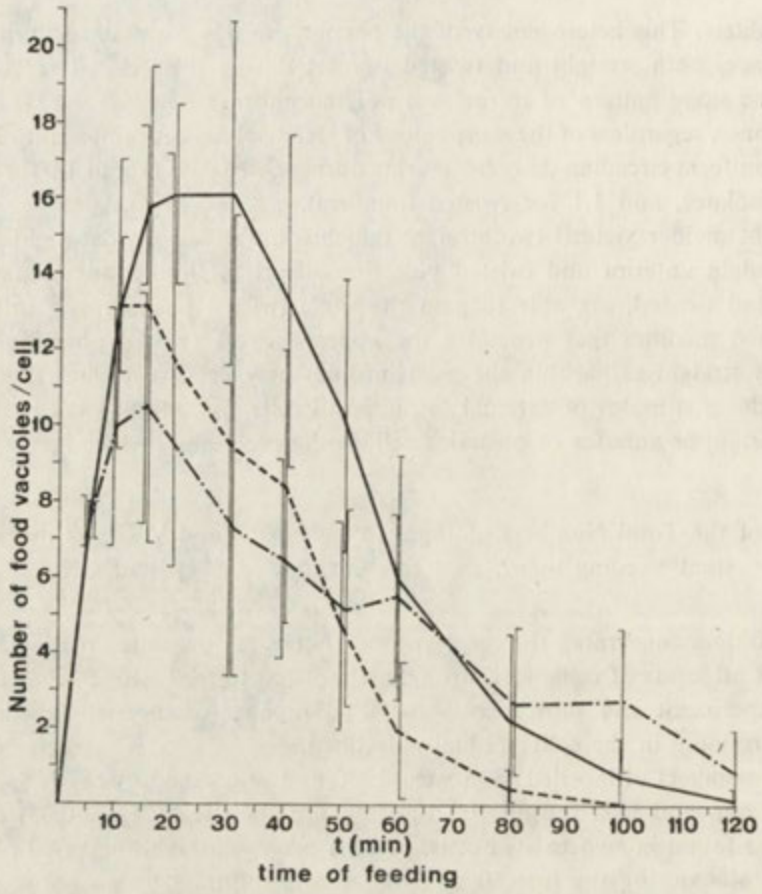


Fig. 1. Kinetics of mean total number of PLP-labelled food vacuoles per individual cell in different kinds of cells as a function of time of feeding with label. *Abscissa* — phagocytosis time (min) spent in the presence of label. *Ordinate* — mean average numbers of ingested food vacuoles labelled with PLP per cell. Experiment performed as described in section Material and Methods: *wt* cells — heavy lines, *sc 6* straight cells — dashed line, *sc 6* twisted cells — dashed and dotted line. Every mean comprizes pooled data of 30 cells, bars represent standard deviation values of means

## Rates of Ingestion and Egestion of Food Vacuoles during 30 min in *wt*, *sc 6* Straight and *sc 6* Twisted Cells

The rates of uptake of food vacuoles during 30 min of feeding were calculated from the data presented in Figs 1 and 2 as sums of total input, total output and maximal total number of PLP labelled food vacuoles residing within the cell cytoplasm (Sawicka et al. 1983) in the particular type of cells.

During 30 min the *wt* and straight *sc 6* cells produced an equal average number of food vacuoles (respectively 23.0 and 25.1 food vacuoles per cell). *sc 6* twisted

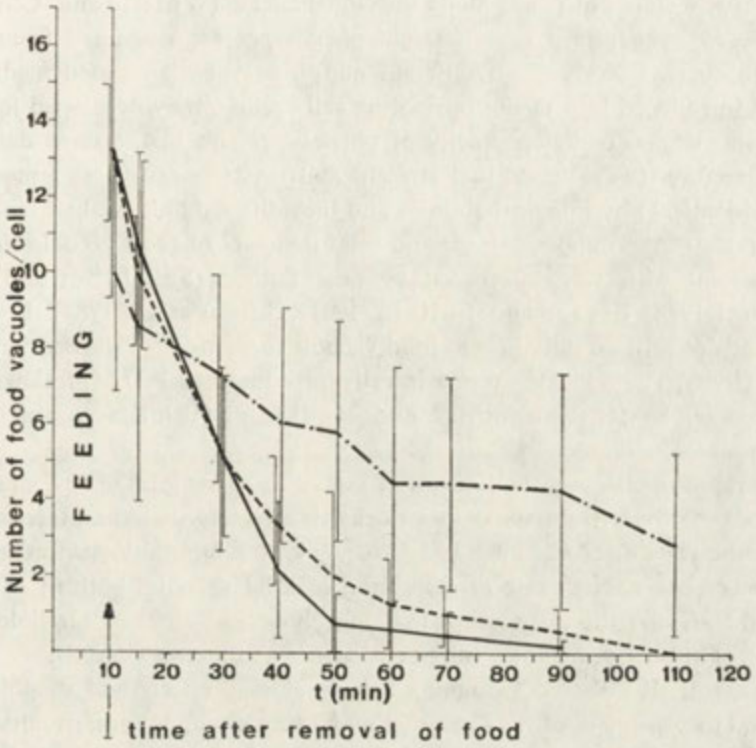


Fig. 2. Kinetics of decrease of mean total number of PLP-labelled food vacuoles ingested by individual cells of different kinds during 10 min of feeding as a function of time of subsequent incubation in PLP-depleted medium. Other explanations and legends as in Fig. 1

phenotype produced less ($p = 0.05$) food vacuoles than *wt* cells, i.e., about 15.8.

Egestion of ingested food vacuoles in *wt* and straight *sc 6* involved defecation of about 8 food vacuoles during 30 min since the start of feeding. During this period the *sc 6* twisted cells extruded a variable number of food vacuoles (high *sd* values) averaging to 2.6 food vacuole per cell.

## Discussion

The presented data revealed that twisted phenotypes are generated in ageing *sc 6* cells in the presence of a specific culture medium. This twist is produced during the interphase period of the cell-cycle. Thus divisional morphogenesis does not generate *per se* the cortical twist of the offspring, but merely separates differently shaped daughters originating from less twisted anterior and more twisted posterior parts of the parental twisted cell. Although the heterogeneity of phenoty-

pes within *sc 6* clones increases along the clonal ageing (Whittle and Chen-Shan 1972) in every generation some straight phenotypes are generated from anterior fission products. Sister cells of different morphology twist in used medium. However, if introduced into media promoting cell-cycling, they developed into clones of the same degree of heterogeneity of phenotypes and of the same daily fission rates. Therefore it is assumed that straight and twisted *sc 6* sisters represented similar or identical physiological abilities and they differed only in their morphology.

The rates of the uptake, release and total numbers of food vacuoles in *wt* cells are consistent with values reported by other authors (Smith-Sonneborn and Rodermel 1976, Berger and Pollock 1981, Cohen et al. 1984). In all three tested kinds of cells an initial rapid food vacuole formation is followed by a decline of this activity. These kinetics tested in cells introduced to P.U.M. follows the pattern noted by Smith-Sonneborn and Rodermel (1976) for ageing *Paramecium tetraurelia*.

The rate of uptake and the kinetics of loss of food vacuoles in *sc 6* straight phenotype do not differ from those in *wt* cells. It suggests that the presence of *sc 6* allele in the cells does not alter phagotrophy until a morphological expression of its presence occurs. High rate of defecation of food vacuoles both in *sc 6* and *wt* cells further favors the assumption that morphological and not physiological impairment of the food vacuoles turn-over occurs in the twisted cells.

We suggest that altered swimming behaviour may affect food vacuole uptake, and dorsal displacement of the cytoproct may delay a random opportunity (Berger and Pollock 1981) that food vacuole is extruded by the cytoproct. Such food vacuoles trapped within the cytoplasm were also observed when food vacuole movement within the cytoplasm was impaired in *wt* double *Paramecium tetraurelia* (Kaczanowska and Garlińska 1981). An alternative assumption that the function of displaced cytoproct is mechanically impaired is less likely, since a displaced cytoproct in twisted *sc 6* cells is not shut down (Dubielecka and Kaczanowska 1984).

All these data prove that the helical twist and morphological displacement of the cortical organelles may affect the swimming behaviour and food vacuoles internalization, and decreases the probability of their defecation.

ACKNOWLEDGEMENTS

We are much indebted to the late Professor Dr. T. M. Sonneborn for the generous supply of the stocks used in this study.

We acknowledge a partial support of this work from the grant of the Polish Academy of Sciences to Dr. A. Kaczanowski.

## REFERENCES

Allen R. D. 1974: Food vacuole membrane growth with microtubule – associated membrane transport in *Paramecium*. J. Cell Biol., 63, 904–922.

Allen R. D. and Wolf R. W. 1974: The cytoproct of *Paramecium caudatum*: Structure and function, microtubules and fate of food vacuole membranes. J. Cell Sci., 14, 611–631.

Berger J. D. and Pollock C. 1981: Kinetics of food vacuole accumulation and loss in *Paramecium tetraurelia*. Trans. Am. Microsc. Soc., 100, 120–133.

Cohen J., Garreau de Loubresse N. and Beisson J. 1984: Actin microfilaments in *Paramecium*: Localization and role in intracellular movements. Cell Motility, 4, 443–468.

Dubielecka B. and Kaczanowska J. 1984: Experimental studies on positioning and sizing of the cytoproct in *Paramecium tetraurelia* J. Exp. Zool., 229, 349–359.

Frankel J. and Heckmann K. 1968: A simplified Chatton-Lwoff silver impregnation procedure for use in experimental studies with ciliates. Trans. Am. Microsc. Soc., 87, 317–321.

Hanson E. D. 1962: Morphogenesis and regeneration of oral structures in *Paramecium aurelia*: An analysis of intracellular development. J. Exp. Zool., 150, 45–68.

Kaczanowska J. 1977: Morphometrical studies on screwy 1° mutant of *Paramecium tetraurelia*. Fifth Int. Congr. Protozool., (ed. S. H. Hunter), New York, p. 295.

Kaczanowska J. and Garlińska T. 1981: Endocytosis and exocytosis of doublets of *Paramecium tetraurelia*. Acta Protozool., 20, 135–144.

Kaneda M. and Hanson E. D. 1974: Growth, patterns and morphogenetic events in the cell cycle of *Paramecium aurelia*. In: *Paramecium* – a Current Survey (ed. W. J. van Wagtendonk), Elsevier Publ. Comp., Amsterdam, pp. 210–262.

Preer J. B. 1975: The hereditary symbionts of *Paramecium tetraurelia*. Soc. Exp. Biol., 29, 125–144.

Sawicka K., Kaczanowski A. and Kaczanowska J. 1983: Kinetics of ingestion and egestion of food vacuoles during cell-cycle of *Chilodonella steini*. Acta Protozool., 22, 157–167.

Smith-Sonneborn J. and Rodermel S. R. 1976: Loss of endocytic capacity in ageing *Paramecium*. The importance of cytoplasmic organelles. J. Cell Biol., 71, 575–588.

Sokal R. R. and Rohlf F. J. 1969: Biometry (eds. Freeman et al.), San Francisco.

Sonneborn T. M. 1963: Does preformed structure play an essential role in cell heredity? In: Nature of Biological Diversity (ed. J. M. Allen), McGraw-Hill Book Comp., New York, San Francisco, Toronto and London, pp. 165–221.

Sonneborn T. M. 1970: Methods in *Paramecium* research. In: Methods in Cell Physiology, Vol. 4 (ed. D. M. Prescott), Academic Press, New York and London, pp. 241–339.

Sonneborn T. M. 1974: *Paramecium aurelia*. In: Handbook of Genetics, Vol. 2, (ed. R. C. King), Plenum Press, New York, pp. 465–594.

Whittle J. R. S. and Chen-Shan L. 1972: Cortical morphogenesis in *Paramecium aurelia*: mutants affecting cell shape. Genet. Res. Camb., 19, 271–279.

ACTA PROTOZOOLOGICA
Vol. 25, No. 3, pp. 315–324 (1986)

# Measurement of Intracellular Ion Activities in Protozoan Cells with Ion-selective Microelectrodes

Stanisław FABCZAK

Department of Cell Biology, Nencki Institute of Experimental Biology, Polish Academy of Sciences, 3 Pasteur Str., 02-093 Warszawa, Poland

*Received on* 20 January 1986

*Synopsis.* Determination of intracellular ion activities is a crucial factor for understanding the physiology of living cells, therefore a number of methods to measure ionic concentrations or ion activities in their interior have been developed. The most direct way to measure ion activities is by means of ion-selective microelectrodes (ISMs) introduced into cell cytoplasm. Since ISMs can be now routinely fabricated, the determination of ion activities of $Na^+$, $K^+$, $H^+$, $Mg^{2+}$ and $Cl^-$ ions and monitoring of their changes even in small cells is possible. The main aim of this article is to outline some of the theoretical and practical aspects underlying the ISM construction and its application for measuring ion activities in the cytoplasm of protozoan cells *in vivo*.

It is now generally accepted that the bioelectrical activity of living cells depends on the transmembrane concentration (activity) gradients of different ions. Each individual ion remains in its characteristic ionic equilibrium condition expressed by the Nernst equation:

$$E_i = \frac{RT}{Fz_i} \ln \frac{a_i^o}{a_i^i}, \tag{1}$$

where $E_i$ is the equilibrium potential for the "$i$" ion, $R$, $T$ and $F$ are thermodynamical constants, $z_i$ is "$i$" ion valency and $a_i^o$ and $a_i^i$ are ion activities on internal ($i$) and external ($o$) membrane sides. The electrical potential difference (EMF) across the cell membrane is a function of equilibrium potentials ($E_i$) for particular ions occurring in the cell cytoplasm and the external solution. In order to estimate the contribution of an ion in the active and passive functional properties of the membrane, both the intra- and extracellular ion activities should be measured.

These activities might be deduced from EMF measurements across cell membrane with the aim of ISMs.

The first ISM for intracellular measurements *in vivo* was a glass pH microelectrode manufactured by Caldwell (1954). The later development of $Na^+$ and $K^+$ selective glasses (Eisenman et al. 1957) and a number of ion exchanger-resins (Walker 1971, Khuri et al. 1974, Oehme and Simon 1976, Kraig and Nicholson 1976, Di Polo et al. 1976, Oehme et al. 1976, Brown et al. 1976) have recently extended the application of ISMs for the intracellular measurement of most physiologically important inorganic ions in a variety of cells of higher organisms and unicellular protozoan ones (Fabczak 1983, Fabczak and Kuźnicki 1985).

Theory of ISMs. ISM is a sensor containing an electrochemical liquid membrane as an essential component. The membrane is composed of a cation-selective ligand in a water immiscible solvent. When a membrane is introduced between two aqueous solutions, an electrical potential difference (EMF) appears. The EMF value is described by the Nicolsky–Eisenman equation (Nicolsky 1937, Eisenman 1967, Durst 1974):

$$E = E_o + \frac{RT}{Fz_i} \ln \left[ \frac{a_i' + \sum_j K_{ij} (a_j')^{z_i/z_j}}{a_i'' + \sum_j K_{ij} (a_j'')^{z_i/z_j}} \right], \tag{2}$$

where $E_o$ is a constant reference potential, $a_i'$ and $a_i''$ are the activities of the "$i$" ion with charge $z_i$ on both sides of selective membrane, $a_j'$ and $a_j''$ are the activities of an interfering "$j$" ion with $z_j$ charge on both membrane sides and $K_{ij}$ is the selectivity coefficient for the "$i$" ion in respect to the "$j$" one. In a sample solution consisting of both ions the EMF across the selective membrane with constant internal filling solution (Fig. 1) is described by Eqn. (2) as:

$$E = E_o' + \frac{RT}{Fz_i} \ln [a_i'' + \sum_j K_{ij} (a_j)^{z_i/z_j}], \tag{3}$$

where $E_o'$ is the constant reference potential for the ISM assembly, $a_i$ and $a_j$ are the ion activities of the "$i$" ion and interfering "$j$" one in sample solution, respectively. In solution with no ion interference (i.e., when $K_{ij} = 0$) Eqn. (3) is reduced to the Nernst form:

$$E = E_o' + \frac{RT}{Fz_i} \ln a_i \tag{4}$$

or

$$E = E_o' + S \log a_i, \tag{5}$$

where $S$ is a slope factor which indicates the change in the EMF value of ISM at a ten-fold change of $a_i$ in sample solution. Therefore, the EMF response for the ideal ISM to the ten-fold change of $a_i$ of a single-charged cation is given by:

$$S = \frac{RT}{F} \log 10 = 59.16 \text{ mV} \quad (\text{at } 25°\text{C}). \tag{6}$$

In practice, in physiological solutions consisting of different ions, ISMs are exposed to some ion interference and ISM responses must be described by Eqn. (3). Often it is difficult to describe the ISM value by Eqn. (3) because the selective coefficient, $K_{ij}$, does not necessarily have a fixed value in the course of experimentation. As has been shown the $K_{ij}$ depends on the ionic strength of sample solution (Armstrong and Garcia-Diaz 1980) and tip diameter (Bolton and Vaughan-Jones 1977) of an ISM.

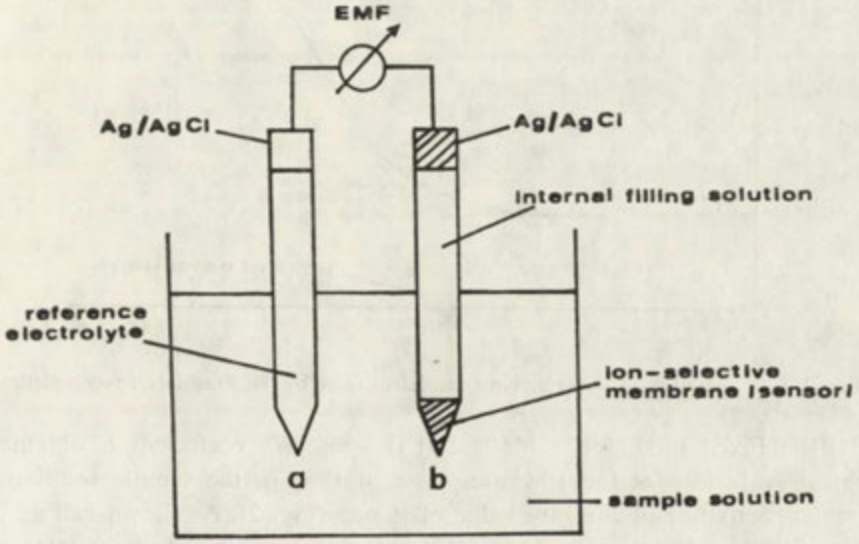


Fig. 1. Schematic diagram of an electrode assembly circuit with conventional (a) and ion-selective electrodes (b)

ISM Selectivity Coefficient. A number of different methods for the assessement of the $K_{ij}$ for the ISMs have been described (Thomas 1977, Simon et al. 1978, Bailey 1980). In general, the methods used fall into the following groups:

(I) the Separate Solution Method (SS) in which the $K_{ij}$ is obtained experimentally by comparison of EMF generated by ISM in a single-electrolyte solution. In the sample solution consisting of "$i$" ion with activity $a_i$, the EMF is given by the Eqn. (5):

$$E_i = E_o + S \log a_i \tag{7}$$

whereas in the solution with interfering "$j$" ion only, the EMF is described by the Eqn. (3):

$$E_j = E_o + S \log K_{ij} (a_j)^{z_i/z_j}. \tag{8}$$

With the aim of both Eqns (7) and (8) the value of $K_{ij}$ can be estimated as:

$$K_{ij} = 10^{(E_j - E_i)/S} a_i (a_j)^{z_i/z_j}. \tag{9}$$

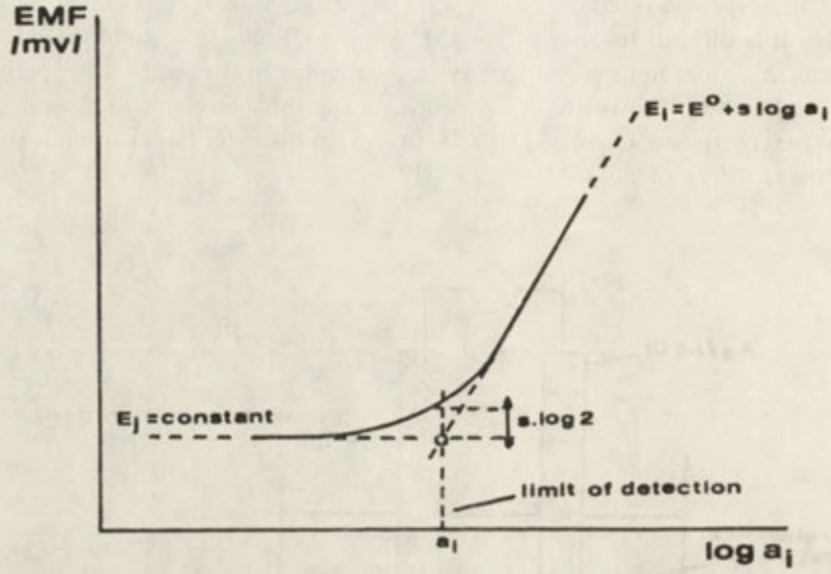


Fig. 2. Determination of the selectivity coefficient ($K_{ij}$) by the fixed interference method

(II) the Fixed Interference Method (FI) where $K_{ij}$ coefficient is obtained by graphical evaluation of the EMF response of ISM in the sample solution with different $a_i$ activity and constant value of $a_j$ one (Fig. 2). As shown in Fig. 2 the $a_i$ value for $K_{ij}$ calculation from Eqn. (9) is found as the point at the intersection of the two asymptotes corresponding to $E_i$ and $E_j$, respectively (i.e., at the point of $E_i = E_j$):

$$K_{ij} = \frac{a_i}{(a_j)^{z_i/z_j}} . \tag{10}$$

(III) the Fixed Primary Ion Method (FPI) which is the reverse of the FI-method. Here the EMF responses of ISMs is obtained in the sample solution with varied $a_j$ activities and constant activity of primary "$i$" ion, and EMF values are plotted as a function of log $a_j$. Coefficient $K_{ij}$ can be calculated then by Eqn. (10) in the same way as in the FI-method. The $K_{ij}$ values obtained by these methods will to some degree depend on the external condition chosen (i.e., concentration of the

sample electrolyte in the SS-method and concentration of interfering electrolyte in the two other ones). Therefore, in order to compare the $K_{ij}$ coefficients obtained by different methods, the experimental conditions should be precisely specified (i.e., ion activities, pH, temperature or the value of association constant to estimate ion activity etc.). The detection limit of ISM's for specified chemical or biological systems is given by the same value of $a_i$ chosen for $K_{ij}$ calculation in the FI-method (Fig. 2).

Electrode Construction. A procedure for making liquid membrane ISMs involves usually the following steps:

(I) glass selection; the best glass are borosilicate capillaries, because of their high reactivity with siliconizing agents (Hair and Hertl 1973),

(II) capillary cleaning; cleaning of glass tubings of oily contaminants improves the result of the following siliconization (Johannson and Torok 1946). It can be done simply by their immersion in hydrochloric acid with subsequent rinsing with ethanol and boiling in distilled water or keeping in hot ethanol vapour and then drying (Walker 1971),

(III) capillary pulling; cleaned and dried glass capillaries are pulled with a commercially available puller with the settings to give the desired tip diameter,

(IV) bevelling; since the ISM operational characteristics depend on the tip diametre (Armstrong and Garcia-Diaz 1980), bevelling has been used to obtain micropipettes with relatively large working surface of the microelectrode tip and can still penetrate the cell without causing damage (Dahl and Isenberg 1980, Marban et al. 1980). The bevelling apparatus commercially or noncommercially available can be used with satisfactory results (Odgen and Citron 1978, Lederer et al. 1979),

(V) siliconization (silanization); the liquid membrane sensors for ISMs are highly water-immiscible, therefore, before their introduction into the tip of a micropipette it is necessary to make its inner wall hydrophobic by treating it with an organic silicon agent (Johannson and Torok 1946, Thomas 1978, Tsien and Rink 1980). This is important not only for the mechanical stability of the liquid selective membrane in the microelectrode tip, but also will decide of the subsequent performance of ISM. In general, under-siliconization of the inner electrode wall will lead to the forming a thin layer of relatively high conductivity, thereby shunting the EFM of the ISM. On the other hand, over-siliconization will partially or completely block the ISM tip and induce undesirable high ISM resistance. The number of siliconization procedures has been described. Usually the electrode tip is dipped into a fresh solution of 3% tri-N-butylchlorosilane in chloronaphthalene until a column of silicone solution fills the tip to the height of about 200–500 μm and later it is baked at 100°C for one hour to complete the silanization procedure (Coles and Taskopoulos 1977, Berrige and Schlue 1978, Djamgoz and Laming 1981),

(VI) filling with sensor; a small quantity of the liquid sensor can be introduced into the micropipette tip after siliconization with injection as far down the electrode shank from the back or simply by suction of the liquid sensor through the open electrode tip to the desired height (Lux and Neher 1973, Djamgoz and Laming 1981),

(VII) filling with reference solution; following the introduction of the sensor into the microelectrode tip, the rest of the microelectrode is filled with reference solution (Fig. 1) and the end of a Ag/AgCl wire is sealed to the electrode shank to complete the ISM assembly. When the liquid sensor is sucked through the open tip, the electrode is usually filled with reference electrolyte first. The latter method is recommended when filamented glass tubing is available,

(VIII) microelectrode shielding; fluctuations of the sample solution level in the calibration or experimental chambers might cause large capacitative artifacts. It can be avoided by application to the ISM of a signal-driven guard or by painting the electrode shank with a conductive paint.

Electrode Calibration. Prior to applying ISMs in the experiment, they have to be calibrated by measuring their electrical responses (EMF) in series of standard solutions consisting of varying concentrations of the ion to be detected. In general, the calibration solutions, besides the primary ion should contain other

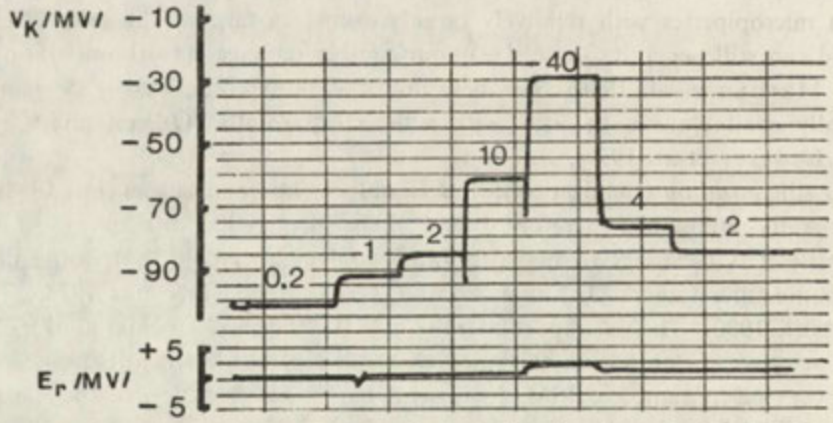


Fig. 3. Preimpalment calibration of the potassium-selective microelectrode ($K^+$-ISM). The EMF responses of both the conventional reference microelecrode ($E_R$) and the $K^+$-ISM ($E_K$) were recorded in standard solutions with potassium activity ($a_K$) of 0.2, 1, 4, 10 and 40 mM

ions as well, to mimic the intracellular composition of ions as closely as possible. Figure 3 illustrates the EMF values of the $K^+$-ISM during calibration in standard solutions of KCl+Tris/HCl or in solutions of KCl+NaCl with constant ionic strength of 40 mM ($K^+$-activity coefficient is 0.75). Both microelectrodes, the conventional reference and selective one were filled with 0.1 M KCl, while the ISM tip was filled with $K^+$-ion-exchanger liquid (Corning Co. cat. No. 477317). The

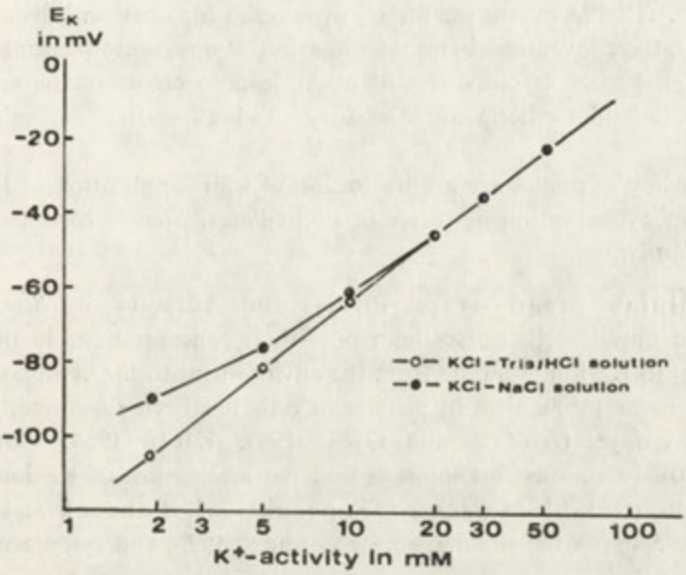


Fig. 4. EMF response from Fig. 3 plotted vs. log of $K^+$ activities ($a_K$). Coefficient of $K^+$ ion activity is 0.75. The calibration points can be fitted by Eqn. 3 to within 1 mV at the $K_{KNa} = 1.38 \times 10^{-2}$

obtained ISM electrical responses in calibration solutions were plotted vs. $K^+$-ion activities (Fig. 4). As shown in Fig. 4 the EMF values for $K^+$-ISM were linear in the calibration solutions of KCl+Tris/HCl in the range of $a_K$ of 1–100 mM and in solutions of KCl+NaCl in the range of 10–100 mM of $a_K$. Each tenfold change of $a_K$ in these ranges gives the EMF difference by 56 mV. However, at low ion activity for $K^+$ ions in solutions of KCl+NaCl, the EMF values deviate from the straight line, because the large $Na^+$ interference in respect to the primary $K^+$ ion, especially below $a_K$ of 10 mM.

Electronics. ISMs have electrical resistance ranging from $10^9$ to $10^{11}$ ohms, owing mainly to their ion-selective component and, therefore, they require the use of preamplifiers with very high input impedance of $10^{14}$ or even $10^{15}$ ohms which will draw the negligible current from the electrode (Thomas 1977, Tsien 1980). Such high-resistance electrodes suffer from external electrical interferences, thus, both experimental and calibration chambers require careful electrical shielding with a metallic enclosure.

Intracellular Measurements. During the puncture of the cell with ISM, the recorded electrical response ($E_i'$) is the sum of the transmembrane electrical potential ($E_m$) and the ion electrochemical potential ($E_i$) associated with "$i$" ion activity. To obtain the $E_i$ value separately, the membrane potential should be simultaneously measured with a conventional microelectrode and subtracted from ISM response:

$$E_i = E_i' - E_m = E_o + S \log a_i. \qquad (11)$$

Therefore, reliable measurements of $E_i$ may be obtained only when both microelectrodes, the conventional and the ion-selective one, sense the same membrane potential ($E_m$). Errors in measurement of $E_i$ lead to errors in the estimation of $a_i$, therefore, reliable criteria are necessary to check satisfactory microelectrode impalements.

The following examples are an illustration of some application of ISMs to measurements of cytosolic ion activities in two ciliates, *Stentor coeruleus* and *Paramecium caudatum*.

Intracellular Steady-state Potassium Activity in *Stentor* Cells. Neurone and muscle cells posses high potassium concentrations in the cell cytoplasm, owing to $K^+$ ion pumping from the environment to the cytoplasm. The presence of a similar mechanism in protozoan cells has been suggested, but not definitively proved yet (Andrus and Giese 1963, Klein 1964, Conner 1967, Hilden 1970). In the first attempts to find the mechanism of $K^+$ ion regulation in *Stentor* cells, the $K^+$-ISM was used (Fabczak 1983, Fabczak and Kuźnicki 1985). Figure 5 shows the simultaneous recordings of $E_m$ and cytoplasm potassium

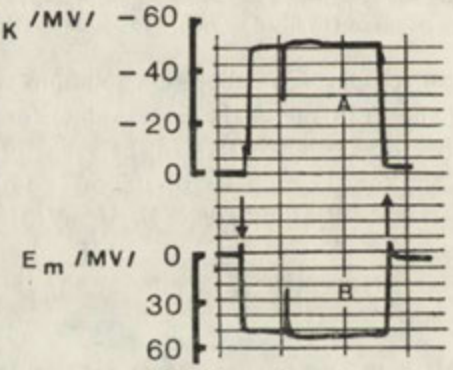


Fig. 5. Simultaneous recordings of membrane potential ($E_m$) and $K^+$ electrochemical potential ($E_K$) across *Stentor* cell membrane

activity ($E_K$). In resting conditions intracellular potassium activity ($a_K$) and membrane potential ($E_m$) were found to be 15.2 mM and −50.8 mV, respectively. In the *Stentor* cells adapted to low temperature a significant decrease in internal $a_K$ was noticed. These findings suggest that *Stentor* cells regulate intracellular $a_K$ level by active transport of potassium to the cell cytoplasm.

Calcium Current and Intracellular pH in *Paramecium* Cells. It has been shown that changes in extra- and intracellular $H^+$ activities of different cells in higher organisms may modify the structure and function of membrane ion channels. In *Paramecium* cells the effect of internal pH changes ($pH_i$) on the calcium channel function and membrane excitability has been investigated under voltage-

clamp conditions (Umbach 1982). Cytoplasmic $pH_i$ was measured with $H^+$-ISM (Thomas 1978). Under standard external conditions the resting $pH_i$ was 6.8. Alkalization of cell cytoplasm enhanced the early $Ca^{2+}$ current, while internal acidification depressed it. Extracellular pH changes had little effect on $pH_i$ or membrane potential. It was concluded that $H^+$ ions can affect the $Ca^{2+}$ current by direct interaction with sites located near the ion channel.

## REFERENCES


Andrus W. W. and Giese A. C. 1963: Mechanism of sodium regulation in *Tetrahymena pyriformis* strain W. J. Cell Comp. Physiol., 61, 17–30.

Armstrong W. and Garcia-Diaz J. F. 1980: Ion-selective microelectrodes: theory and technique. Fed. Proc., 39, 2851–2859.

Bailey P. L. 1980: Analysis with Ion-selective Electrodes. 2nd ed., Heyden, London.

Berrige M. J. and Schlue W. R. 1978: Ion-selective electrode studies on the effects of 5-hydroxytryptamine on the intracellular level of potassium in an insect salivary gland. J. Exp. Biol., 72, 204–216.

Bolton T. B. and Vaughan-Jones R. D. 1977: Continuous direct measurement of intracellular chloride and pH in frog skeletal muscle. J. Physiol., Lond., 270, 801–833.

Brown H. M., Pemberton J. P. and Owen J. D. 1976: A calcium-selective microelectrode suitable for intracellular measurement of calcium (II) activity. Analytica Chim. Acta, 85, 261–276.

Caldwell P. C. 1954: An investigation of the intracellular pH of crab muscle fibers by means of micro-glass and micro-tungsten electrodes. J. Physiol., 126, 169–180.

Coles J. A. and Tsacopoulos H. 1977: A method of making fine double-barrelled potassium-sensitive microelectrodes for intracellular recording. J. Physiol., 270, 12–14 P.

Conner R. L. 1967: Transport phenomena in protozoa. Chem. Zool., 1, 309–350.

Dahl G. and Isenberg G. 1980: Decoupling of heart muscle cells. Correlation with increased cytoplasmic calcium activity and with changes of nexus ultrastructure. Nature, 286, 845–850.

Di Polo R., Requena J., Bringley F. J., Mullins L. J., Scarpa A. and Tiffert T. 1976: Ionized calcium concentrations in squid axons. J. Gen. Physiol., 67, 433–467.

Djamgoz M. B. A. and Laming R. J. 1981: Intracellular measurement of ionic activity. Trends Neurosci., 4, 280–283.

Durst R. A. 1974: Ion-selective electrode in biologic fluids. In: Ion-selective Microelectrodes (eds. Berman H. J. and Hebert N. C.), New York, 13–21.

Eisenman G., Rudin D. O. and Cosby J. R. 1957: Glass electrode for measuring sodium ions. Science, 126, 831–834.

Eisenman G. 1967: The origin of the glass electrode potential. In: Glass Electrodes for Hydrogen and other Cations, (ed. Eisenman G.), New York, 1133–1173.

Fabczak S. 1983: Measurements of intracellular $K^+$-activity in *Stentor coeruleus* with use of an ion-selective microelectrode. Acta Protozool., 22, 175–181.

Fabczak S. and Kuźnicki L. 1985: Intracellular sodium and potassium ion activities in *Stentor coeruleus*. II Ogólnopolska Konferencja Biologii Komórki, Warszawa, 35–36.

Hair M. L. and Hertl W. 1973: Reactivity of boria-silica surface hydroxyl groups. J. Physiol. Chem., 77, 1965–1969.

Hilden S. 1970: Sodium and potassium levels in *Blepharisma intermedium*. Exp. Cell Res., 61, 246–256.

Johannson O. K. and Torok J. J. 1946: The use of liquid dimethylsilicones to produce water reppelant surfaces on glass-insulator bodies. Proc. I.R.E. Wares, Electrons, 3, 296–302.

Klein R. L. 1964: Effect of active transport inhibitors on K movements in *Acanthamoeba* sp. Exp. Cell Res., 34, 231–238.

Khuri R. N., Bogharian K. K. and Agulian S. K. 1974: Intracellular bicarbonate in single muscle fibres. Pflugers Arch., 349, 285–294.

Kraig R. P. and Nicholson C. 1976: Sodium liquid ion exchanger microelectrode used to measure large extracellular sodium transients. Science, 199, 725–726.

Lederer W. J., Spindler A. J. and Eisner D. A. 1979: Thick slurry bevelling. Pflugers Arch., 381, 287–288.
Lux H. D. and Neher E. 1973: The equilibration time course of $K^+$ in cat cortex. Exp. Brain Res., 17, 190–205.
Marban E., Rink T., Tsien R. W. and Tsien R. Y. 1980: Free calcium in heart muscle at rest and during contraction measured with $Ca^{2+}$-sensitive microelectrodes. Nature, 286, 845–850.
Nicolsky B. P. 1937: Theory of the glass electrode. Part I, theoretical. Zh. Fiz. Khim., 10, 495–501.
Oehme M. and Simon W. 1976: Microelectrode for potassium ions based on a neutral carrier and comparison of its characteristics with cation exchanger sensor. Analytica Chim. Acta, 86, 21–25.
Oehme M., Kessler M. and Simon W. 1976: Neutral carrier $Ca^{2+}$-microelectrode. Chimia, 30, 204–206.
Ogden T. E. and Citron M. C. 1978: The jet stream microbeveller: an inexpensive way to bevel ultrafine glass micropipettes. Science, 20, 649–651.
Simon W., Amman D., Oehme M. and Marf W. E. 1978: Calcium-selective microelectrodes. Ann. N.Y. Acad. Sci., 307, 52–69.
Thomas M. V. 1977: Microelectrode amplifier with improved method of input-capacitance neutralization. Med. Biol. Engn. Comput, 15, 450–454.
Thomas R. C. 1978: Ion-sensitive Intracellular Microelectrodes. Academic Press, London, 110 pp.
Tsien R. Y. 1980: Low-cost active-probe electrometer with special features for testing ion-selective microelectrodes. J. Physiol., 308, 6P–8P.
Tsien R. Y. and Rink T. J. 1980: Neutral-carrier ion-selective microelectrodes for measurement of intracellular free calcium. Biochim. Biophys. Acta, 599, 623–638.
Umbach B. J. 1982: Changes in intracellular pH affects calcium currents in *Paramecium caudatum*. Proc. R. Soc., 216, 209–224.
Walker J. L. 1971: Ion-specific liquid ion-exchanger microelectrodes. Ann. Chem., 43, 89 A–92 A.

ACTA PROTOZOOLOGICA
Vol. 25, No. 3, pp. 325–330 (1986)

# Cholesterol-enriched Liposomes Affect Food-vacuole Formation in *Tetrahymena pyriformis*

Hanna FABCZAK

Department of Cell Biology, Institute of Experimental Biology, Polish Academy of Sciences, 3 Pasteur Str., 02-093 Warszawa, Poland

*Received on* 20 January 1986

*Synopsis.* The food-vacuole formation was investigated in *Tetrahymena pyriformis* after incubation of the ciliates in a suspension of cholesterol containing phospholipid liposomes and then treated with carmine, an artificial vacuole-inducing agent. Observations carried out on single cells have shown that preincubation at lower cholesterol concentration (cholesterol to lecithin ratio C:P 0.7) caused rapid enhancement of food-vacuole formation rate while higher cholesterol concentration (C:P 1) lowered the cell phagocytic activity below the control level. These findings suggest that food-vacuole formation rate is strongly determined, besides other parameters, by functional membrane properties of *Tetrahymena* which are modified by cell incubation with liposome-containing cholesterol.

The functional effect of cholesterol on the orientation, configuration, rotary and linear diffusion of lipid molecules in biological membranes composed of a mixture of various phospholipids with different degrees of saturation of fatty acids has been established (Kruijff 1974). The presence of higher concentrations of this sterol in biological membranes results in altered microviscosity of the lipid bilayer (Schapiro and Barchi 1981).

The enrichment or impoverishment of cell membranes in cholesterol modifies the permeability of membranes of mammalian erythrocytes for nonelectrolyte molecules and anions (Deuticke and Ruska 1976, Grunze and Deuticke 1974). Changes in the permeability of the membrane for cations have been also observed in the case of passive and active transport (Cooper et al. 1975, Kroes and Ostwald 1971, Drabikowski et al. 1972, Madden et al. 1979) and this in turn is, connected with processes of cell excitability (Zyzek et al. 1983, Szydłowska-Fabczak 1982, 1983, Fabczak 1985).

Sterol-phospholipid interaction is believed to be of importance in the membranes of organisms that contain cholesterol or related compounds. Cholesterol

when added to phospholipids acts as a universal equalizer and alters the phase properties of the bilayers (Rothman and Engelman 1972).

Cholesterol and related sterols are not synthesized by the ciliate, *Tetrahymena pyriformis*, and sterol is not required for growth (Conner at al. 1971). Tetrahymanol and a minor isomer, diplopterol, are the polycyclic alcohols found when this organism is grown in a sterol-free medium (Mallory and Conner 1971, Mallory et al. 1963). Tetrahymanol seems to perform the same structural function assumed by sterols in other eukaryotic cells. The ability to replace tetrahymanol with cholesterol or ergosterol in the membrane systems of *Tetrahymena* offers a novel opportunity to study the changes in several functional properties of the membrane of this ciliate. The results presented deal with the influence of incubation of *Tetrahymena* cells with liposomes of two cholesterol–phospholipid ratios on the cell phagocytic activity.

## Material and Methods

Preparation of liposomes. The phospholipid liposomes were prepared in accordance with the modified method of Batzri and Korn (1973). An ethanol solution containing egg lecithin (P) (Merck) and cholesterol (C) (Serva) in molar proportions of 0.7 and 1 was rapidly injected with a syringe into 1 mM TRIS/HCl and 1 mM $CaCl_2$ buffer solution. The suspension was concentrated during 30 to 60 min on an Amicon YM-100 membrane with stirring under $N_2$ pressure of 0.2 MPa. The obtained liposome preparation was concentrated finally to 20 mM of lipids.

Cell culture. Stock cultures of *Tetrahymena pyriformis* were grown in 2% protease peptone (Difco) with yeast extract (Difco). The three-day-old culture was harvested and washed three times with buffer solution by the use of a centrifuge at 800×g. The cells chosen for the experiments were starved for 20 h before each experiment.

Phagocytosis assay. Starved *Tetrahymena* cells (about $10^6$ cells/ml) were divided into two groups. The first group of ciliates was left in buffer solution (control group) and the second was placed in the suspension of previously prepared liposomes with definite C:P ratio in the buffer solution and incubated for a standard time period (from 30 to 210 min). The final lipid concentration in this suspension did not exceed 25 μm. Every 15 min a sample of control cells (1 ml) and those incubated with liposomes with liposomes were taken and immersed in the carmine suspension for a period of 5 min to induce phagocytic activity. The carmine suspension was prepared with 20 mg powdered carmine (BDH) in 10 ml of distilled water by careful stirring in a porcelain mortar and then filtrated to obtain granules of 1 to 5 μm in diameter. The cell phagocytic activity was studied by quantitative evaluation of the mean number of vacuoles containing carmine, formed by an individual cell. Prior to calculations the samples of *Tetrahymena* cells (50 cells) were fixed in 2.5% glutaraldehyde solution.

## Results

Single cell observations showed distinctly that preincubation of *Tetrahymena* with liposomes causes changes in the rate of food-vacuole formation after treatment with carmine. As shown in Fig. 1 a and Table 1, the treatment of cells with pho-

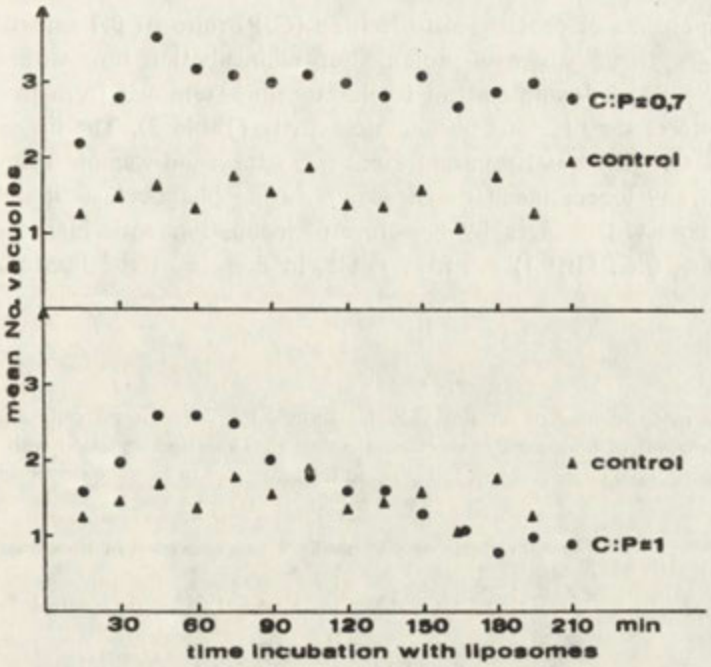


Fig. 1. The mean number of food vacuoles formed by *Tetrahymena pyriformis* after preincubation with phospholipid liposomes of cholesterol to lecithin ratios 0.7 and 1.0 and exposure to carmine suspension for 5 min

Table 1

The mean number of carmine vacuoles formed by *Tetrahymena pyriformis* during preincubation with phospholipid liposomes of cholesterol to lecithin rations 0.7 and 1.0. Time exposure of the cell to carmine suspension was 5 min

| Incubation time with liposomes in min | Ratio of phospholipid to cholesterol in liposomes | | |
|---|---|---|---|
| | C:P = 0.7 | C:P = 1.0 | Control |
| 15 | 2.2±0.3 | 1.6±0.2 | 1.3±0.2 |
| 30 | 2.8±0.1 | 2.0±0.1 | 1.5±0.2 |
| 45 | 3.5±0.2 | 2.6±0.4 | 1.7±0.2 |
| 60 | 3.2±0.3 | 2.6±0.2 | 1.4±0.3 |
| 75 | 3.1±0.2 | 2.5±0.1 | 1.8±0.4 |
| 90 | 3.0±0.3 | 2.0±0.2 | 1.6±0.1 |
| 105 | 3.1±0.2 | 1.8±0.3 | 1.9±0.4 |
| 120 | 3.0±0.5 | 1.6±0.2 | 1.4±0.1 |
| 135 | 2.8±0.2 | 1.6±0.4 | 1.5±0.3 |
| 150 | 3.1±0.3 | 1.3±0.3 | 1.6±0.2 |
| 165 | 2.7±0.2 | 1.1±0.2 | 1.1±0.1 |
| 180 | 2.9±0.5 | 0.8±0.4 | 1.8±0.5 |
| 195 | 3.0±0.3 | 1.0±0.2 | 1.3±0.2 |
| 210 | 2.8±0.1 | 0.9±0.1 | 2.0±0.3 |

spholipid liposomes at cholesterol to lecithin (C:P) ratio of 0.7 caused a gradual rise of phagocytic activity with prolongation of incubation time with subsequent "saturation" at the double control level. Liposome removal from the cell environment restores the previous phagocytic activity (Table 2). The liposome preincubation at C:P ratio of 1 transiently enhances the food-vacuole formation rate as well and any longer incubation leads to strong phagocytosis inhibition (Fig. 1 b). The observed changes by liposome preincubation with higher cholesterol concentrations (i.e., C:P 1) are irreversible, in despite of the liposome removal (Table 2).

Table 2

The mean number of carmine vacuoles formed by *Tetrahymena* cells after removal of liposomes from external solution. Time preincubation with phospholipid liposomes was 120 min and time exposure to carmine suspension was 5 min

| Time after liposome removal in min | Ratio of phospholipid to cholesterol in liposomes | | |
|---|---|---|---|
| | C:P = 0.7 | C:P = 1.0 | Control |
| 0 | 3.0±0.5 | 1.6±0.2 | 1.4±0.1 |
| 30 | 2.1±0.3 | 1.2±0.1 | 1.6±0.2 |
| 60 | 1.7±0.1 | 1.0±0.3 | 1.8±0.5 |
| 90 | 1.8±0.3 | 1.1±0.2 | 2.0±0.3 |

For determination of the cholesterol amount effectively incorporated into *Tetrahymena*, cells were kept for 2 h in a liposome suspension of C:P 1. The preliminary data showed that the amount of cholesterol incorporated by the cell rises gradually with incubation time to attain the value of 2 n moles of cholesterol uptake per 1 mg of cell protein after 2 h incubation.

## Discussion

The change in the phagocytic activity in *Tetrahymena* cells due to liposome incubation at different cholesterol concentrations is characterized by strong inhibition of cell phagocytosis in respect to the control (Fig. 1 a, b), especially, at higher cholesterol concentrations. A similar phenomenon was noticed by Stuart (1962). An intravenous injection of 30 mg of cholesterol oleate caused inhibition of the cells phagocytosis of the reticulo-endothelial system in spleen of the mouse for a two- or three-day period, while smaller doses of cholesterol had no effect.

The data obtained in the present study concerning the effects of cholesterol on the phagocytic activity and analysis of cholesterol uptake by the cell of *Tetra-*

*hymena* and the results obtained by other authors (Poste and Papahadjopoulos 1976) confirm the suggestion that the cells might take up the phospholipid liposomes by endocytosis. Recently it has been shown that *Tetrahymena* in the presence of free cholesterol may partially replace tetrahymanol, specific for *Tetrahymena* membrane, by external cholesterol (Conner et al. 1982). Cholesterol incorporated by the cell is transformed to 7, 22, bis-dehydro-cholesterol causing distinct diminution of cell size and an increase of the content of saturated fatty acids. These observations correspond to those in previous works dealing with the same problem by Fergusson et al. (1975).

It has been frequently demonstrated in *in vivo* studies and in model membrane investigations that an alteration in the amount of cholesterol in the membrane can influence membrane lipid composition, the function of membrane-bound enzymes and its fluidity. Conner (1982) suggests that sterol supplementation in *Tetrahymena* i.e., replacement of cell tetrahymanol by cholesterol can influence the cellular metabolism, possibly *via* an effect on cell membrane fluidity. The observed in the present work correlation between cholesterol uptake and inhibition of food-vacuole formation rate suggests that the prolonged incubation of *Tetrahymena* cells with phospholipid liposomes containing high concentration of cholesterol may affect the cell phagocytic activity presumably by modulation of cell membranes fluidity.

The higher rate of vacuole formation in cells incubated with lower concentrations of cholesterol (i.e., liposomes of C:P 0.7) and the initial transient one with liposomes having C:P ratio 1 is probably due to the additive action of carmine and liposomes as phagocytosis-inducing agents.

## REFERENCES

Batzri S. and Korn E. D. 1973: Single bilayer liposomes prepared without sonication. Biochim. Biophys. Acta, 298, 1015–1019.

Conner R. L., Mallory F. B., Landrey J. R., Ferguson K. A., Kaneshiro E. S. and Ray E. 1971: Ergosterol replacement of tetrahymanol in *Tetrahymena* membranes. Biochem. Biophys. Res. Commun., 44, 995–1000.

Conner R. L., Landrey J. R. and Czarkowski N. 1982: The effects of specific sterols on cell size and fatty acid composition of *Tetrahymena pyriformis*. J. Protozool., 29, 105–109.

Cooper R. A., Arner E. C., Wiley J. A. and Shattils J. 1975: Modification of red cell membrane structure by cholesterol-rich lipid dispersion. J. Clin. Invest., 55, 115–126.

Deuticke G. and Ruska C. 1976: Changes of nonelectrolyte permeability in cholesterol loaded erythrocytes. Biochim. Biophys. Acta., 223, 638–653.

Drabikowski W., Sarzała M. G., Wroniszewska A., Łągwińska F. and Drzewiecka B. 1972: Role of cholesterol in the $Ca^{2+}$ uptake and ATP-ase activity of fragmented sarcoplasmic reticulum. Biochim. Biophys. Acta, 274, 158–171.

Fabczak H. 1985: Changes in behaviour of *Paramecium caudatum* caused by incubation in various cholesterol concentrations. Acta Protozool., 24, 117–124.

Ferguson K. A., Davis F. M., Conner R. L., Landrey J. R. and Mallory F. B. 1975: Effect of sterol replacement *in vivo* on the fatty acid composition of *Tetrahymena*. J. Biol. Chem., 250, 6998–7005.

Grunze M. and Deuticke B. 1974: Changes of membrane permeability due to extensive cholesterol depletion in mammalian erythrocytes. Biochim. Biophys. Acta, 356, 125–130.

Kroes J. and Ostwald R. 1971: Erythrocyte membrane — effect of increased cholesterol content on permeability. Biochim. Biophys. Acta, 249, 647–650.
de Kruijff B. 1974: Studies on the role of sterols in membranes. Ph. D. Thesis, 1 - 53.
Madden T. D., Chapmann D. and Quin P. J. 1979: Cholesterol modulates activity of calcium dependent ATP-ase of the sarcoplasmic reticulum. Nature, 279, 538–541.
Mallory F. B., Gordon J. T. and Conner R. L. 1963: The isolation of the pentacyclic triterpenoid alcohol from protozoan. J. Am. Chem. Soc., 85, 1362–1363.
Mallory F. B. and Conner R. L. 1971: Dehydrogenation and dealkylation of various sterols by *Tetrahymena pyriformis*. Lipids, 6, 149–153.
Poste G. and Papahadjopoulos D. 1976: Influence of vesicle composition on mechanism(s) of vesicles incorporation into cells. Lipid vesicles as carriers for introducing materials into cultured cells. Proc. Natl. Acad. Sci. USA, 73, 1603–1607.
Rothman J. E. and Engelman D. M. 1972: Phospholipid molecular mechanism for interaction with cholesterol. Nature New Biol., 237, 42–44.
Shapiro H. K. and Barchi R. L. 1981: Alteration of synaptosomal plasma membrane cholesterol content: membrane physical properties and cation transport proteins. J. Neurochem., 36, 1813–1819.
Stuart E. 1962: Effect of cholesterol oleate on the phagocytic function of the reticulo-endothelial system. Nature, 196, 78–79.
Szydłowska-Fabczak H. 1982: Modification of motile behaviour in *Paramecium octaurelia* by cholesterol. Acta Protozool., 21, 61–67.
Szydłowska-Fabczak H. 1983: Stabilizing effects of cholesterol on changes in membrane permeability induced in *Paramecium octaurelia* by lysolecithin and valinomycin. Acta Protozool., 22, 169–173.
Zyzek F., Desmazes J. P., Gourdij D., Dufy B. and Georgescauld D. 1983: Modification of membrane cholesterol content effects electrical properties release of cultured pituitary cells. Experientia, 39, 56–58.

ACTA PROTOZOOLOGICA
Vol. 25, No. 3, pp. 331–338 (1986)

# Modelling the Insulin Receptor in the *Tetrahymena*. Time-dependence of Receptor Formation, Down-regulation and Imprinting[1]

György CSABA and László KÖHIDAI

Department of Biology, Semmelweis University of Medicine, H-1445, Budapest, Hungary

*Received on* 26 November 1985

*Synopsis.* The insulin receptor formed (amplified) in *Tetrahymena* during primary exposure to the hormone has shown the phenomenon of down-regulation, most distinctly after preexposure for 3–6 h. The establishment of hormonal imprinting induced by primary interaction takes a certain time: the effect of 1-h preexposure (imprinting) reached a statistically significant degree after 24 and 48 h. It depends on the duration of down-regulation whether or not the effect of imprinting is measurable after 24 h.

The unicellular *Tetrahymena*, which represents a very low level of phylogenesis, is able to respond to hormones of higher organisms (Csaba 1981). At its primary interaction with the hormone, hormonal imprinting takes place, which increases the binding capacity of the hormone receptor, and cellular response to hormone reexposure(s) as well (Csaba 1980, 1984, 1985). Thus imprinting gives rise to amplification of the binding structures, which persist over as many as 500 subsequent cell generations (Csaba et al. 1982 a). In earlier experiments with amino acid type hormones, even a very low ($10^{-18}$M), in itself functionally inactive hormone concentration gave rise to imprinting, indicating that, between certain limits, the amount of interacting hormone plays little role, while the time factor is decisive, for at least 1-h exposure was required to induce imprinting (Csaba et al. 1982 b).

In the present study a polypeptide hormone, insulin was examined for interdependence between imprinting and the time factor, in other words, for the length of exposure required to induce imprinting in the *Tetrahymena*. Much information has been accumulated on the insulin binding capacity and binding properties of hepatocytes and adipocytes (Gammeltoft et al. 1978). The receptor binds the insulin molecule specifically, and binding elicits cellular response to insulin through poorly understood mediator mechanism. Subsequently, the bound insulin becomes

[1] Supported by the Scientific Research Council, Ministry of Health, Hungary 16/1-04/432/Cs

internalized in coated vesicles, and becomes degraded intracellularly, while the receptor structure re-enters the cytoplasmic membrane via recycling (Gammeltoft et al. 1978, Gorden et al. 1980). Binding of a larger dose of insulin (and of other polypeptide hormones in general) (Gorden et al. 1980, Djiane et al. 1979) accounts for down-regulation, i.e., for a temporary decrease in, or failure of, insulin binding (Marshall and Olefsky 1980, Pezzino et al. 1980). Down-regulation is presumably consequent upon increased internalization and decreased recyclization of the receptor, and on certain postreception events (Marshall and Olefsky 1980) as well, although inhibition of receptor neogenesis could also play a role (Reed and Lane 1980).

We demonstrated earlier that binding of FITC-labelled insulin to *Tetrahymena* can be either displaced or inhibited by non-labelled insulin (Csaba et al. 1985). Since, like mammalian cells, *Tetrahymena*, too, possesess internalizable coated pits and coated vesicles (Csaba et al. 1984 a), we expected that those changes in binding capacity, which characterize the mammalian insulin receptor, could also appear in *Tetrahymena*. Since imprinting is a proof of receptor formation, we used it as index to study insulin receptor behaviour in *Tetrahymena* and simultaneously, the influence of possible down-regulation on hormonal imprinting at the unicellular level.

## Material and Methods

*Tetrahymena pyriformis* GL cells, cultured in 0.1% yeast extract containing 1% Bacto Tryptone medium (Difco, Michigan, USA) at 28°C, were used in the logarithmic phase of growth. After 24 h, the cells were treated on three different schemes, as follows:

First series. The cells were exposed to $10^{-6}$M insulin (Semilente, Novo, Copenhagen, Denmark), for 1 h, after which they were returned to plain medium and examined for insulin binding immediately, and 1, 3, 6, 24 and 48 h after the exchange of medium.

Second series. The cells were exposed to insulin for 1, 3, 6, 24 or 48 h, and were examined for insulin binding immediately after treatment, without return to plain medium.

Third series. The cells were treated with insulin for the same lengths of time as in the second series, but were returned to plain medium for 24 h, and sampled for insulin binding tests only thereafter.

All samples were fixed in 4% formaline, washed in two changes of PBS (0.05 M phosphate buffer in 0.9% saline), and exposed to fluoresceine-isothiocyanate-labelled insulin (FITC, BDH Chemicals Ltd., Poole, England) for 1 h. After incubation, the samples were washed in several changes of PBS, spread on slides, and dried for determination of the intensity of fluorescence in a Zeiss Fluoval cytofluorimeter, which was connected with a HP-41C calculator for statistical evaluation of the results. The values given by the cytofluorimeter are arbitrary units. This renders possible the comparison of treated cells with control ones, but the calculation of absolute values of insulin bound is impossible. Twenty cells were assayed for fluorescence at each level of insulin treatment, and each experiment was performed in five replicates, thus the enclosed Figures show the mean of 100 measurements in each series. The mean values are given (in the Figures) in percentage, related to the control as 100.

## Results

Six hours after 1 h insulin exposure the binding of labelled insulin did not differ from the control. At 24 and 48 h the difference in binding is biologically and mathematically significant alike (Fig. 1).

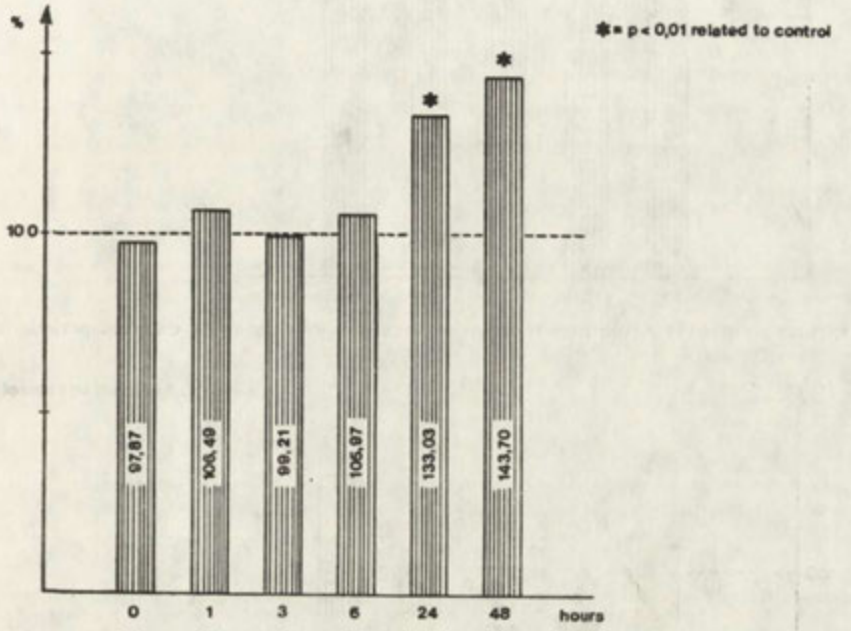


Fig. 1. Effect of 1 h insulin pretreatment (imprinting) on the binding of FITC-labelled insulin to *Tetrahymena* after staying for different periods in normal medium

In the permanent presence of hormone (and measuring labelled insulin binding without delay) the 1 h treatment did not cause down regulation. Although a biologically significant decrease had been observed between 3 and 24 h due to the high deviation only the 48 h difference (from the control) was significant mathematically (Fig. 2).

Twenty four hours after 1 to 48 h insulin treatment, the cells treated for 3and 6 h decreased, treated for 48 h increased their insulin binding, significantly (Fig. 3).

## Discussion

The establishment of imprinting took a relatively long time. Insulin binding still did not differ from the control at 6 h after the 1-h exposure, either because the lasting presence of insulin on the surface of the cells prevented further (labelled) insulin binding, or because the negative influence of down-regulation counteracted

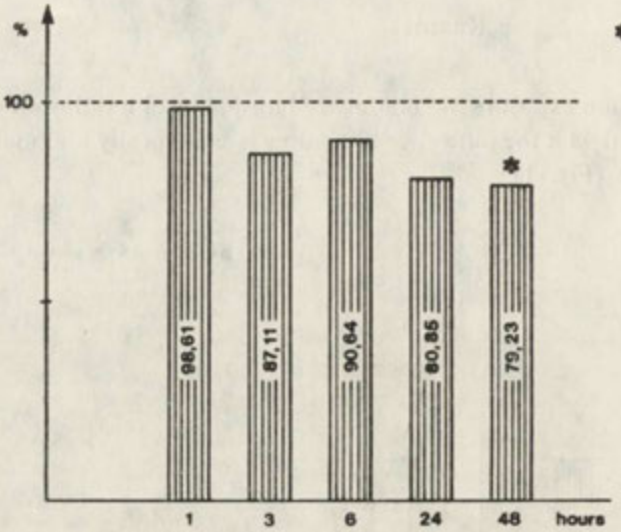


Fig. 2. Binding of FITC-insulin to *Tetrahymena* treated with insulin for different periods of time

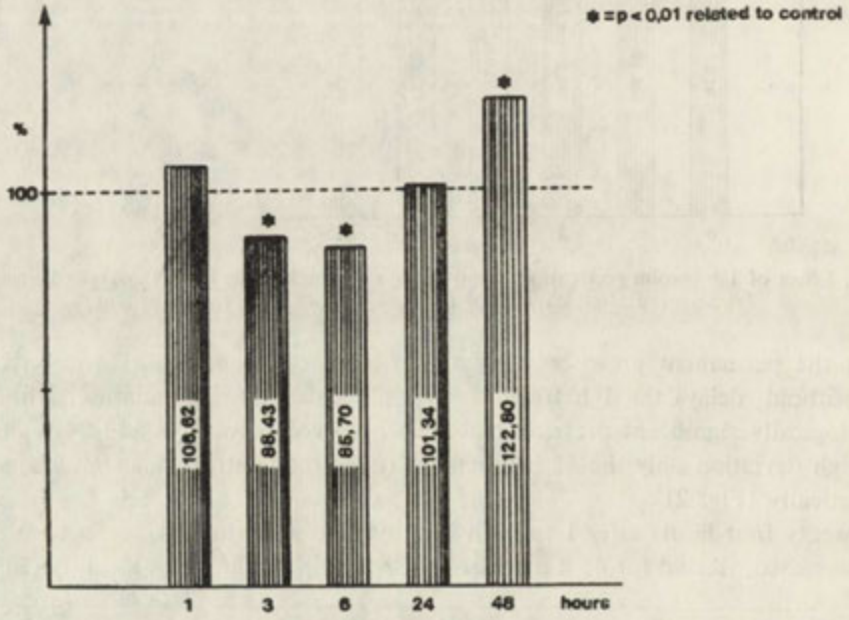


Fig. 3. Effect of insulin treatment of different periods of time to insulin binding after 24 h stay in normal medium

the positive influence of insulin, or thirdly, simply because the establishment of imprinting required a longer time than 6 h. The effect of the imprinting was in fact measurable at 24 h.

The *Tetrahymena* cells divide every 3–4 h in culture. This fact, and internali-

zation of the bound ligand, which is characteristic of polypeptide hormones (Pezzino et al. 1980), seem to disprove that the insulin used for the induction of imprinting was still present on the surface of the daughter cells in a fully inhibitory concentration at 6 h. At the same time, the fact that imprinting took full effect by 48 h, during which more than 10 generation changes had taken place, strongly suggests that imprinting, once it had occurred, becomes, an endogenous property of the cell.

The direct effect of down-regulation was not demonstrable immediately after exposure, but increased measurably with the progression of time. One might, naturally, postulate that fewer receptors had become saturated in 1 than in 48 h, but the possibility of this saturation difference is low since, in principle, 1 h is sufficient for full receptor saturation. If, however, the actual number of active receptors depended on the quantitative relation (equilibrium) between internalized and recycled receptor structures, increase in internalization and a parallel decrease in recyclization could well occur with the progression of time. Such shift of equilibrium between the actual numbers of active and inactive (internalized) receptor structures could account for a time dependent decrease in FITC-labelled insulin binding at reexposure. The applied insulin concentration, $10^{-6}$M, was relatively high, but it was required to produce a well measurable effect in the given conditions of experiment. Extracellular insulin decomposition is low (1–6%/h), but there is evidence that the liver cells degrade 40% of bound insulin within 1 h (Gammeltoft et al. 1978, Gammeltoft 1984). No similar data are available on the *Tetrahymena*, but the present findings unequivocally suggest that down-regulation can also occur in unicellular organisms.

The third experimental series has thrown a light on the interrelationships between different lengths of primary exposure and establishment of imprinting within 24 h. While preexposure for 1 h did induce imprinting within 24 h, preexposure for 3 or 6 h had a negative rather than positive influence on insulin binding within the same time period. The binding capacity of the cells preexposed for 24 h, did not differ from the control after 24 h, but increased considerably over it by 48 h. An interaction between imprinting and down-regulation can well be held responsible for this phenomenon. One-hour preexposure to insulin did not elicit down-regulation in the *Tetrahymena*, whereas 3-h and 6-h preexposure did. It appears that the 24-h hormone withdrawal period following upon preexposure was too short for expiration of the effects of downregulation (by these short treatments), and for manifestation of the effects of prolonged imprinting as well, whence the latter were not strong enough to supersede the negative influence of the former.

It was interesting to note that the effects of down-regulation were still demonstrable in the hepatocellular membrane of rats 24 h after *in vivo* insulin treatment (Vigneri et al. 1978). Thus the period of 24 h might generally be too short for the expiration of down-regulation phenomena.

Remarkably, while preexposure (imprinting) for 24 h had counter-balanced

down-regulation to the extent of maintaining the control level, preexposure for 48 h had, despite a much stronger down-regulating influence, induced an appreciable degree of imprinting, which was already demonstrable 24 h later. However, with the continuous internalization and degradation of the hormone taken into consideration, the explanation lies close at hand that all insulin added to the medium for preexposure had been degraded between 6 and 24 h, and the *Tetrahymena* cells "consuming" it had increased in number (hence the return of the binding value to the control level), thus insulin was no longer present in the next 24 h, which were sufficient for the establishment of imprinting.

The foregoing considerations support the earlier implication (Csaba et al. 1982 b) that the time factor is of primary importance for the establishment of hormonal imprinting. The dynamic membrane structures of the unicellular are, in all probability, incessantly scanning the environment for information, and require a certain time to assemble to configurations capable of an adequate response. The present findings strongly suggest that the mechanism of hormonal imprinting involves a stage of down-regulation not only in higher organisms, but also in the *Tetrahymena*, from which we imply that the "inherent" insulin receptor of mammals, and the induced insulin receptor of the *Tetrahymena*, are similar structures, as already suggested by earlier studies along this line (Csaba et al. 1984 b, Kovács et al. 1985).

## REFERENCES

Csaba G. 1980: Phylogeny and ontogeny of hormone receptors: the selection theory of receptor formation and hormonal imprinting. Biol. Rev., 55, 47–63.

Csaba G. 1981: Ontogeny and Phylogeny of Hormone Receptors. Karger, Basel.

Csaba G. 1984: The present state in the phylogeny and ontogeny of hormone receptors. Horm. Metab. Res., 16, 329–335.

Csaba G. 1985: The unicellular *Tetrahymena* as model cell for receptor research. Int. Rev. Cytol., (in press).

Csaba G., Gruszczynska M., Madarász B. and Sudár F. 1984 a: Coated pits and coated vesicles in unicellulars (*Tetrahymena*, *Critidia*) and in Hydra. Acta Morphol. Acad. Sci. Hung., 32, 181–186.

Csaba G., Kovács P. and Inczefi-Gonda Á. 1984 b: Insulin binding sites induced in the *Tetrahymena* by rat liver receptor antibody. Z. Naturforsch., 39 e, 183–185.

Csaba G., Németh G. and Vargha P. 1982 a: Development and persistence of receptor "memory" in a unicellular model system. Exp. Cell Biol., 50, 291–294.

Csaba G., Németh G. and Vargha P. 1982 b: Influence of hormone concentration and time factor on development of receptor memory in a unicellular (*Tetrahymena*) model system. Comp. Biochem. Physiol., 73 B, 357–360.

Csaba G., Németh G., Kovács P., Vargha P. and Vas Á. 1985: Receptor level action of polypeptide hormones (insulin, glucagon, FSH, TSH, ACTH) and nonhormone polypeptides on the *Tetrahymena*. BioSystems, 17, 227–231.

Djiane J., Clauser H. and Kelly P. A. 1979: Rapid down regulation of prolactin receptors in mammary gland and liver. Biochem. Biophys. Res. Commun., 90, 1371–1378.

Gammeltoff S. 1984: Insulin receptors: binding kinetics and structure-function relationship of insulin. Physiol. Rev., 64, 1321–1378.

Gammeltoff S., Kristensen L. O. and Sestoft L. 1978: Insulin receptors in isolated rat hepatocytes. J. Biol. Chem., 253, 8406–8413.

Gorden P., Carpentier J.-L., Freychet P. and Orci L. 1980: Morphologic probes of polypeptide hormone receptor interactions. J. Histochem. Cytochem., 28, 811–817.
Kovács P., Csaba G. and Bohdaneczky E. 1985: Immunological evidence of the induced insulin receptor in *Tetrahymena*. Comp. Biochem. Physiol., 80 A, 41–42.
Marshall S. and Olefsky J. M. 1980: Effects of insulin incubation on insulin binding, glucose transport and insulin degradation by isolated rat adipocytes. J. Clin. Invest., 66, 763–772.
Pezzino V., Vigneri R., Pliom N. B. and Goldfine I. D. 1980: Rapid regulation of plasma membrane insulin receptors. Diabetologie, 19, 211–215.
Reed B. C. and Lane M. D. 1980: Insulin receptor synthesis and turnover is differentiating 353-L1 preadipocytes. Proc. Natl. Acad. Sci. USA, 77, 285–289.
Vigneri R., Pliam N. B., Cohen D. C., Pezzino V., Wong K. Y. and Goldfine I. D. 1978: *In vivo* regulation of cell surface and intracellular binding sites by insulin. J. Biol. Chem., 253, 8192–8197.

ACTA PROTOZOOLOGICA
Vol. 25, No. 3, pp. 339–344 (1986)

# Developmental Stage Dependent Alterations in the Net Surface Charge of *Acanthamoeba castellanii*

Aleksandra PRZEŁĘCKA and Ewa PERKOWSKA

Department of Cell Biology, Nencki Institute of Experimental Biology, Pasteura 3 Str., 02-093 Warszawa, Poland

*Received on* 8 January 1986

*Synopsis.* Trophozoites, which are the vegetative stage of the amoeba, and cysts behave differently in the electric field: Trophozoites display an anodic electrophoretic mobility equaling — 1.88 μm/s/V/cm whereas cysts — a slightly cathodic one equaling +0.15 μm/s/V/cm, both measured at pH 7.2. The reported results indicate that the morpho-chemical reorganization of the trophozoite surface occurring during the encystation is associated with a loss of its net negative charge.

*Acanthamoeba castellanii* is a small free living amoeba isolated from soil moisture by Neff (1957). Its life cycle includes two developmental stages: a trophozoite representing the vegetative stage and exhibiting a continuous pinocytotic activity, the rate of which exceeds about 100 times that observed in mammalian macrophages, and a cyst — enabling the cell to survive the unfavorable environmental conditions (Bowers and Olszewski 1972, Korn 1974). The differentiation of the trophozoite into a cyst is accompanied by the appearance of a cyst wall, about 1 μm thick, covering the surface of the protoplast. The plasma membrane of the trophozoite differentiating into a cyst undergoes structural alterations involving the disappearance of surface residues capable of binding ruthenium red (RR) and cationized ferritin (CF), or of reacting with concanavalin A (Con A) (Przełęcka and Sobota 1982). However, these compounds may associate with the external layer of the cyst wall which indicates the presence of negatively charged residues therein. The question arises whether the net change of the cyst wall approximates that of the trophocyte or not. The present study is an attempt at solving this problem with the use of the method of cell free electrophoresis.

## Material and Methods

Trophozoites and fully formed cysts of *Acanthamoeba castellanii*, Neff strain (1957) grown axenically under standarized laboratory conditions were used. Trophozoites were obtained from 4-day cultures being at the exponential growth phase of the cells. Encystment was induced by

transferring the cells into a non-nutrient ionic medium as described previously (Sobota and Przełęcka 1981). The population density and the percentage of trophozoites and of cysts in each sample were estimated by microscopic examination using Bürker's microchamber for cell counting.

Cells washed out from the culture medium were suspended in the medium of 0.01 M Tris-HCl (pH 7.2) and 0.1 M sucrose, where they were subjected to a free electrophoresis. The instrument used was the Kern's LK-30 model (Aarau, Switzerland) provided with a calibrated optical system in which one division of the ocular micrometer corresponded to 350 μm. The electrophoretic mobility of the cells was determined by estimating the length of their transit during 5 min, when a constant direct current was passing through the electrophoretic chamber.

## Results and Discussion

Samples of *Acanthamoeba* containing over 90 per cent of trophozoites in the buffer-sucrose solution, pH 7.2, display an electrophoretic mobility of −1.88 μm/s /V/cm. This is the mean value of 26 determinations from 8 experiments (Table 1). A relatively large standard deviation is probably due to some diversity in cell size and shape (Pl. I 1–4). The mean is somewhat higher than the corresponding figures obtained for other free living cells. Thus, the human blood cells: trombocytes, lymphocytes, eosinophils and erythrocytes show an electrophoretic mobility amoun-

Table 1

Electrophoretic mobility of trophozoites of *Acanthamoeba castellanii*. Tris-HCl 0.01 M plus 0.1 M sucrose, pH 7.2, H = 4.3 V/cm

| Batch | Number of cells used for the experiment | | Electrophoretic mobility, μm/s/V/cm, mean±S.D. (number of determinations in parentheses) |
|---|---|---|---|
| | total ($\times 10^6$) | trophozoites (%) | |
| 1 | 27 | 92 | |
| 2 | 29 | 95 | |
| 3 | 25 | 100 | −1.88±0.20 |
| 4 | 49 | 94 | (26) |
| 5 | 153 | 92 | |
| 6 | 14 | 90 | |
| 7 | 11 | 100 | |
| 8 | 36 | 100 | |

ting to −0.91, −1.05, −1.08, and −1.08 μm/s/V/cm respectively (Mehrishi 1972, Pimenta and de Souza 1982). The electrophoretic mobility of *Trypanosoma cruzi*, a protozoan parasite of vertebrates at the developmental stage of trypomastigote living in the host blood stream, equals −1.14 μm/s/V/cm (de Souza et al. 1977).

Table 2

Electrophoretic mobility of cysts of *Acanthamoeba castellanii*. Tris-HCl 0.01 M plus 0.1 M sucrose, pH 7.2, H = 4.3 V/cm

| Batch | Number of cells used for the experiment | | Electrophoretic mobility, μm/s/V/cm, mean±S.D. (number of determinations in parentheses) |
|---|---|---|---|
| | total ($\times 10^6$) | cysts % | |
| 1 | 3 | 90 | |
| 2 | 13 | 99 | |
| 3 | 14 | 99 | |
| 4 | 19 | 99 | |
| 5 | 11 | 95 | |
| 6 | 55 | 97 | +0.15±0.20 |
| 7 | 9 | 95 | (63) |
| 8 | 10 | 95 | |
| 9 | 9 | 95 | |
| 10 | 35 | 99 | |
| 11 | 34 | 98 | |
| 12 | 34 | 98 | |
| 13 | 35 | 100 | |
| 14 | 40 | 100 | |
| 15 | 40 | 99 | |
| 16 | 40 | 99 | |
| 17 | 30 | 100 | |

Chemically, the plasma membrane of the *Acanthamoeba* trophozoites consists of about 1/3 protein, 1/3 lipid and 1/3 lipophosphoglycan (Korn and Wright 1973, Korn et al. 1973). A high content of the latter macromolecule rich in acidic residues seems to be responsible for a high rate of the anodic movement of these cells.

*Acanthamoeba* cells differentiated into cysts and covered with a fully formed wall behave in the electric field differently from the trophozoites. Under the same experimental conditions the cysts display either no electrophoretic movement, or only a fairly small shift towards the cathode and not the anode (Table 2). The electrophoretic mobility of cysts (based on the results of 63 determinations from 17 experiments) is +0.15 μm/s/V/cm. This value evidently layes within the limits of the measurements error. It indicates that in cysts the average surface charge is close to zero, when measured at pH 7.2.

There was only one case of the cyst movement towards the anode. But the cysts used in this experiment descend from a subculture which appeared to be contaminated with bacteria sticking fast to their wall (Pl. I 5). After a very careful washing (centrifugation in the buffer solution repeated over 10 times) the cysts, set free of bacteria, which fact was checked by microscopic observation, behaved

like the majority of the others, that is at pH 7.2 they did not show any electrophoretic mobility.

The wall of the cysts is formed by a thin peripheral layer of protein, presumably phosphoprotein, and a more thick one of cellulose adhering to the cell. Protein and cellulose are about 33 and 35 per cent of the wall constituents respectively. Besides, the wall contains lipids (about 5 per cent) and a significant amount of inorganic matter — up to 8 per cent of the ash content (Neff et al. 1964, Neff and Neff 1969). The results of this study indicate that the profound changes in the morpho-chemical constitution of the surface occurring during the encystation of *Acanthamoeba* account for profound changes in the electrostatic properties of the cell. The surface residues of the cysts were found to belong to protein with an isoelectric point at the pH close to 7.2.

It is difficult to define the electrostatic properties of the plasma membrane of the naked cysts, deprived of the wall. However, the lack of the surface residues capable of reacting with RR or with CF (Przełęcka and Sobota 1982) suggests that the surface of the naked cysts differs from that of the trophozoites in regard to its net charge as well. The developmental changes in the net charge of the surface have been demonstrated in the above mentioned *Trypanosoma*. As was shown by de Souza et al. (1977) the epimastigote, a form living in the tissues, displays a rate of electrophoretic migration nearly three times higher than that recorded for the trypomastigote, a form living in the host blood stream.

In the case of sea urchin eggs (Oshima 1975, 1982), the electrokinetic potential of fertilized eggs with their fertilization membrane intact differs from that of the egg proper, deprived experimentally of the fertilization membrane and of the hyaline layer. In order to understand whether a similar phenomenon can be observed in the cyst of *Acanthamoeba castellanii*, it is necessary to study the electrophoretic mobility of individual cells and not of cell populations as has been the case so far.

ACKNOWLEDGEMENTS

We wish to thank prof. L. Wojtczak and dr. M. Nałęcz for access to the apparatus and for instructing us in its use. We are grateful to Mrs K. Mrozińska for her helpful assistance in maintaining the cultures of the amoeba.

REFERENCES

Bowers B. and Olszewski T. E. 1972: Pinocytosis in *Acanthamoeba castellanii*. Kinetics and morphology. J. Cell Biol., 53, 681–694.

Korn E. D. 1974: Biochemistry of endocytosis. In: Biochemistry of Cell Walls and Membranes (ed. C. F. Fox), Butterworth, Woburn (Mass.), pp. 1–26.

Korn E. D., Deaborn D. G., Fales H. M. and Sokoloski E. A. 1973: A major polisaccharide constituent of the amoeba plasma membrane contains 2-aminoethyl phosphonic acid and 1-hydroxy-2-aminoethyl-phosphonic acid. J. Biol. Chem. 248 2257–2259.

Korn E. D. and Wright P. L. 1973: Macromolecular composition of an amoeba membrane. J. Biol. Chem., 248, 439–447.
Mehrishi J. N. 1972: Molecular aspects of the mammalian cell surface. In: Progress in Biophysics and Molecular Biology (eds. J. A. V. Butler and D. Noble), Pergamon Press, Oxford, Vol. 25.
Neff R. J. 1957: Purification, axenic cultivation and description of soil amoeba, *Acanthamoeba* sp. J. Protozool., 4, 176–182.
Neff R. J., Benton W. F. and Neff R. H. 1964: The composition of the mature cyst wall of the soil amoeba, *Acanthamoeba* sp. J. Cell Biol., 23, 66 A.
Neff R. J. and Neff R. H. 1969: The biochemistry of amoebic encystment. Symp. Soc. Exp. Biol., 23, 51–81.
Oshima N. 1975: Electrophoretic mobility of sea-urchin eggs during the division cycle. Dev. Growth Differ,. 17, 19–25.
Oshima N. 1982: Electrophoretic movement of fertilized sea-urchin eggs. J. Cell Sci., 55, 105–113.
Pimenta P. F. P. and de Souza W. 1982: Surface charge of eosinophils. Binding of cationic particles and measurement of cellular electrophoretic mobility. Histochemistry, 74, 569–576.
Przełęcka A. and Sobota A. 1982: Growth phase dependent alterations in the surface coat of *Acanthamoeba castellanii*. Acta Histochem., 71, 219–229.
Sobota A. and Przełęcka A. 1981: Developmental changes in the localization of calcium binding sites in *Acanthamoeba castellanii*. Histochemistry, 71, 135–144.
De Souza W., Argello C., Martinez-Palomo A., Gonzales-Robles A. and Chiari E. 1977: Surface charge of *Trypanosoma cruzi*. Binding of cationized ferritin and measurements of cellular electrophoretic mobility. J. Protozool., 24, 411–415.

## EXPLANATION OF PLATE I

1–4: Photomicrograph of trophozoites of *Acanthamoeba castellanii*. Cells differing in size, shape and the number of nuclei are seen; unstained, phase contrast, bar — 5 μm
5: Photomicrograph of cysts of *Acanthamoeba castellanii* descending from a batch contaminated with bacteria. The bacteria are sticking to the surface of the cyst wall; unstained, bar — 5 μm

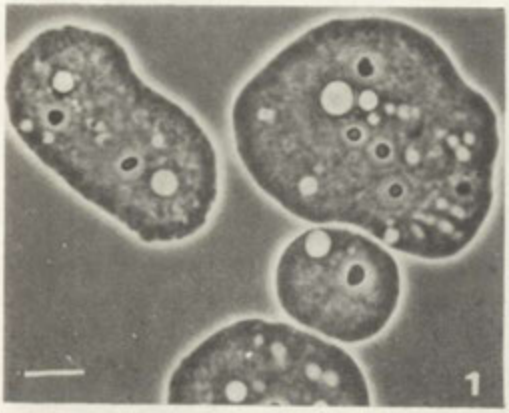


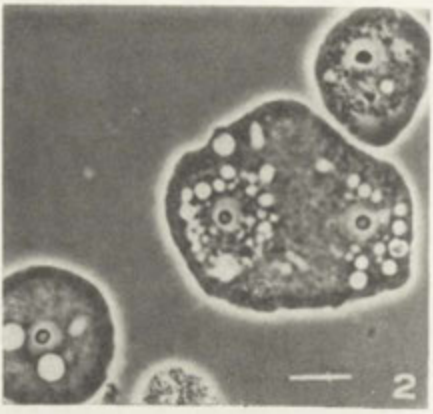


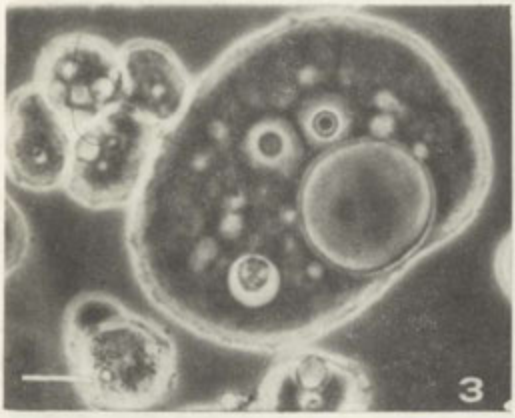


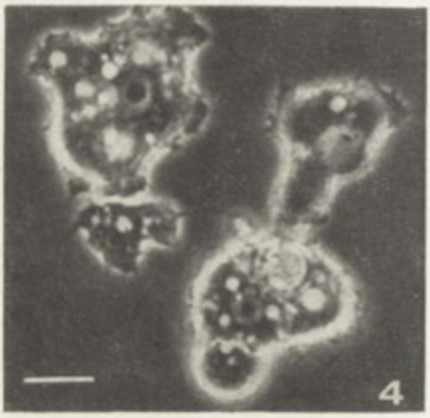


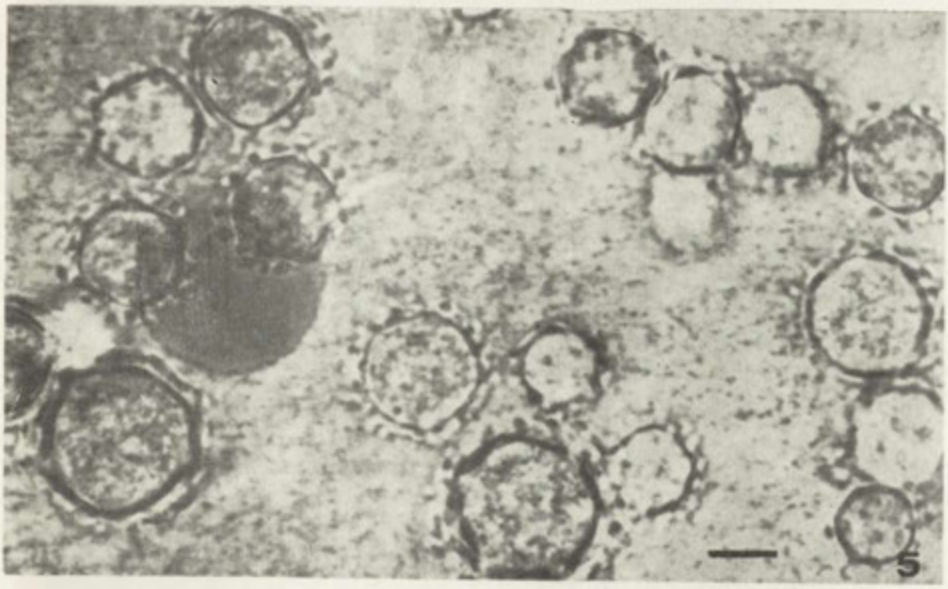


A. Przełęcka et E. Perkowska auctores phot.

ACTA PROTOZOOLOGICA
Vol. 25, No. 3, pp. 345–350 (1986)

# Further Study of the Infectivity of *Holospora obtusa*, a Macronucleus Specific Bacterium of the Ciliate *Paramecium caudatum*

Masahiro FUJISHIMA

Biological Institute, Faculty of Science, Yamaguchi University, Yamaguchi 753, Japan

*Received on* 12 December 1985

*Synopsis.* The gram-negative bacterium *Holospora obtusa* is a macronucleus-specific symbiont of ciliate *Paramecium*, which can penetrate the macronuclear envelopes of *P. caudatum*, *P. multimicronucleatum* and *P. aurelia* species, complex but stable maintenance of the infected bacteria in the host nucleus is achieved only in certain strains of *P. caudatum*. In the present study, it was found that the bacterium cannot penetrate the macronuclear envelopes of *P. woodruffi* and *P. calkinsi*. The result suggests that a property of the macronuclear envelope that is necessary for it to be recognized and infected by *H. obtusa* is not provided in these two species of *Paramecium*.

In the ciliate *Paramecium* six species of *Holospora* are known to occur as endonuclear symbionts (Hafkine 1890, Preer 1969, Ossipov et al. 1980, Borchsenius et al. 1983). All of them exhibit not only a species specificity but also a nuclear specificity in their habitats: *H. obtusa* in the macronucleus of *P. caudatum*, *H. elegans* and *H. undulata* in the micronucleus of *P. caudatum*, *H. caryophila* in the macronucleus of *P. biaurelia*, *H. curviuscula* in the macronucleus of *P. bursaria*, and *H. accuminata* in the micronucleus of *P. bursaria*. They show two morphologically distinct forms in their life cycle: a reproductive short form (1.5–2.0 μm in length) and an infectious long form (5.0–20.0 μm in length). The former is observed predominantly in nuclei of vegetatively growing host cells and the latter in those of starved cells. Only the long form can infect the specific nucleus, via the food vacuoles, when a homogenates of *Holospora*-bearing cells or purified holosporas are added to *Holospora*-free cells (Preer 1969, Ossipov and Ivakhyuk 1972, Ossipov et al. 1975, Görtz and Dieckmann 1980, Görtz and Fujishima 1983, Fujishima and Görtz 1983, Fujishima and Nagahara 1984, 1985, Fujishima and Fujita 1985).

Recently, Fujishima and Fujita (1985) elucidated that the capacity of *Paramecium* for infection with *Holospora* can be separated from its ability to main-

tain the symbionts. They showed that *H. obtusa* infects not only the macronucleus of *P. caudatum*, but also the macronuclei of *P. multimicronucleatum* and 14 species of the *P. aurelia* complex, and that the bacteria that infected the macronuclei of *P. multimicronucleatum* and the *P. aurelia* species complex always disappear from the nuclei and stable maintenance of the infected bacteria in the host nucleus is achieved in a highly specific fashion in certain strains of *P. caudatum*. Furthermore, they found that the macronuclei of *P. jenningsi*, *P. bursaria*, *P. trichium*, *P. duboscqui* were never infected by the bacterium. These results indicate that a property of the macronucleus that is necessary for it to be recognized and infected by *H. obtusa* is commonly provided by *P. caudatum*, *P. multimicronucleatum* and 14 species of the *P. aurelia*, but not by *P. jenningsi*, *P. bursaria*, *P. trichium* and *P. duboscqui*.

To examine the infectivity of *H. obtusa* against various *Paramecium* species has a worthwhile value in evolutionary implications of the species. It was the purpose of the study reported here to test the infectivity of *H. obtusa* in other *Paramecium* species, *P. woodruffi* and *P. calkinsi*.

## Materials and Methods

### Cells and Culture Conditions

Stock Ok-6 of *Paramecium woodruffi* and stock Ok-10 of *P. calkinsi* were kindly supplied from Dr. S. I. Fokin, Leningrad State University. Stock GT703S2 of *P. caudatum* syngen X was supplied from Dr. K. Hiwatashi's stocks at Tohoku University.

The culture medium used was 1.25% (w/v) fresh lettuce juice in Dryl's solution (Dryl 1959), inoculated with a non-pathogenic strain of *Klebsiella pneumoniae* one day before use (Hiwatashi 1968). In ordinary cultures several hundred cells were inoculated into 2 ml culture medium in 18 mm×180 mm test tubes and then 4 ml, 10 ml and 10 ml of fresh medium were added on successive days. The cultures were kept at 25°C.

The original *Holospora obtusa*-bearing strain C101 (syngen unknown) of *P. caudatum* was collected in Münster, FRG, by Dr. H.-D. Görtz. Later, the bacteria infected strain GT703S2 of *P. caudatum* and this newly infected strain was used for obtaining the bacteria used in the present study.

### Infection

Infection of *H. obtusa* (i.e., penetration by the bacterium of the host nuclear envelope) was achieved as follows. Infectious long form of *H. obtusa* was isolated from homogenates of mass cultures of *H. obtusa*-bearing paramecia with a Percoll density gradient centrifugation (Fujishima and Nagahara 1984, 1985). *H. obtusa*-bearing cells were harvested and washed three times with Dryl's solution by centrifuging at 160 g for 2 min. The cell pellet was mixed with 4 volumes of Dryl's solution and homogenized by hand in a Teflon homogenizer at 0–4°C. Then, the homogenate was mixed with 75% Percoll (Pharmacia Fine Chemicals) containing 0.25 M sucrose and centrifuged 38,000 g for 1.5 h at 2°C. After the centrifugation, infectious long form of *H. obtusa* deposited as a band. The band region was collected from bottom of the centrifuge tube and was-

hed with Dryl's solution to remove Percoll by centrifuging at 1000 g for 10 min. The isolated *H. obtusa* was stored in a refrigerator until was used in experiment.

Recipient cells and bacteria were mixed in depression slides at 1000 cells/ml and $4\times10^5$ bacteria/ml, respectively, at 25°C. Samples of the cells were examined at 1, 6 and 24 h after the mixing by Nomarski differential interference microscopy at magnification of ×1000.

## Results

When cells of stock GT703S2 of *P. caudatum* and the isolated *H. obtusa* were mixed, the first bacteria appeared in the recipient macronucleus within 15 min after the mixing. This result indicated that the isolated bacteria had a strong infectivity. However, the macronuclei of *P. woodruffi* and *P. calkinsi* were not infected by the bacteria, though bacteria were observed in their food vacuoles and cytoplasm and some were apparently in contact with the macronuclear envelope. In order to check reproducibility of the results, each infection experiment was repeated five times, but the results were always negative. Thus, it appears that a property of the macronucleus, necessary for it to be recognized and infected by *H. obtusa*, is not provided by *P. woodruffi* and *P. calkinsi*.

## Discussion

*Holospora obtusa*, as well as another species of *Holospora*, is incorporated into food vacuoles of the host cells, migrates from there to the cytoplasm, penetrates the macronuclear envelope and grows exclusively in the nucleus. By light and electron microscopy, one end of the infectious long form of this bacterium can be distinguished from the other as being non-refractile and electron-translucent. The non-refractile tip is never observed in the reproductive short forms (Görtz 1983). The infectious long form always penetrates the macronuclear envelope with this special tip and never with one another. Furthermore, *H. obtusa* never penetrate the micronuclear envelope. Therefore, it is strongly suggested that an affinity between this special tip of the bacterium and the host nuclear envelope is responsible for the nuclear specificity of the infectivity of *H. obtusa*.

Fujishima and Fujita (1985) reported that *Paramecium* species can be divided into two different groups on the basis of its ability to be infected by *H. obtusa*: *P. caudatum*, *P. multimicronucleatum* and *P. aurelia* species complex belong to a group which macronuclei are infected by *H. obtusa*, and *P. jenningsi*, *P. bursaria*, *P. trichium* and *P. duboscqui* belong to the other group in which macronuclei are never infected by the bacterium. Present study showed that *P. woodruffi* and *P. calkinsi* belong to the latter group, suggesting that macronuclear envelopes of *P. woodruffi* and *P. calkinsi* are somewhat different from those of *P. caudatum*, *P. mul-*

*timicronucleatum* and *P. aurelia* species complex as well as of *P. jenningsi*, *P. bursaria*, *P. trichium* and *P. duboscqui*. This difference in the infectivity of the macronuclei of *Paramecium* species by *Holospora* can be expected to provide us new information which concerns the evolutionary relationships among *Paramecium* species. Therefore, the infectivity of *Paramecium* species with other macronucleus-specific *Holospora*, *H. caryoplila* and *H. curviuscula*, should also be tested in future study.

Although it has been found that the property of the macronucleus necessary for it to be recognized by the bacterium is acquired in close association with initiation of structural or fundamental differentiation in the macronucleus (Fujishima and Görtz 1983), its physical property is unclear. Recently, Fujishima and Nagahara (1984, 1985) succeeded to isolate the infectious long form of *H. obtusa* from mass cultures of *H. obtusa*-bearing paramecia. If the isolated bacteria can infect isolated macronuclei, this *in vitro* infection system will provide a good opportunity to detect what kinds of differences of the nuclear envelopes can be recognized by the bacterium. Furthermore, such studies will also provide new data not only for evolutionary implications of *Paramecium* species but also for the macro- and the micronuclear differentiation from a common fertilization nucleus, because *Holospora* species infect specific nucleus of the two kinds of nuclei and the property of the nucleus needed for an infection by the bacterium is acquired when nuclear differentiation begins.

## REFERENCES

Borchsenius O. N., Skoblo I. I. and Ossipov D. V. 1983: *Holospora curviuscula* — A new species of macronuclear symbiotic bacteria of *Paramecium bursaria*. Tsitologiya, 25, 91–97.

Dryl S. 1959: Antigenic transformation in *Paramecium aurelia* after homologous antiserum treatment during autogamy and conjugation. J. Protozool., 6 (suppl.), 25.

Fujishima M. and Görtz H.-D. 1983: Infection of macronuclear anlagen of *Paramecium caudatum* with the macronucleus-specific symbiont *Holospora obtusa*. J. Cell Sci., 64, 137–146.

Fujishima M. and Nagahara K. 1984: Isolation of endonuclear symbiont *Holospora obtusa* from mass cultures of *Paramecium caudatum*. Proc. 55th Ann. Meet. Zool. Soc. Japan (abstr.), 36.

Fujishima M. and Nagahara K. 1985: Isolation of endonuclear symbiont *Holospora obtusa* from mass cultures of *Paramecium caudatum*. In: Progress in Protozoology, Abstr. Seventh int. Congr. Protozool., 301.

Fujishima M. and Fujita M. 1985: Infection and maintenance of *Holospora obtusa*, a macronucleus-specific bacterium of the ciliate *Paramecium caudatum*. J. Cell Sci., 76, 179–187.

Görtz H.-D. and Dieckmann J. 1980: Life cycle and infectivity of *Holospora elegans* Hafkine, a micronucleus-specific symbiont of *Paramecium caudatum* (Ehrenberg). Protistologica, 16, 591–603.

Görtz H.-D. and Fujishima M. 1983: Conjugation and meiosis of *Paramecium caudatum* infected with the micronucleus-specific bacterium *Holospora elegans*. Eur. J. Cell Biol., 32, 86–91.

Görtz H.-D. 1983: Endonuclear symbionts in ciliates. Int. Rev. Cytol. (suppl.), 14, 145–176.

Hafkine W. M. 1890: Maladies infectieuses des paramecies. Annls Inst. Pasteur, Paris 4, 145–162.

Hiwatashi K. 1968: Determination and inheritance of mating type in *Paramecium caudatum*. Genetics, Princeton 58, 378–386.

Ossipov D. V. and Ivakhnyuk I. S. 1972: Omega-particles — micronuclear symbiotic bacteria of *Paramecium caudatum* clone MI-48. Cytologia, 14, 1414–1419.

Ossipov D. V., Skoblo I. I. and Rautian M. S. 1975: Iota-particles, macronuclear symbiotic bacteria of ciliate *Paramecium caudatum* clone M115. Acta Protozool., 14, 263–280.

Ossipov D. V., Borchsenius O. N. and Podlipaev S. A. 1980: Some peculiarities in organization of nuclear apparatus in a ciliate, *Paramecium bursaria*, infected with symbiotic bacteria, *Holospora acuminata*. Acta Protozool., 19, 315–326.

Preer L. B. 1969: Alpha, an infectious macronuclear symbiont of *Paramecium aurelia*. J. Protozool., 16, 570–578.

ACTA PROTOZOOLOGICA
Vol. 25, No. 3, pp. 351–354 (1986)

# *Ceratomyxa tartoori* sp. n. *(Myxozoa)* from the Gall-bladder of a Marine Teleost *(Clupeidae)* of West Bengal, India

N. K. SARKAR

Department of Zoology, R. B. C. College, Naihati 743165, West Bengal, India

*Received on* 17 April 1985, *revised on* 10 January 1986

*Synopsis.* A new myxosporidan *Ceratomyxa tartoori* sp. n. (*Myxozoa*) is described from the gall-bladder of a marine teleost *Opisthopterus tartoor* Day (*Clupeidae*) caught from the West Bengal coastal water of Bay of Bengal, India. The characteristics of the parasite are as follows: spore arched, coelozoic, suture distinct — sutural diameter 16.12 μm, breadth of the spore 212.0 μm, with two to five equal appendages of the shell valves, polar capsule two, spherical (6.3 μm) or broadly ovoidal (6.29 μm× ×5.50 μm) with occasional presence of three to four polar capsules. The extruded polar filament is 25.0 μm long.

While the investigation was carried out about the parasitic protozoa of Indian marine fishes, a myxosporidan parasite has been found to infest the gall-bladder of a teleost *Opisthopterus tartoor* Day (*Clupeidae*), caught from the coastal water of Bay of Bengal at Digha, West Bengal, India during the winter of 1984–85.

## Material and Methods

All autopsies were performed from fresh and frozen fish. The fish was collected from Digha beach of Bay of Bengal, West Bengal, India. The parasite was studied from the fresh wet smears of the infected gall-bladder treated with Lugol's iodine solution and also from the dry smears stained with Giemsa after fixation in absolute methanol. The extrusion of the polar filament was achieved with saturated aquaous solution of urea. All the measurements were taken in micrometer (μm). The Figures have been drawn with the aid of a camera lucida.

## Observations

### *Ceratomyxa tartoori* sp. n.

Vegetative form: Not seen.

Spore: These were coelozoic, found floating in the bile. The spore body was hemispherical in sutural view with highly convex, round anterior surface and almost

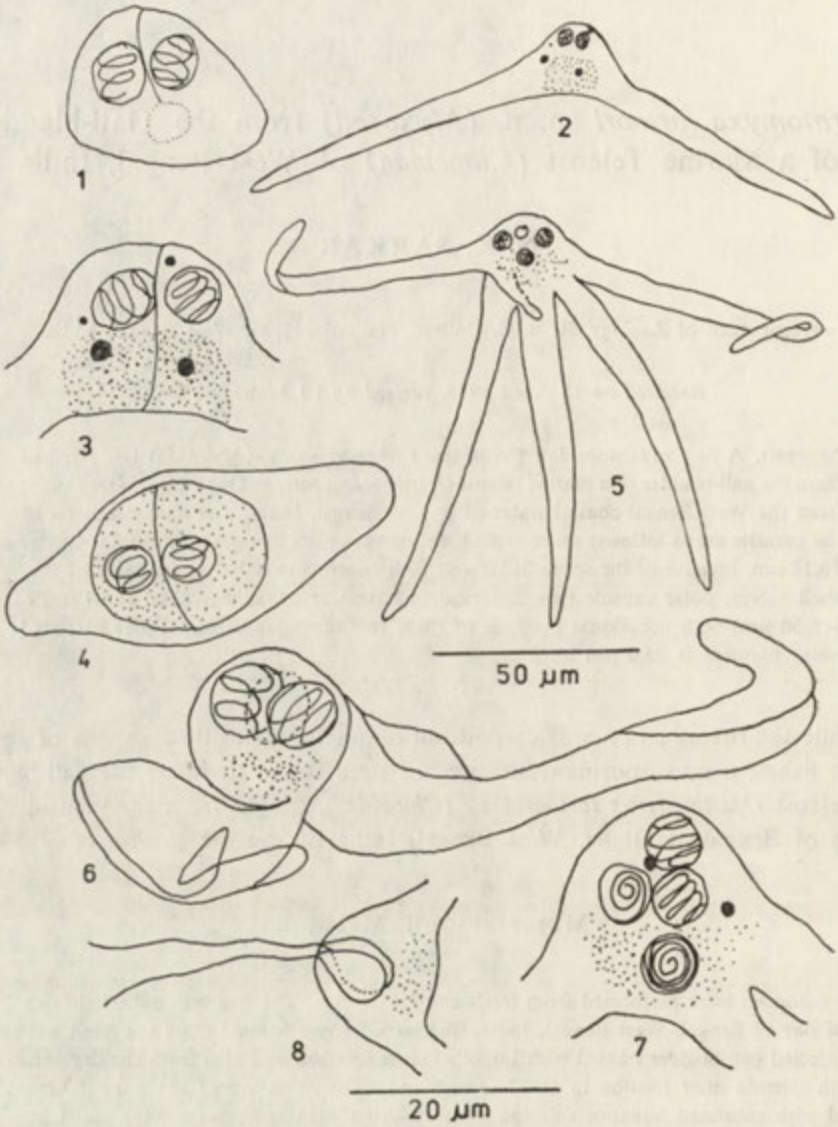


Fig. 1. 1–8 — Spores of *Ceratomyxa tartoori* sp. n. *1* — An early spore, *2* — A mature spore with two polar capsules and two equal appendages of the shell valves, *3* — Enlarged sutural view of the spore body, *4* — A mature spore in top view, *5* — A mature spore with three polar capsules and five equal appendages of the shell valves, *6* — A mature spore with three polar capsules and two appendages of the shell valves, *7* — A mature spore with four polar capsules showing different arrangement of the polar filament, *8* — A mature spore with two polar capsules showing extruded polar filament

flat posterior surface (Fig. 1 *1–4*). The shell valves were two, very thin and smooth — each had very thin and long prolongation or appendage forming about 45° angle with the sutural axis. Usually there were two lateral appendages. However, the spores with three to five appendages were also found (Fig. 1 *5*, *7*). The polar capsules were two — one on each side of the nearly straight, thin-walled suture. However, the spores with three to four polar capsules were also noticed (Fig. 1 *6*, *7*). The polar capsules were spherical or nearly ovoidal with a very short neck (Fig. 1 *8*). In spores with three to four polar capsules, the direction of opening of the polar capsules were variable (Fig. 1 *7*). Each polar capsule had three to four coils of polar filament and when extruded attained a maximum length of 28.0 μm (Fig. 1 *8*). The appendages of the shell valves were equal in length and similar in shape having widest at the base and narrowing down towards the roundly pointed tip. The sporoplasm was in the form of a small granular mass towards the flat surface of the spore with two large nuclei. The smaller capsulogenous nuclei were also found either at the base or in front of the polar capsule. No iodinophilous vacuole was found. The demarcation between the main spore body (containing the polar capsules and sporoplasm) and its appendages was not present which supports the view that the appendages were the hollow prolongations of the shell valves.

Measurements (based on twenty fresh spores, mean is given with range within the parenthesis):

Sutural diameter of the spore — 16.12 (14.0–19.0)
Breadth of the spore — 212.00 (167.00–234.00)
Diameter of the polar capsule — 6.30 (6.0–7.0)
or
Length of the polar capsule — 6.29 (5.0–7.0)
Width of the polar capsule — 5.50 (5.0–7.0)
Length of the extruded polar filament — 25.00 (20.0–28.0)
Incidence: One infected out of five examined
Infection locus: Gall-bladder
Pathogenicity: Not apparent
Host: *Opisthopterus tartoor* Day
Locality: Digha coast of Bay of Bengal, West Bengal, India
Date of collection: 30 December, 1984

## Discussion

The myxosporidan, in having arched spore, hollow and conical shell valve and its breadth much more than twice the sutural diameter, is assigned to the genus *Ceratomyxa* Thelohan, 1892. As its general morphology of the spore is concerned, it superficially resembles *Ceratomyxa mesospora* Davis, 1917 (dimension 8 μm × 50 μm – 65 μm), *C. aggregata* Davis, 1917 (6 μm–7 μm × 50 μm–70 μm) *C. californica* Jameson, 1929 (7.5 μm,–9.0 μm × 48 μm–59 μm), *C. hilsae* Chakravarty, 1939 (10 μm × 25 μm–40 μm) and *C. sagarica* Choudhury and Nandi, 1973 (3.5 μm ×

×31 μm) reported from the gall-bladders of *Cestracion zygaena*, *Leiostomus xanthurus* and *Micropogon undulatus*, *Polistotrema stouti*, *Hilsa ilisha* and *Boleophthalmus boddaerti* respectively. Moreover, it also resembles *C. aggregata* in having diad and triad spores. However, the present parasite differs from all the above mentioned species by two to five hollow appendages of shell valves, tetrad spores (having four polar capsules) and its very large dimension. In view of such distinct differences, the myxosporidan has been considered a new species for which the name *Ceratomyxa tartoori* sp. n. has been proposed after the name of the host.

Material: Syntypes on slide No. MxC–3 is kept in author's collection and soon will be deposited to the National Collection of the Zoological Survey of India, Calcutta.

## ACKNOWLEDGEMENT

Author expresses sincere gratitudes to Prof. A. Pramanik, Head of the Department of Zoology R. B. C. College for laboratory facilities.

## REFERENCES

Chakravarty M. M. 1939: Studies on myxosporidia from the fishes of Bengal with a note on the myxosporidian infection in aquaria fishes. Arch. Protistenkd., 92, 169–178.

Choudhury A. and Nandi N. C. 1973: Studies on myxosporidan parasites (*Protozoa*) from an estuarine Gobid fish of West Bengal. Proc., Zool. Soc. (Calcutta), 26, 45–55.

Davis H. S. 1917: The myxosporidia of the Beaufort region. A systematic and biologic study. Bull. Bur. Fish. U.S., 35, 201–243.

Jameson A. P. 1929: Myxosporidia from California fishes. J. Parasitol., 16, 59–68.

ACTA PROTOZOOLOGICA
Vol. 25, No. 3, pp. 355–358 (1986)

# *Sphaerospora sphaerocapsularae* sp. n. *(Myxospora, Bivalvulida)* a Parasite of Eel, *Anguilla anguilla* (L.)

Jadwiga WIERZBICKA

Institute of Ichthyology, Academy of Agriculture, Kazimierza Królewicza 4, 71-550 Szczecin, Poland

*Received on* 6 January 1986

*Synopsis.* A new species, *Sphaerospora sphaerocapsularae*, is described. The parasite was found in the urinary bladder of eel, *Anguilla anguilla* (L.) caught in the Lake Dąbie adjacent to the River Odra mouth.

During studies on parasitic protozoans in *Anguilla anguilla* (L.), sporozoans of the genus *Sphaerospora* Thélohan, 1892 were found. Morphologically, they differ from the hitherto known species of the genus (Kudo 1919, Šulman 1966, 1984, Evlanov 1981, Wierzbicka 1986). The differences observed prompted the author to describe the protozoans as a new species, *Sphaerospora sphaerocapsularae* sp. n.

## Materials and Methods

The fishes examined were caught in the Lake Dąbie, connected with the mouth section of the River Odra. The materials were collected in July and September 1985. A total of 13 eels, *Anguilla anguilla* (L.), were examined, their length (l.t.) and weight ranged within 42–65 cm and 120–530 g, respectively. The observations were made on fresh materials. Those scraped off of the urinary bladder were examined under the microscope, smears on glass plates, stained using Pappenheim's technique (May-Grünwald and Giemsa) were made as well. Drawings of spores were made from both fresh materials and stained mounts. A total of 30 fresh and 30 stained spores were measured.

## Description of *Sphaerospora sphaerocapsularae* sp. n. (Figs. 1 and 2)

Host species: eel, *Anguilla anguilla* (L.)
Location host: urinary bladder

Location of finding: Lake Dąbie (NW Poland)
Extent of infestation: out of 13 fish specimens examined, one was found to contain numerous spores, invasion incidence of 7.69%.

The spores are oval, the anterior end being clearly flattened (when looking from the suture). Spore width is slightly lower than its thickness. The halves of a spore are connected with a poorly visible, straight suture. Delicate striata run parallel to the suture over the whole surface of the spore (they are visible on fresh materials only). Two polar capsules, almost spherical in shape, are located near the anterior margin on a plane perpendicular to that of the suture and occupy about one-third of the spore. Their tapering ends are very short and open far away from

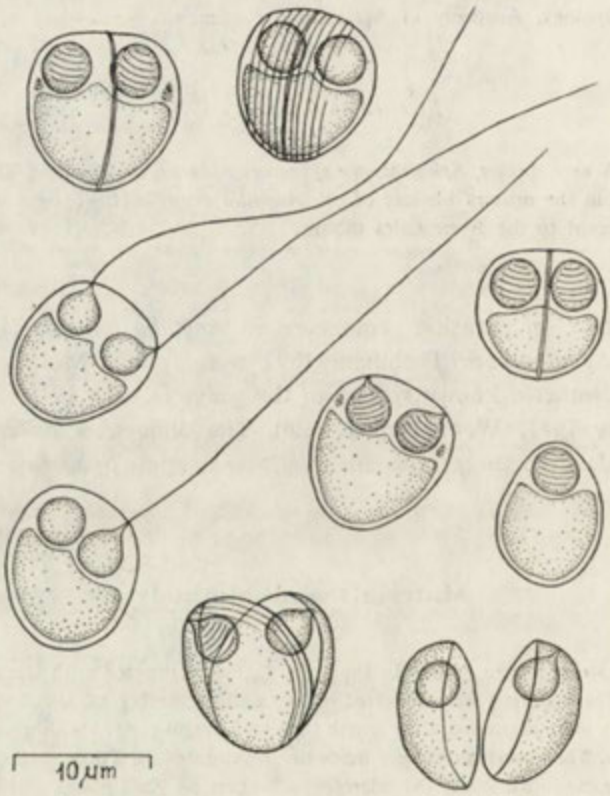


Fig. 1. Spores of *Sphaerospora sphaerocapsularae* sp. n. (fresh)


Fig. 2. Spores of *Sphaerospora sphaerocapsularae* sp. n. (stained)

the suture, almost on the opposite margins of the spore (Figs. 1 and 2). The capsules usually contain spirally coiled filaments, six coils being visible in each. The remaining part of the spore is filled with embryonic sporoplasm. Some (fresh) spores were observed to contain small oval structures causing a stronger light refraction than the rest (Fig. 1). They presumably are the nuclei of polar capsules.

Dimensions of spores (in μm):

| | fresh | stained |
|---|---|---|
| Spore length | 10.4–12.8 (11.39±0.65)* | 8.4–11.2 (9.83±0.72) |
| Spore thickness | 9.6–12.0 (10.38±0.55) | 8.0–10.0 (8.80±0.50) |
| Spore width | 8.0–9.2 – | – |
| Polar capsule width | 2.8–3.8 (3.41±0.29) | 2.4–3.4 (2.97±0.26) |
| Polar capsule length | 3.6–4.4 (4.08±0.23) | 3.2–4.4 (3.65±0.42) |
| Polar filament length | about 40.0–45.0 | – |

* arithmetic mean of a sample and its standard deviation are given in parentheses.

Among the materials examined, only four spores with ejected polar filaments were found. The location of spores on the suture plane was rare, too.

The vegetative stages will be described in the next paper.

## Discussion

The sporozoans *Sphaerospora sphaerocapsularae* sp. n. differ from the *Sphaerospora* species described in the available literature to date (Kudo 1919, Šulman 1966, 1984, Evlanov 1981, Wierzbicka 1986) in the location of openings of their polar capsules. In *S. sphaerocapsularae*, they are placed far away from the suture, almost on the opposite sides of the spore. The literature shows the polar capsule openings in the *Sphaerospora* species to be located close to the suture; frequently the top parts of the capsules touch the suture. However, neither figures nor descriptions of *S. sphaerica* Dogiel, 1948 from the urinary bladder of *Sphaeroides pardalis* from the Sea of Japan, *S. minuta* Konovalov, 1967 from the urinary bladder and ducts of *Esox lucius* from Kamtschatka (Šulman 1984), and *S. galinae* Evlanov, 1981 from the kidneys canaliculi of *Tinca tinca* from lakes off Kaliningrad show the polar capsules openings. On the other hand, the shape of spores in the abovementioned species differ from that of *S. sphaerocapsularae*. Moreover, the posterior part of the *S. galinae* spore contains transverse ribs (Evlanov 1981), while the striation in *S. sphaerocapsularae* is parallel to the suture line. The spores of the newly described species have no test thickenings typical of *S. minuta*; the surface of spores *S. sphaerica* is smooth. *S. sphaerocapsularae* sp. n. differs from *S. anguillae* Wierzbicka, 1986 found in the urinary bladder of *Anguilla anguilla* in shapes of spores and polar capsules as well as in the absence of filamentous processes.

## REFERENCES

Evlanov I. A. 1981: Novye vidy miksosporidij iz ryb Kaliningradskoj oblasti. Parazitologija, 15, 168–170.

Kudo R. 1919: Studies on *Myxosporidia*. A synopsis of genera and species of *Myxosporidia*. Ill. Biol. Monogr., 5, 245–503.

Šulman S. S. 1966: Miksosporidii fauny SSSR. Izd. "Nauka", Moskva–Leningrad, 507 pp.

Šulman S. S. (ed.) 1984: Opredelitel parazitov presnovodnyh ryb fauny SSSR. I. Parazitičeskie prostejšie. Izd. AN SSSR, Leningrad, p. 75–251.

Wierzbicka J. 1986: *Sphaerospora anguillae* sp. n. (*Myxospora, Bivalvulida*), a parasite of eel, *Anguilla anguilla* (L.). Acta Protozool., 25, (in press).

ACTA PROTOZOOLOGICA
Vol. 25, No. 3, pp. 359–362 (1986)

# *Thelohanellus bengalensis* sp. n. and *Myxidium mystusium* sp. n. *(Myxozoa)*: Two New Myxosporida from Indian Fresh Water Teleosts

N. K. SARKAR and S. RAY CHOUDHURY

Department of Zoology, Rishi Bankim Chandra College, Naihati 743165, West Bengal, India

*Received on* 4 October 1985

*Synopsis.* The two new myxosporida viz., *Thelohanellus bengalensis* sp. n. and *Myxidium mystusium* sp. n. (*Myxozoa*) are described from the gall-bladders of *Catla catla* Ham. and *Mystus vittatus* Day respectively. Their respective mensural data are: spore — 10.95 μm × 6.59 μm and 13.08 μm × 5.89 μm, polar capsule — 5.42 μm × 3.47 μm and 4.46 μm in diameter.

While investigation was carried out for the parasitic protozoa of Indian teleosts, two new myxosporidans have been found to be infested in the gall-bladders of the two fresh water teleosts from West Bengal, India.

## Material and Methods

The fishes collected from the local fish market were thoroughly examined for the protozoan parasites. The parasites treated with Lugol's iodine solution and the dry smears stained with Giemsa after fixation in absolute methanol, were carefully studied under the oil immersion lens of an Olympus research microscope. The extrusion of the polar filament was achieved with 2.5% KOH solution. The measurements were taken in micrometer (μm). The figures were drawn with the aid of a camera lucida (Prism type).

## Observations

### *Thelohanellus bengalensis* sp. n.

Description: The vegetative or trophozoite stages were not seen.

The spores were coelozoic, small, broadly pyriform to cylindroconical in valvular view (Fig. 1 *1*) and almost S-shaped in sutural view (Fig. 1 *2*). The suture was

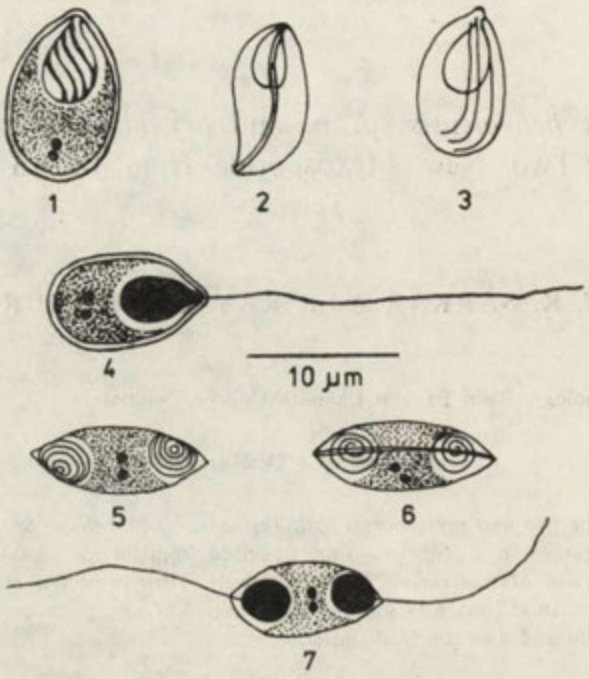


Fig. 1. *1–4* — Spores of *Thelohanellus bengalensis* sp. n., *1* — A spore in valvular view — Lugol's iodine, *2* — A spore in sutural view — Lugol's iodine, *3* — A spore showing peculiar longitudinal striations — Lugol's iodine, *4* — A spore showing extruded polar filament — Giemsa stained, *5–7* — Spores of *Myxidium mystusium* sp. n., *5* — A spore in slightly oblique view — Lugol's iodine, *6* — A spore in sutural view — Lugol's iodine, *7* — A spore showing extruded polar filament — Giemsa stained

S-shaped and ridged. The two shell valves were thick-walled, usually smooth but 3–4 longitudinal striations which were bent posteriorly, rarely visible (Fig. 1 *3*). The polar capsule was one — broadly pyriform with 4–6 coils of polar filament. When extruded, the polar filament attained a maximum length of 52.5 µm (Fig. 1 *4*). The extracapsular cavity was filled with finely granular, sickle shaped mass of sporoplasm with a pair of round nuclei in it. The iodinophilous vacuole was not found.

Measurements: Thirty fresh spores have been measured, mean value is given with range within the parenthesis.

Length of the spore — 10.95 (10.0–12.0)
Width of the spore — 6.59 (5.5–7.5)
Length of the polar capsule — 5.42 (3.75–7.0)
Width of the polar capsule — 3.47 (3.0–4.5)
Infection locus: Gall-bladder
Pathogenicity: Not apparent
Incidence: Two infected (weight — 1 kg) out of 15 examined
Host: *Catla catla* Ham.
Locality: Chinsurah, West Bengal, India
Date of collection: 13 May, 1985

Remark: In having close mensural data of the spore, the present species resembles *Thelohanellus mrigalae* Tripathi, 1952 reported from the head region between the eyes, *T. boggoti* Quadri, 1962 reported from the gills and *T. chelae* Lalitakumari, 1969 reported from the bile of *Cirrhina mrigala*, *Labeo boggot* and *Chela becaila* respectively. The spore of the present myxosporidan also shows very close similarity with the spore of *T. mrigalae* in valvular view. However, it differs from the later species and also from the above mentioned myxosporida by broadly S-shaped spore in sutural view and ridged S-shaped distinct suture. The myxosporidan in study is, therefore considered to be a new species and the name *Thelohanellus bengalensis* sp. n. is proposed.

Material: Syntypes on slide No. MxT-10 is kept in the author's collection and soon will be deposited to the National Collection of the Zoological Survey of India, Calcutta.

*Myxidium mystusium* sp. n.

Description: No trophozoite or other vegetative stages were found. The spores were found floating in the bile. They were fusiform with pointed ends (Fig. 1 *5*). The suture was slightly curved, ridged and very distinct (Fig. 1 *6*). The shell valves were smooth. The two polar capsules — one on either end of the spore, were spherical to ovoidal with 4 to 5 coils of polar filament in each capsule. The polar filament, when extruded fully, attained a maximum length of 36.0 μm (Fig. 1 *7*). The extracapsular cavity was filled with biconcave granular mass of sporoplasm. The iodinophilous vacuole was absent but a pair of sporoplasm nuclei was always present.

Measurements: Thirty fresh spores have been measured, mean value is given with range within the parentheses.

Length of the spore — 13.08 (11.0–16.65)
Width of the spore — 5.89 (5.0–7.49)
Diameter of the polar capsule — 4.46 (3.33–7.49)
or
Length of the polar capsule — 4.83
Width of the polar capsule — 4.50
Infection locus: Gall-bladder
Pathogenicity: Not apparent
Incidence: One infected out of 22 examined
Host: *Mystus vittatus* Day
Locality: Chinsurah, West Bengal, India

Remark: The present myxosporidan, in mensural data, resembles *Myxidium heteropneustesi* Chakravarty, 1943, *M. aori* Lalitakumari, 1969 and *M. boddaerti* Choudhury and Nandi, 1973 reported from the gall-bladders of *Heteropneustes fossilis*, *Macrones aor* and *Boleophthalmus boddaerti* respectively. However, the

parasite in study differs from *M. heteropneustesi* by the smooth shell valves, distinct suture and spherical polar capsule. It also disagrees with *M. aor* in having larger spore and longer polar filament. Moreover, it is markedly different from *M. boddaerti* in having no lateral extension of the spore and smaller, spherical polar capsule. In view of such differences, I propose the present myxosporidan a new species and name it as *Myxidium mystusium* sp. n.

Material: Syntypes on slide No. MxMy-7 are kept in the author's collection and soon will be deposited to the National Collection of the Zoological Survey of India, Calcutta.

ACKNOWLEDGEMENT

Grateful acknowledgement is made to Prof. A. Pramanik, Head of the Department of Zoology, R. B. C. College, for laboratory facilities.

REFERENCES

Chakravarty M. 1943: Studies on *Myxosporidia* from the common food fishes of Bengal. Proc. Indian Acad. Sci. Sect. B, 18, 21–35.

Choudhury A. and Nandi N. C. 1973: Studies on myxosporidian parasites (*Protozoa*) from an estuarine gobbid fish of West Bengal. Proc. Zool. Soc. Calcutta, 26, 45–55.

Lalitakumari P. S. 1969: Studies on parasitic protozoa (*Myxosporidia*) of fresh water fishes of Andhra Pradesh, India. Riv. Parassitol., 30, 154–225.

Quadri S. S. 1962: On a new myxosporidian *Thelohanellus boggoti* n. sp. from an Indian fresh water fish *Labeo boggot*. Arch. Protistenk., 106, 218–222.

Tripathi Y. R. 1952: Studies on parasites of Indian fishes. I. *Protozoa*: *Myxosporidia* together with a check list of parasitic protozoa described from Indian fishes. Rec. Indian Mus., 50, 63–89.

## NOTICE TO AUTHORS

ACTA PROTOZOOLOGICA is intended as a journal serving for the publication of original papers embodying the results of experimental or theoretical research in all fields of protozoology with the exception of faunistic notices of the local character and purely clinical reports. The papers should be concise and will not be accepted if they have been previously published elsewhere. After acceptance by the Editors papers will be printed in the possibly shortest time.

Papers are accepted in English, French, German and Russian. Every paper should begin with the name and postal address of the laboratory, name and the surname of the author and title in the language of the text. The titles in German and French should be translated into English according to the demands of Current Contents. The paper should be accompanied by synopsis in the language of the text not exceeding 100 words and by short summary in one of 4 languages accepted in the Journal. In the Russian text also the name and the postal address of the laboratory, legends of tables, plates and text illustrations must be translated, the translation of the summary may be somewhat more extensive, and the name of the author should be given additionally also in the Latin characters.

Manuscripts should be doublespaced typescript (30 lines on one side of a sheet) with a normal margin. No elements of the text should be fully typed in capitals nor in spaced set (only underlining with pencil is admittable). In decimal fractions points not commas should be used. The generally accepted abbreviations and symbols are recommended. Nomenclature must agree with the International Code of Zoological Nomenclature, London 1961. The original and one carbon copy of the whole text material should be supplied.

References must be cited in the text indicating only the author and year thus:

"Kinosita (1954) found that, etc."

Only all references cited in the text should be listed. The list must be arranged as follows:

Ehret C. F. and Powers E. L. 1959: The cell surface of *Paramecium*. Int. Rev. Cytol., 8, 97–133.

Gelei J. von 1939: Das aussere Stützgerustsystem des Parameciumkörpers. Arch. Protistenk., 92, 245–272.

Titles of references are given in their original language (not translated). In papers written in English, French or German, the Cyrillic type of the Russian is transliterated according to the international system (ISO Recommendation R 9 September). This regulation is not applied to names if there exists in their traditional spelling. Also author may freely choose in transliteration of his own name. In Russian papers, the Russian references are cited in Cyrillic, the others in the Latin characters, but they must be listed all together in the Latin alphabetical order.

The following material should be supplied on separate sheets 1. the running tittle for the page headlines, 2. tables, 3. legends for text figures, 4. legends for plates. Line-drawings will be published in the text, photographs and raster figures on separate plates. No coloured photographs can be published presently. Lettering on photographs and drawings should be marked in pencil. With no regard to the language of the text, only the Latin lettering, arabic numerals or generally accepted symbols are admittable for marking on illustrations. Numbering of text-figures, plates and tables must be also marked in pencil, as well in the legends as in the text.

Galley proofs are sent to the authors. Authors receive 75 reprints without covers.

In preparation:

I. Wita and K. M. Sukhanova: Seasonal Modifications in the Life Cycle of *Parastasia fennica* (Michajłow, 1966) — D. Chardez: Thecamoebiens des plages de la Mer du Nord en Angleterre — N. Wilbert: Ciliaten aus dem Interstitial des Ontario Sees — R. Mathur and D. M. Saxena: Inhibition of Macromolecule Syntheses in a Ciliate Protozoan, *Tetrahymena pyriformis* by Hexachlorocyclohexane (HCH) Isomers — W. Kasprzak, T. Mazur and E. Hadaś: Biochemical Changes of *Acanthamoeba* Following Attenuation and the Role of Cysts in Retaining the Characteristics of Strains — T. Michałowski, P. Szczepkowski and P. Muszyński: The Nutritive Factors Affecting the Growth of the Rumen Ciliate *Diploplastron affine* on vitro — A. Czapik et N. Wilbert: Sur une nouvelle espèce de cilié *Paranophrys carnivora* sp. n. (*Scuticociliatida*) — S. L. Kazubski and S. A. M. El-Tantawy: A Ciliate *Paratrichodina africana* sp. n. (*Peritricha, Trichodinidae*) from *Tilapia* Fish (*Cichlidae*) from Africa — S. A. M. El-Tantawy and S. L. Kazubski: The Trichodinid Ciliates from Fish *Tilapia nilotica* from the Delta of Nile (Egypt) — S. L. Kazubski: The Trichodinid Ciliates from Fish *Tilapia* sp. from Victoria Lake (Kenya) and Description of *Trichodina equatorialis* nom. nom. nov. — C. K. Sinha: Occurrence of *Trypanosoma mukasai* Hoare, 1932 in *Talapia mossambica* (Peters) from India — S. Ghose, S. K. Ray and D. P. Haldar: *Neohirmocystidae* fam. n., a New Family of Septate Gregarines (*Apicomplexa*: *Sporozoea*) from Insects — V. N. Hoogar and S. D. Amoji: *Leidyana bimaculata* a New Cephaline Gregarine Parasite of a Cricket, *Gryllus bimaculatus* De Geer: C. K. Sinha: *Hepatozoon mucosus* sp. n. from Indian Rat Snakes, *Ptyas mucosus* (Linnaeus) — N. K. Sarkar: A New Myxosporidian *Myxidium sciaenae* sp. n. (*Myxozoa*: *Myxididae*) from the Gall Bladder of Marine Teleost of West Bengal, India

**Warunki** prenumeraty

Prenumeratę **na kraj** przyjmują i informacji o ocenach udzielają urzędy pocztowe i doręczyciele na wsi oraz Oddziały RSW „Prasa-Książka-Ruch" w miastach.
Prenumeratę ze zleceniem wysyłki **za granicę** przyjmuje RSW „Prasa-Książka-Ruch", Centrala Kolportażu Prasy i Wydawnictw, ul. Towarowa 28, 00-958 Warszawa, konto NBP XV Oddział w Warszawie Nr 1153-201045-139-11. Wysyłka **za granicę** pocztą zwykłą jest droższa od prenumeraty krajowej o 50% dla zleceniodawców indywidualnych i o 100% dla zlecających instytucji i zakładów pracy.

**Terminy przyjmowania prenumerat na kraj i za granicę:**
— do dnia 10 listopada na I półrocze roku następnego i cały rok następny,
— do dnia 1 czerwca na II półrocze roku bieżącego.

Bieżące i archiwalne numery można nabyć lub zamówić we Wzorcowni Ośrodka rozpowszechniania Wydawnictw Naukowych PAN, Pałac Kultury i Nauki, 00-901 Warszawa, oraz w księgarniach naukowych „Domu Książki".

Cena zł 140.—

CONTENTS



Organizing Commitee of the IIIrd Polish Conference of Cell Biology informs that the Conference will be held in 2nd half of June 1988 in Łódź. The interested colleagues are asked to send the preliminary declarations until 30th June 1987 to the address: Department of Plant Cytology and Cytochemistry, Institute od Physiology and Cytology, University of Łódź, Banacha 12/16, 90-237 Łódź, Poland.

Indeks 351334